UNIVERSIDAD EAFIT

DOCTORAL THESIS

---

# Relationship between enamel mechanical, chemical, ultrastructural properties and mammalian bite force

---

***Author:***

Juliana María Fernández-Arteaga

***Supervisor:***

Dr. Alexánder Ossa

*A thesis submitted in fulfillment of the requirements*

*for the degree of Doctor of Philosophy*

September 10, 2021

*When given the choice between being right and being kind, choose kind*

**Wayne Dyer**

# *Abstract*

Mammalian enamel is one of the hardest and most mineralized tissues in the body. Its main function is to support the loads generated during the chewing process. Mechanical, chemical and ultrastructural properties are responsible for providing it with the high resistance necessary to withstand constant loads and for making the animal's tooth functional through its life. Animal bite forces as well as their feeding patterns can influence enamel ultrastructure, improving its behavior when facing chewing loads.

A brief review of enamel mechanical and chemical properties as well as a brief review on mammalian enamel decussation characteristics are presented in chapter $2$. The methodology used in this study is shown in chapter $3$, experimental results in terms of mechanical, chemical and ultrastructural properties are presented in chapter $4$. In Chapter $5$ the results of the experimentation are analyzed in terms of their statistical correlations and the relationship between enamel properties, bite force, and feeding patterns of the analyzed specimens. Finally the conclusions of this investigation are shown in chapter $6$.

The bite force of the analyzed animals ($BFQ$) is related to the elastic modulus of the enamel and that the enamel of the analyzed species shows similar characteristics to human enamel in terms of the variations in mechanical and chemical properties. The properties analyzed were compared in terms of the taxonomic classification or the feeding patterns of the analyzed specimens. The mechanical variables (elastic modulus and hardness) do not seem to be related to taxonomic classification or feeding patterns. The decussation fraction is greater than $0.8$ regardless of the taxonomic classification or feeding patterns, enamel thickness and decussated thickness are statistically correlated with decussated band thickness, this could indicate that these variables are important in delaying crack growth. Ultrastructural variables do not seem to depend on taxonomic classification or feeding patterns.

*I want to dedicate this thesis to my family.*

*With special gratitude to my loving parents, Carlos and Marta, whose words of encouragement were always there during this long journey.*

*I dedicate this work and I especially thank my best friend and great love Alejandro, for being there for me throughout the doctoral program. You were my biggest inspiration.*

# *Acknowledgements*

I would like to express my sincere gratitude to my supervisor Dr. Alexánder Ossa for his guidance and invaluable discussions. I appreciate his patience, support, motivation and immense knowledge.

Special thanks to Dr. Dwayne Arola from the Materials Science and Engineering department at the University of Washington for the continuous support during this investigation.

Finally, this doctoral project was possible thanks to the scholarship program $647 - 2014$ from Ministerio de Ciencia, Tecnología e Innovación, Minciencias.

# Contents

# List of Figures

# List of Tables

# 1 Introduction

Dental enamel, one of the hardest tissues in the body, surrounds the dental crown, and is responsible for providing resistance to crack growth in order to prevent tooth fracture (Yahyazadehfar, Bajaj, and Arola, 2013; Thompson, 2020). This important characteristic is given by enamel prism decussation, that is, the existence of a wavy path created by variations in the curvature of enamel prisms when crossing each other while traveling from the dentino-enamel junction (DEJ) to the outer enamel surface (Berkovitz and Shellis, 2018c; Thompson, 2020).

Enamel decussation is essential in tooth resistance to crack growth (Gao et al., 2016). To date, there are multiple investigations related to enamel decussation patterns in humans (Shimizu and Macho, 2008; Bajaj and Arola, 2009b; He et al., 2013; Lucas et al., 2016; Pro and Barthelat, 2019; Beniash et al., 2019), but little research on the importance of this pattern in other mammals (Rensberger and Wang, 2005; Weng et al., 2016; Yilmaz, Koldehoff, and Schneider, 2018; Carreon and Funkenbusch, 2019; Arango-Santander et al., 2020), specifically taking into account bite forces and feeding patterns (Yahyazadehfar, Bajaj, and Arola, 2013; Lucas et al., 2016).

Mechanical, chemical, and ultrastructural properties of mammalian enamel may be related. Changes in the value of one of these properties can produce changes in the others or, on the contrary, be compensated due to their stability. Characterizing the relationship between these properties, the bite force and the eating habits of mammals could help to better understand enamel properties and its fundamental role in protecting the tooth against fracture and the consequences that this would bring for the animal life.

# 2 Literature review

Teeth and their structure are well known and studied. Teeth and especially enamel, allow obtaining information on ancient species due to its long-time of degradation and structural nature (Macchiarelli and Bailey, 2007; Teaford, 2007; Xing, Martinón-Torres, and Bermúdez de Castro, 2018; Thompson, 2020). Teeth should remain functional throughout the animal lifespan, as their fracture can be catastrophic and cause dental failure, starvation and death (Lucas and van Casteren, 2015; Ungar, 2015; van Casteren and Crofts, 2019). Dietary habits of different mammals present a risk of occurrence of dental fracture. However, this risk is compensated through a specialized structure, the enamel, which receives the force of the chewing load (Peres Line and Duarte Novaes, 2005). In this chapter a review of the mechanical, chemical and ultrastructural properties of enamel is presented in order to understand the importance of the research carried out in this thesis.

## 2.1 Mammalian feeding

Mammals are endothermic animals, they regulate their body temperature through a combination of a high metabolic rate and an insulating layer of hair. Being endothermic gave mammals the ability to be independent of the environment, and thus the potential to colonize almost every region of the planet as they evolved (Berkovitz and Shellis, 2018b). Animal survival is determined, in part, by the ability to acquire and store energy, which in turn depends on the ease of the animal to detect, capture and acquire food (Svanbäck and Bolnick, 2019).

Mammalian evolution involved changes in their oral cavity: shape and size of the maxillary bones and dentition, temporomandibular joint configuration and, the ability to process food through chewing (Berkovitz and Shellis, 2018b). Regarding dentition, the development of the tribosphenic molar was essential for mammalian evolution. Tribosphenic molar combined crushing and shearing functions, and

provided the morphological base for the subsequent evolution of the different dental morphologies used today by mammals (Davis, 2011; Price et al., 2012).

### 2.1.1 Bite forces

The mechanical loads produced during chewing are determined by the animal's bite force. In some mammals, these forces can overcome the fracture tolerance that arise during chewing and are typically characterized by maximum bite force (Wilmers and Bargmann, 2020). In larger mammals, chewing forces can easily overcome the fracture tolerance given by prism decussation (Maas and Dumont, 1999). Teeth functionality depends on the structure and integrity of the enamel (Lucas et al., 2008). It has been proved that enamel thickness and ultrastructure, as well as tooth geometry, are essential to determine the force that a tooth can withstand without fracturing (Maas and Dumont, 1999; Constantino et al., 2009).

The magnitude of bite force depends not only on the size and body mass, but also on the morphology of the skull and on the eating habits (the force required to process food is determined by the type of food: some foods break easily, while others are tougher) (Ellis et al., 2009; Kim et al., 2018). Some foods must be divided into small pieces for an efficient digestive process while others simply need to be small enough to be swallowed, then, the most effective tooth structure to process food varies with food mechanical properties (Evans and Pineda-Munoz, 2018). Mammalian teeth are adapted to interact with 3 types of food: plants and grasses (herbivores), meat (carnivores) and, insects and worms (insectivores), a diet that consists of the combination of these 3 types of food (omnivores) is present in several mammals (Berkovitz, 2013). As teeth have the particularity of being adapted to the functions that they must perform, they present highly variable structures (Hillson, 2005).

Bite force is highly correlated with body size, so it is necessary to separate these values to have a valid comparison of force between animals of different sizes, taking this into account, bite force quotient ($BFQ$) allows the comparison of bite forces in taxa of greatly differing body masses (Meers, 2002; Christiansen, 2007). Another advantage of using BFQ is being able to make more meaningful comparisons based on small data sets (Wroe, McHenry, and Thomason, 2005). When normalized for body mass, bite forces (i.e. $BFQ$) differ significantly between the various feeding categories (herbivores,

carnivores, insectivores, and omnivores). Mammals that feed on tough fibrous plant material and carnivores that feed on large prey have high $BFQ$, while the $BFQ$ is low among specialized insectivores. Omnivores and carnivores that eat small prey have more moderate $BFQ$ for their size (Wroe, McHenry, and Thomason, 2005; Christiansen and Wroe, 2007; Wroe and Milne, 2007).

## 2.2 The tooth

Mammalian tooth's quality is given by a complex dental morphology that differs according to the functions of each tooth and by an increasing complexity of the enamel structure (von Koenigswald and Pfretzschner, 1991). The tooth consists of a crown, which is exposed in the mouth, and one or more roots embedded in the maxillary bone (Hillson, 2005; Berkovitz and Shellis, 2018b) (Fig. 2.1). Each tooth is made up of several tissues: 1) a hard, highly mineralized, inert acellular tissue called enamel, 2) a less mineralized, more resistant and vital tissue, called dentin, which serves as a substrate for enamel and, 3) pulp, a soft connective tissue that in turn is the substrate for dentin.. In mammals, teeth are attached to the jaw by connective tissues that support them (cementum, periodontal ligament, and alveolar bone), which provide the flexibility necessary to withstand the forces exerted by chewing (Nanci, 2017; Berkovitz and Shellis, 2018b).

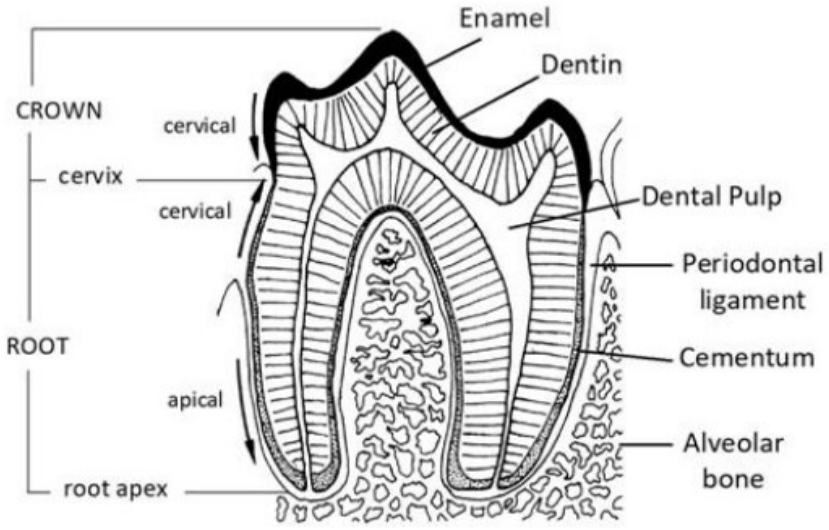


**Figure 2.1:** Schematic of a tooth (Berkovitz and Shellis, 2018b)

Teeth have important functions such as chewing (and speech in the case of humans), but they also serve as attack and defense weapons. Teeth must remain firmly attached to the jaw bones to fulfill these functions (Nanci, 2017). Some vertebrate species replace their dentition several times throughout their life span (polyphyodont). However, humans and most mammals only develop two sets of teeth: deciduous and permanent teeth (diphyodont) (Giacaman, Perez, and Carrera, 2016). In addition, enamel does not have living cells, therefore it is not remodeled nor is it possible to recover the tissue when it fractures or wears out (Teaford, 2007; Yilmaz, Schneider, and Swain, 2015).

### 2.2.1 Tooth morphology

Mammalian dentition is made up of repeating functional units (teeth) that are arranged along a curvilinear axis (hemimandibles). Most mammals have heterodont dentition, that is, different types of teeth can be differentiated in the dental arch: the anterior teeth (incisors and canines) and the posterior (or cheek) teeth (premolars and molars). The number and the arrangement of each of these types of teeth (that is, the dental formula) and its exact morphology depend mainly on the feeding pattern of these animals (Zhao, Weiss, and Stock, 2000; Hillson, 2005).

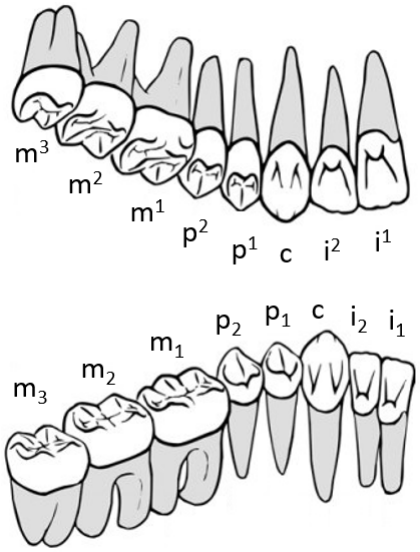


**Figure 2.2:** Schematic of human upper and lower permanent dentition: incisors (i), canines (c), premolars (p), and molars (m). -Superscript numbers denote upper teeth and subscript numbers denote lower teeth- (Hillson, 2005)

Each type of tooth has a particular shape and function (van Casteren and Crofts, 2019). The incisors, due to its triangular shape, function as instruments for biting and cutting food. The canines, which are conical in shape and have a prominent cusp, function to pierce or tear food and also to kill and immobilize the prey. The premolars, due to their prominent cusps, usually have a puncturing and crushing role. Finally the molars, that have a wide masticatory surface, grind food during chewing (Fehrenbach and Popowics, 2015). The variations in the morphology of the posterior teeth are greater than in the anterior teeth, this variation degree is related with the different requirements for breaking down the food (Fig. 2.2)(Rensberger, 2000; Berkovitz and Shellis, 2018b).

## 2.3 Enamel

Tooth enamel is one of the hardest and most mineralized tissues in the body. Its composition (by weight) is: 96% inorganic material, 3% water, and 1% protein (Ramakrishnaiah et al., 2015; Nanci, 2017; Berkovitz, Holland, and Moxham, 2017; Mansoor et al., 2019). The inorganic enamel material is a crystalline calcium phosphate (hydroxyapatite) substituted with carbonate ions (Sakae, 2006; Giacaman, Perez, and Carrera, 2016). Enamel is found in the outermost layer of the crown of the tooth. Its main function is to protect the underlying dental tissues (dentin and pulp) from the mechanical forces produced during chewing and from the chemical environment present in the mouth (An et al., 2012; Yilmaz, Schneider, and Swain, 2015). Because of its exceptionally high mineral content, enamel is a brittle tissue (Nanci, 2017). Even though mammalian tooth enamel is a fragile material, it is capable of withstanding high bite forces imposed thousands of times a day during the chewing process (Chai et al., 2009b). Composition, mechanical properties and hierarchical ultrastructure allow the enamel to resist the mechanical forces applied during chewing (Popowics and Herring, 2006). The analysis of damage tolerance in dental enamel to the different types of foods present in the diet of mammals can be approached from 2 points of view: 1) Variations in enamel thickness and 2) variations in enamel ultrastructure (Teaford, 2007).

### 2.3.1 Enamel ultrastructure

To achieve fracture tolerance, enamel possesses a hierarchical ultrastructure (von Koenigswald and Clemens, 1992; Bechtle, Ang, and Schneider, 2010; Yilmaz, Schneider, and Swain, 2015; Beniash et al., 2019). The fundamental unit of enamel is a hydroxyapatite crystallite (level 0), these crystallites are grouped (level 1) to form the prisms ($\approx$ 5 µm diameter) and the interprismatic enamel, a thin layer ($\approx$ 0.5 µm) that surrounds each prism (level 2). The prisms are grouped to form the next hierarchical level (level 3): enamel types, which are defined according to prism orientation, radial enamel is formed by prisms that are parallel to each other and decussated enamel is formed by prisms that cross each other with different orientations. Finally, the "*Schmelzmuster*" (enamel pattern; level 4), defines the three-dimensional distribution of the different enamel types in a tooth (Fig. 2.3) (Maas and Dumont, 1999; Yilmaz, Schneider, and Swain, 2015).

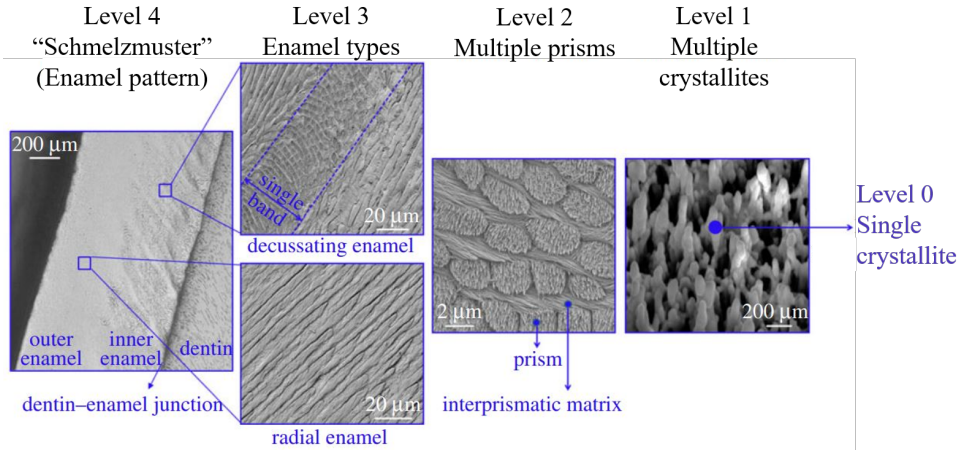


**Figure 2.3:** Overview of the hierarchical organization in bovine enamel (Yilmaz, Schneider, and Swain, 2015)

Mammalian enamel ultrastructure has been evaluated using polarization microscopy, X-ray diffraction, electron microscopy, electron diffraction, and so forth (Lynch et al., 2010; Bergqvist and von Koenigswald, 2017; Yilmaz, Koldehoff, and Schneider, 2018; Zhang et al., 2020b; Koldehoff, Swain, and Schneider, 2020).

#### 2.3.1.1 Level 1 - Crystallites

Enamel apatite crystallites (30 nm thick and 70 nm wide) are very long and are not all parallel to the prism long axis (Berkovitz, Holland, and Moxham, 2017). The shape of the crystallite may be different between species and may also become irregular as the size of the crystallite increases during enamel maturation (Maas and Dumont, 1999). The crystallites within the prisms have two main orientations: in the central region of the prism (head), the crystallites are oriented along the prism axis (Fig. 2.4a), while towards the tail of the prism, the crystals are gradually tilted, forming an angle about 60° with respect to the prism axis (Fig. 2.4b) (Sakae et al., 2011; Berkovitz, Holland, and Moxham, 2017).

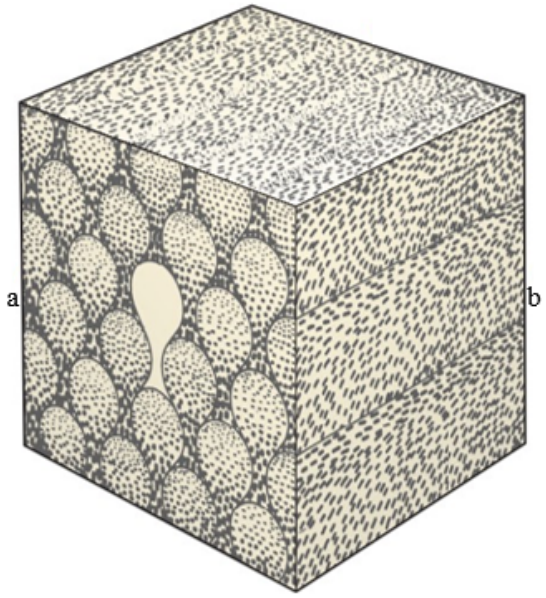


**Figure 2.4:** Schematic representation of crystallite orientation. a) cross-sectional view; b) lateral surface (Berkovitz, Holland, and Moxham, 2017)

#### 2.3.1.2 Level 2 - Prisms

Enamel prisms are rod-shaped (cylindrical) beams of crystallites. The long axis of a prism extends from the DEJ to the outer surface of the tooth (Shore et al., 1995). Crystallites that are outside the prisms are called interprismatic enamel. The difference between prisms and interprismatic enamel is given by the orientation of their crystallites and not by their composition (Maas and Dumont, 1999). The

edges of the prisms are produced by a change in the orientation between the prismatic and interprismatic crystallites (Shore et al., 1995). In these places, there is an accumulation of water and proteins, which generates a new structure called prism sheaths (Maas and Dumont, 1999).

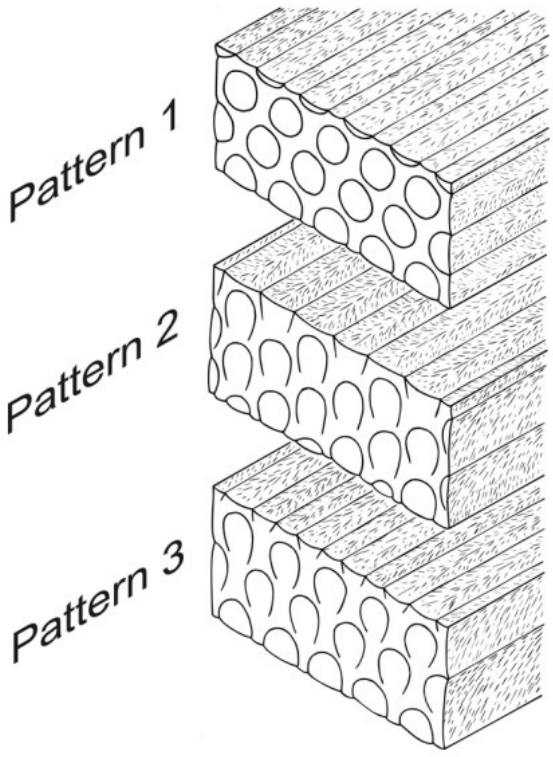


**Figure 2.5:** Isometric views of the prism patterns present in mammalian enamel: Prisms are aligned in staggered rows in patterns I and III and in parallel shapes in pattern II (Hillson, 2005)

In a cross-section, the prisms can have one of three patterns (Fig. 2.5). In pattern I, the prisms have full edges and there is a clear distinction between prisms and interprismatic enamel. In pattern II and III enamel, the edge of the prism is not closed, i.e. the interprismatic enamel anastomoses to the prisms, and there is a gradual change in the orientation between the intraprismatic and interprismatic crystals in the cervical region of the prisms (Yilmaz, Schneider, and Swain, 2015). The prisms of pattern I enamel have a circular shape, while in patterns II and III prisms are key-hole (Maas and Dumont, 1999; Hillson, 2005). Prisms in pattern I and II are aligned in parallel rows, and in pattern III prisms are arranged in staggered rows such that the tail of a prism is between two heads in the next row, giving a key-hole

appearance. These three types of patterns are present in the dentition of mammals but its distribution is variable (Hillson, 2005; Yilmaz, Schneider, and Swain, 2015; Berkovitz, Holland, and Moxham, 2017).

#### 2.3.1.3 Level 3 - Enamel types

The enamel units in which the prisms have similar orientations are defined as enamel types. To analyze and describe the three-dimensional orientation of the prisms, the DEJ serves as a practical reference plane (von Koenigswald and Clemens, 1992). The two most common enamel types are radial enamel and decussating enamel. In radial enamel, all prisms are approximately parallel to each other as they extend from DEJ to the surface. On the other hand, in decussating enamel, the prisms are organized in layers or alternate groups that extend from the DEJ towards the surface in different orientations (Maas and Dumont, 1999) (Fig. 2.6).

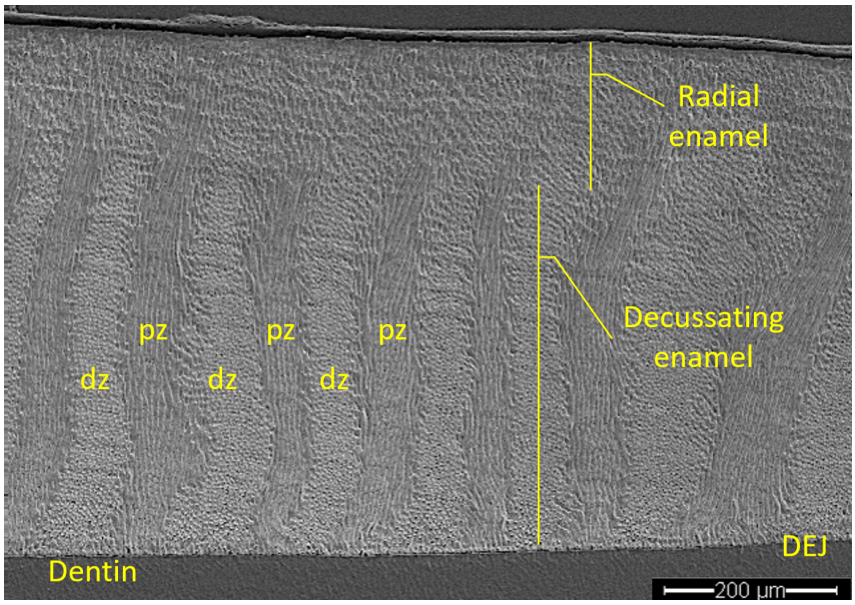


**Figure 2.6:** Longitudinal section of lion (*Panthera leo*) molar enamel (*dz* =diazones, *pz* =parazones)

Enamel decussation produces the optical phenomenon called Hunter-Schreger bands (HSBs), which are the result of the different refractive properties of the prisms with different orientations in the adjacent layers (Fig. 2.7) (Lucas, 2004). HSBs are seen more clearly in longitudinal sections and are found in the two inner thirds of the enamel (Wilmers and Bargmann, 2020). In any enamel section (longitudinal

or transverse), some prism bands will appear to be cut almost transversely (diazones) while neighboring bands will appear to be cut more longitudinally (parazones) (Shore et al., 1995).

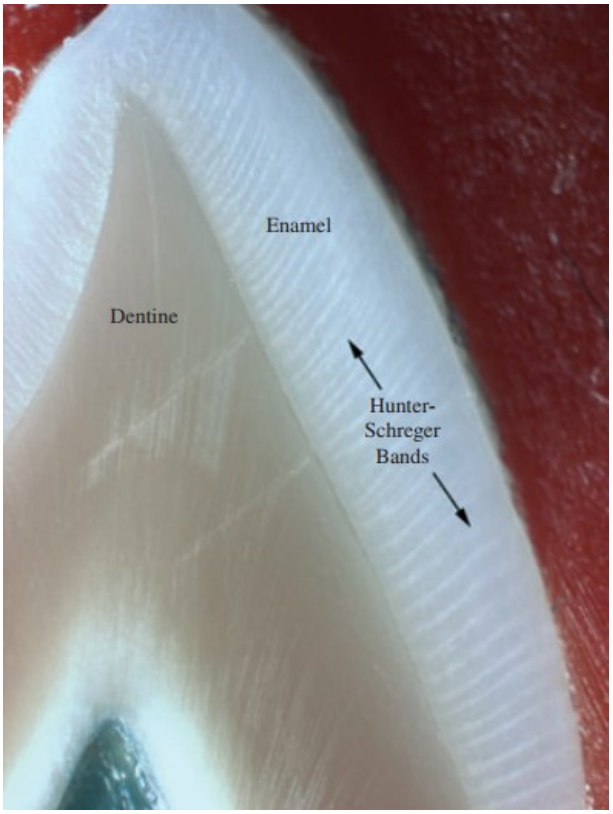


**Figure 2.7:** The appearance of Hunter-Schreger Bands viewed using reflected light (Lynch et al., 2010)

#### 2.3.1.4 Level 4 - Schmelzmuster

Enamel pattern describes the spatial distribution of different enamel types in a tooth (Yilmaz, Schneider, and Swain, 2015). In most mammals, the enamel region near the DEJ (inner enamel) is composed of decussating enamel and the enamel of the dental surface (outer enamel) is radial enamel. The change in the types of enamel produces a slight change in the composition since the protein content of the enamel increases from the outer region to the inner region (Yilmaz, Schneider, and Swain, 2015). The *Schmelzmuster* is different between mammals. These differences may be important in taxonomic

terms, but their main contribution is related to dental function and possibly with animal feeding patterns (Berkovitz and Shellis, 2018c).

### 2.3.2 Role of decussation

Studies on the tooth fracture resistance seem to indicate that the mechanism to prevent damage is to contain the defects rather than avoid them (Chai et al., 2009b). Although enamel high mineralization is a factor that influences on its mechanical properties, enamel's response to stress is modulated by its ultrastructure (Maas and Dumont, 1999). Enamel ultrastructure was recognized as a fundamental factor in the dental function and therefore in mammalian diet in the 80s and 90s (Rensberger and von Koenigswald, 1980; von Koenigswald and Pfretzschner, 1991; Stefen and Rensberger, 1999). It is known that enamel ultrastructure has adapted to the stresses generated during mastication (Constantino et al., 2009). Enamel prism decussation increases the fracture tolerance as the bite forces increase (Rensberger, 2000).

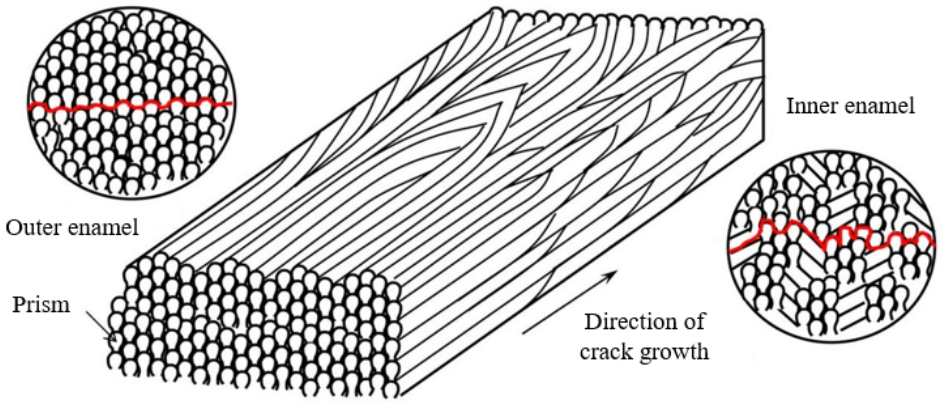


**Figure 2.8:** Schematic diagram of prism orientation in the outer and the inner enamel. Prism curving occurs in the inner enamel resulting in decussation (Bajaj and Arola, 2009a)

The general function of decussation bands is to serve as an important crack stop mechanism, mainly because cracks most commonly occur along the edges of the prism and less frequently across the prisms (von Koenigswald, Holbrook, and Rose, 2011; Berkovitz and Shellis, 2018c). The interface between the outer radial enamel and the inner decussating enamel is a defense mechanism against crack growth.

Inner enamel, the region where the highest degree of decussation occurs, behaves differently than outer enamel. Inner enamel has a messy appearance, which gives it greater resistance to loads and therefore greater protection to the DEJ (Lucas, 2004; Bajaj and Arola, 2009a) (Fig. 2.8). In conclusion, it is easy to create fractures within the enamel, but prism decussation makes it difficult to drive these fractures to failure (Chai et al., 2009a).

### 2.3.3 Enamel characterization

#### 2.3.3.1 Mechanical properties

Measurement of enamel mechanical properties has allowed its characterization and has served to develop restorative materials with similar mechanical properties (An et al., 2012). Enamel is an anisotropic material and its particular mechanical properties depend upon the location and are determined by its hierarchical structure and chemical composition (Cuy et al., 2002; Park et al., 2008; Cheng et al., 2010; He et al., 2013; Zhang et al., 2014).

The most commonly evaluated mechanical properties in enamel are elastic modulus, hardness, and fracture behavior (Cuy et al., 2002; Park et al., 2008; He, 2008; He and Swain, 2009; Zhang et al., 2014; Mansoor et al., 2019). The development of advanced measurement methods has allowed micro and macroscopic tests to be carried out, thereby measuring the mechanical properties on the nanometric scale and in a direction parallel and perpendicular to the prisms (Habelitz et al., 2001; Cuy et al., 2002; He and Swain, 2009).

Hardness and elastic modulus values in human enamel vary from 3 to 6 $GPa$ and from 55 to 130 $GPa$ respectively, both values increase with the distance from the DEJ and with age. Furthermore, hardness and elastic modulus values are related to enamel prisms orientation (Cuy et al., 2002; Park et al., 2008; He and Swain, 2009; Zhang et al., 2014; Mansoor et al., 2019).

Enamel fracture properties have been evaluated using inset compact tension specimens, flexural test (three and four-point bend test), and the indentation fracture toughness approach, among others (Bajaj and Arola, 2009b; Hayashi-Sakai et al., 2012; Yahyazadehfar, Bajaj, and Arola, 2013; Hájková, Jíra,

and Řehounek, 2018). The stress intensity factor $K_{IC}$ as fracture toughness index has been widely used (Bajaj and Arola, 2009b; Yahyazadehfar, Bajaj, and Arola, 2013; Yahyazadehfar and Arola, 2015). However, the use of the indentation fracture toughness $K_C$ has increased (Padmanabhan et al., 2010; Hayashi-Sakai et al., 2012; Hájková, Jíra, and Řehounek, 2018). Using a fracture mechanics method, fracture toughness values of $0.67 \pm 0.12$ and $1.13 \pm 3.93\ MPa \cdot m^{0.5}$ have been reported for external and internal enamel respectively (Zhang et al., 2014).

#### 2.3.3.2 Chemical properties

Mammalian enamel chemical composition, in deciduous and permanent teeth, has been analyzed by means of energy dispersive X-ray spectroscopy (EDS), X-ray diffraction (XRD), Fourier Transform infrared spectroscopy (FT-IR), Raman microspectroscopy, and so forth (He et al., 2011; Xu et al., 2012; Biswas et al., 2012; He et al., 2013; Ghadimi et al., 2014; Zamudio-Ortega et al., 2014; Mansoor et al., 2019; Arango-Santander et al., 2020; Zhang et al., 2020a).

EDS tests showed that in a healthy tooth, the amount of calcium, phosphorus, magnesium and sodium in tooth enamel increases with age, while the amount of carbon, nitrogen and oxygen decreases with age, besides an increase in the amount of calcium and phosphorus from the DEJ towards the outer surface of the enamel was observed (He et al., 2011; Biswas et al., 2012; Mansoor et al., 2019). XRD analysis have allowed to establish the crystallographic dimensions of the hydroxyapatite present in the dental enamel of humans and other mammals, both in healthy and diseased teeth, in addition, it has shown that in healthy teeth, the crystallinity of enamel hydroxyapatite is greater than the crystallinity of dentin hydroxyapatite (Hanlie, Liyun, and Tao, 2006; Eimar et al., 2011). Changes in chemical composition caused by pathologies such as enamel hypomaturation or hypomineralization have been identified using FT-IR analysis (Lopes et al., 2018).

Raman microspectroscopy is non invasive, non destructive, it allows obtaining simple and easy to reproduce results, and the analysis of the samples at the micrometric level (Carden and Morris, 2000; Leroy et al., 2002; Ramakrishnaiah et al., 2015). Raman microspectroscopy allows a complete molecular analysis of mineralized dental tissues and has been frequently used to analyze tooth composition, both

in healthy samples and in those that have undergone treatments or have cavities (Carden and Morris, 2000; Zavala-Alonso et al., 2012; Akkus, Karasik, and Roperto, 2017). The analysis of dental enamel by means of Raman microspectroscopy is focused on the $\nu_1$ phosphate $(960\ cm^{-1})$ and B-type carbonate $(1070\ cm^{-1})$ peaks. Changes in the area and position of these peaks are related to changes in phosphate and carbonate content respectively (Leroy et al., 2002; Zavala-Alonso et al., 2012; Xu et al., 2012).

Finally, the combination of mechanical and chemical analysis has allowed a better characterization of dental enamel in terms of the relationship between its mechanical properties and its composition, for example, it was established that hardness and modulus of elasticity increase in enamel as a consequence of enamel mineralization (Baldassarri, Margolis, and Beniash, 2008; Eimar, 2011; Xu et al., 2012; Akkus, Karasik, and Roperto, 2017; Mansoor et al., 2019).

#### 2.3.3.3 Mammalian enamel decussation

Enamel ultrastructure of the both extinct and extant mammals has been studied over the years due to the ease of extracting information from this tissue given by its long degradation time and structural nature (Boyde, 1964; Boyde, 1997; Stefen, 1999a; Stefen, 1999b; Rensberger and Wang, 2005; Wiszniowska et al., 2010; von Koenigswald, Holbrook, and Rose, 2011; Lucas et al., 2016; Yilmaz, Koldehoff, and Schneider, 2018; Arango-Santander et al., 2020; Zhang et al., 2020a).

In terms of the hierarchical structure of enamel, measurements of the components of the different levels have been made in various animals (Daculsi and Kerebel, 1978; von Koenigswald, 2004; Rensberger and Stefen, 2006; Beniash et al., 2019). In general it has been found that:

- The size of the hydroxyapatite crystals does not vary between the species (Wilmers and Bargmann, 2020).
- The cross section of the prisms is generally circular, however, polygonal shapes have been found, for example, in the enamel of canids and felids (Stefen, 2001; Rensberger and Wang, 2005; Wiszniowska et al., 2010).

- Cross-sectional shapes vary from circular and ellipsoidal patterns to key-hole shaped, and different prism shapes can be found within the enamel covering of an individual tooth (von Koenigswald, 1997; Stefen, 1999a; von Koenigswald, 2009; von Koenigswald, Kalthoff, and Semprebon, 2010; Tabuce et al., 2017; Wilmers and Bargmann, 2020).

- In some species there is only one enamel pattern, however in others, although there is a predominant pattern, there may be a mixture of patterns (Berkovitz and Shellis, 2018c).

- Prism decussation is more developed in mammals that exert high masticatory forces and large occlusal efforts, in turn, is less evident in animals whose diet is based on soft foods. Also, prism decussation is present in animals that have large teeth (molars $6\ mm$ wide or more) (Rensberger, 2000).

- In both radial and decussating enamel, prisms generally deviate from their initial course and exhibit at least one type of curvature. Besides, in some types of radial enamel, the prisms curve in the cervical direction. Besides, in decussating enamel, HSBs may be several prisms wide $(20 - 50)$, named *multiserial* enamel, but there is also *pauciserial* $(4 - 5$ prisms) and *uniserial* enamel $(1$ prism) (Berkovitz and Shellis, 2018c)

- At a higher level, *Schmelzmuster* may show variations between the teeth within a dentition and between different species of mammals. These variations may be important in taxonomic terms, although they are mainly due to differences in the functions of the teeth of each species (Berkovitz and Shellis, 2018c).

Despite what is known about the ultrastructure, as well as about the mechanical and chemical properties of mammalian enamel, this information has not yet been related to bite forces or feeding patterns. Knowing this relationship could lead to a better understanding of the importance of enamel ultrastructure with respect to the stresses to which enamel is subjected during chewing process.

# 3 Materials and methods

The main objective of this study was to characterize the mechanical, chemical and ultrastructural properties of mammalian enamel and their variations in terms of the distance to the DEJ and between the different regions of the tooth. To achieve this goal, nanoindentation tests, Raman microspectroscopy, and SEM imaging were used and performed on enamel samples from selected mammals.

## 3.1 Sample collection and preparation

The dental enamel of 6 different mammalian specimens was analyzed. One tooth from each animal was analyzed in order to characterize dental enamel.

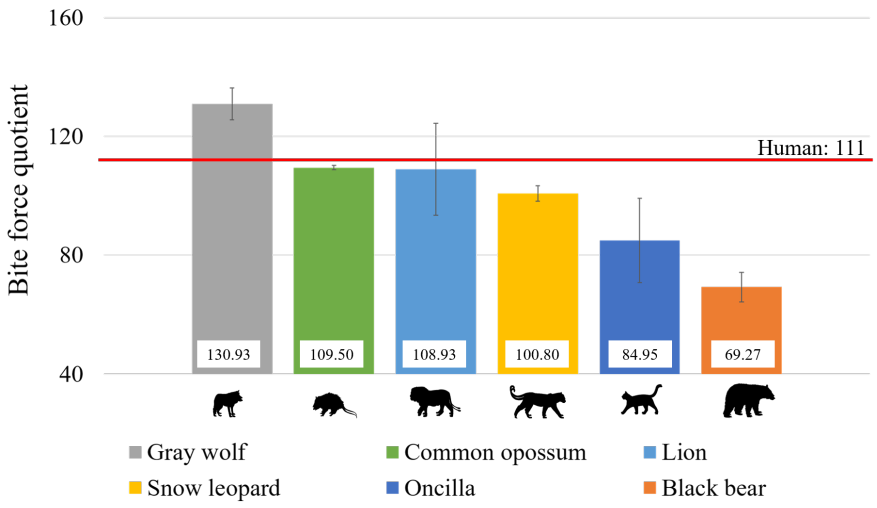


**Figure 3.1:** Average bite force quotient ($BFQ$) for the evaluated specimens (human BFQ is used for comparison purposes only (Hite et al., 2019))

The following animals were chosen according to their $BFQ$ (Wroe, McHenry, and Thomason, 2005; Wroe and Milne, 2007; Christiansen and Wroe, 2007; Wilson et al., 2016): 1) *Canis lupus* Linnaeus, 1758 (Gray wolf), 2) *Didelphis marsupialis* Linnaeus, 1758 (Common opossum), 3) *Panthera*

*leo* Linnaeus, 1758, (Lion), 4) *Panthera uncia* Schreber, 1775 (Snow leopard), 5) *Leopardus tigrinus* Schreber, 1775 (Oncilla), and 6) *Ursus americanus* Pallas, 1780 (Black bear)

Figure 3.1 shows the $BFQ$ values of the animals analyzed in descending order. Samples 1, 3, 4 and 6 were donated by Burke Museum (Burke Museum, 2020) while samples 2 and 5 were donated by Universidad EAFIT's Collection of Macroorganisms and Microorganisms. Samples from Burke Museum belong to specimens that have been storaged for several years, while samples donated by Universidad EAFIT were fresh samples. All the analyzed teeth were molars. The taxonomic classification of the evaluated specimens is shown in table 3.1 (Wilson and Reeder, 2005) and pictures of the specimens that were chosen to analyze tooth enamel are shown in figure 3.2.

**Table 3.1:** Taxonomic classification of the analyzed specimens (Wilson and Reeder, 2005)

| **Class** | Mammalia | | | | | |
|---|---|---|---|---|---|---|
| **Order** | Carnivora | | | | | Didelphimorphia |
| **Sub-Order** | Feliformia | | | Caniformia | | – |
| **Family** | Felidae | | | Canidae | Ursidae | Didelphidae |
| **Genus** | Panthera | | Leopardus | Canis | Ursus | Didelphis |
| **Specimens** | *P. leo* | *P. uncia* | *L. tigrinus* | *C. lupus* | *U. americanus* | *D. marsupialis* |
| **Common name** | Lion | Snow leopard | Oncilla | Gray wolf | Black bear | Common opossum |

Each tooth was sectioned along the longitudinal axis using diamond abrasive cutting equipment with continuous water coolant. Longitudinal cuts were made in order to make measurements longitudinally to the main axis of the prisms, from the external surface of the tooth until the DEJ was reached (Fig. 3.3).

Tooth sections were mounted in cold-cured epoxy resin and the exposed enamel in the resin mount was polished in order to reduce surface roughness and obtain better results in the measurement of the properties of interest in this research. Polishing was performed using silicon carbide abrasive paper from $\#400$ – $\#1200$ mesh and diamond particle suspensions to $0.05\ \mu m$. All samples were kept in


**Figure 3.2:** Images of the specimens that were chosen to analyze tooth enamel. a) Gray wolf, b) Common opossum, c) Lion, d) Snow leopard, e) Oncilla and f) Black bear. (The Smithsonian Institution, n.d.)

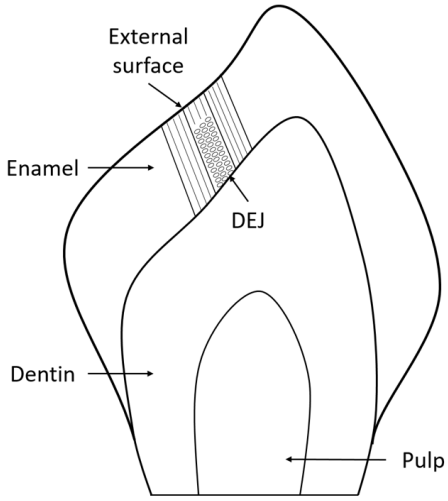


**Figure 3.3:** Longitudinal section of a tooth: Enamel, dentin, and pulp are shown, as well as the external surface and DEJ

Hank's Balanced Salt Solution (HBSS) at 2 $^{\circ}C$ between and during the tests to avoid tissue dehydration.

Measurements were made between 1 and 2 weeks after sample preparation.

## 3.2 Mechanical properties

Elastic modulus $(E)$ and hardness $(H)$ were measured by nanoindentation (Hysitron TI 980 Nanoindenter, Bruker, Massachusetts, US). Oliver and Pharr (1992) method was used to provide elastic modulus and hardness values. Both values were measured in three regions of the tooth (cervical, cuspal and intercuspal) and as a function of the distance to the DEJ in order to identify variations within the dental crown. Four measurements at six equidistant points between the DEJ and the external enamel were performed (Fig. 3.4).

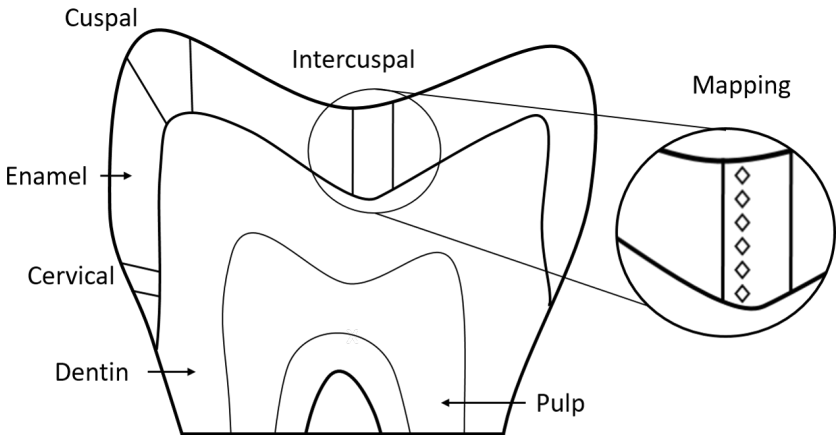


**Figure 3.4:** Schematic illustration of mechanical and chemical properties mapping. The diamonds are representative of the six equidistant points between the DEJ and the external enamel

## 3.3 Chemical properties

A Raman microspectrometer (inVia$^{TM}$, Renishaw, Illinois, US) was used to determine the chemical composition of mammalian enamel with scans performed over the spectral range of $400 - 1900\ cm^{-1}$. The analysis of dental enamel was done by measuring the $\nu_1$ phosphate $(960\ cm^{-1})$ and B-type carbonate $(1070\ cm^{-1})$ peaks. For phosphate peak, peak position $(PP)$, area, and full-widths at half-maximum $(PW)$ were obtained, while only area was obtained for B-type carbonate peak. Both areas were used to calculate the carbonate to phosphate ratio in order to evaluate carbonate substitution $(CO_3)$. Similar to

the procedure followed to estimate mechanical properties, a mapping was also performed from the DEJ to the external enamel in the three regions mentioned above (Fig. 3.4).

## 3.4 Enamel ultrastructure

A scanning electron microscope (Sirion XL30, Phillips, Amsterdam, NL) was used to analyze enamel ultrastructure. Prior to evaluation, each sample was etched with $35\ \%$ phosphoric acid for $20\ s$ and sputtered-coated with gold–palladium. Features of the ultrastructure were examined in secondary electron emission mode.

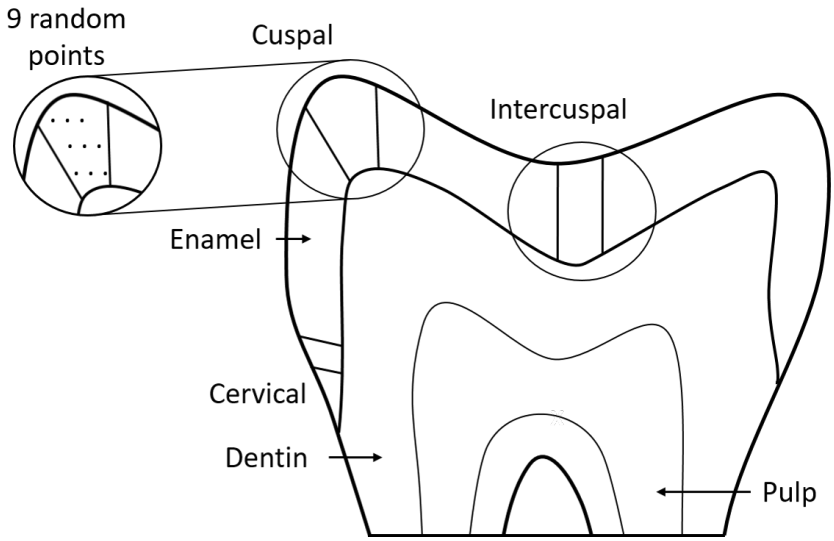


**Figure 3.5:** Schematic illustration of ultrastructue properties measurement

SEM images were obtained from different regions of the enamel and the following parameters were obtained using ImageJ® Software (National Institutes of Health, Bethesda, MD). Each of the ultrastructural properties was measured at 9 random points in each of the 3 regions of interest (Fig. 3.5). In all measurements, SEM images magnification was taken into account, but it is important to clarify that the degree of tooth wear was unknown, so it was assumed that the measured value is the real value for all the analyzed specimens.

### 3.4.1 Ultrastructure description

SEM images were used to make a description of the enamel ultrastructure in terms of prism shape, prism pattern and enamel type of each of the analyzed specimens.

### 3.4.2 Enamel thickness

Enamel thickness $(ET)$ was measured as a perpendicular line from the DEJ to the outer enamel surface (Fig. 3.6). Enamel thickness is an important morphological property since thicker enamel allows to increase resistance to high masticatory loads (Lucas et al., 2008; Constantino et al., 2009).

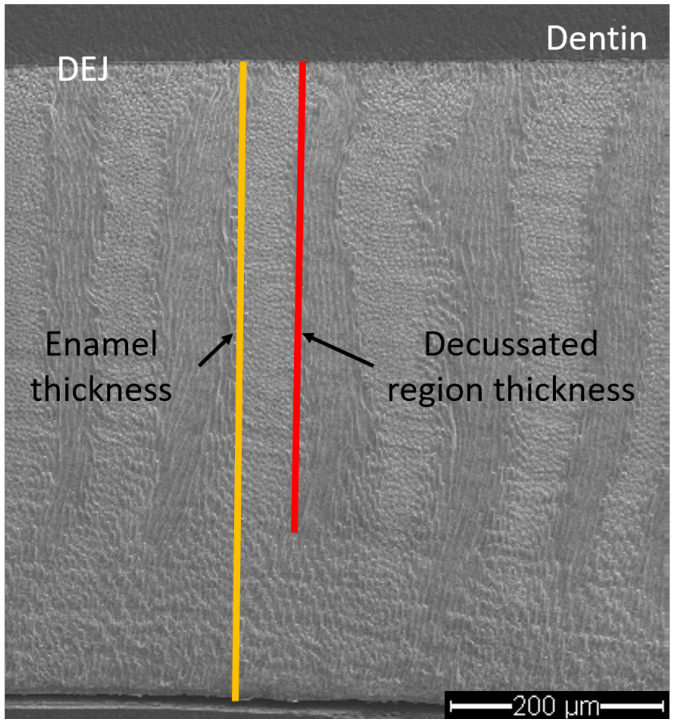


**Figure 3.6:** Measurement of enamel thickness ($ET$, yellow bar) and decussated region thickness ($DT$, red bar) on longitudinal section of Lion (*Panthera leo)* molar

### 3.4.3 Decussated thickness

Decussated thickness $(DT)$ is the thickness of the inner decussated region. It was measured by drawing a straight line, parallel to the decussation bands, from the DEJ to the point where the prism decussation ends, that is, to where the radial enamel begins (Fig. 3.6)

### 3.4.4 Decussated fraction

Decussated fraction $(DF)$ is defined as the fraction of enamel thickness that is composed of decussated rods ($DF = DT/ET$). Decussated fraction can vary from 0 to 1, if the decussated fraction is closer to 0 the decussation percentage is low, while a value closer to 1 means that the decussation percentage is high. A higher decussated fraction would be important in retarding crack extension (Yahyazadehfar, Bajaj, and Arola, 2013).

### 3.4.5 Decussated band thickness

Is given by the thickness of the decussated band in micrometers $(DBT\mu m)$ and was measured by a straight line perpendicular to the main axis of the prisms, which runs from boundary to boundary of each decussation band (Fig. 3.7).

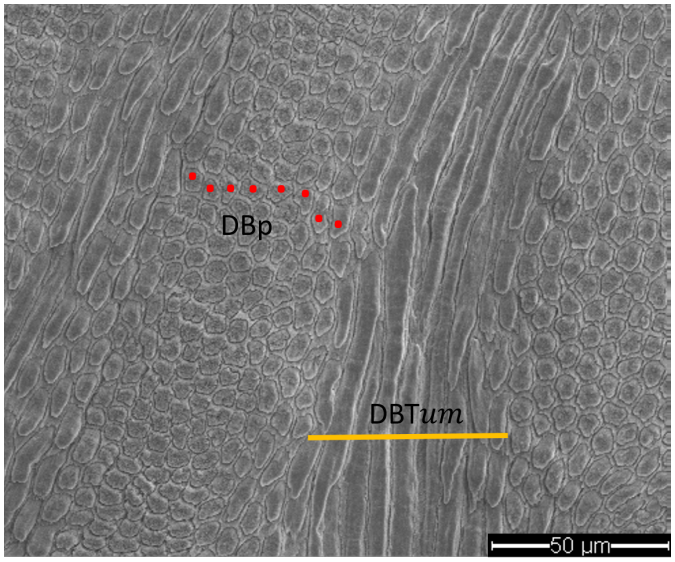


**Figure 3.7:** Decussated band thickness in micrometers ($DBT\mu m$, yellow line) and the number of prisms in the decussation band ($DBp$, red dots) measured on longitudinal section of Lion (*Panthera leo)* molar

### 3.4.6 Number of prisms in decussation band

The number of prisms in a decussated band could be an important factor in tooth fracture resistance since the wider the decussation band, the greater the path that the crack must follow to cause tooth

fracture. Also, more energy would be required to form new cracks as well as greater stresses for crack propagation, this would result in greater fracture resistance. The number of prisms in the decussation band $(DBp)$ (Fig. 3.7) was calculated in the diazones, counting the number of complete prisms that form a line, between the bands boundaries.

### 3.4.7 Prism diameter

Because prism shape varies between specimens, prism diameter $(D)$ was calculated as the diameter of the circumscribed circumference in the prisms in the diazones (Fig. 3.8).

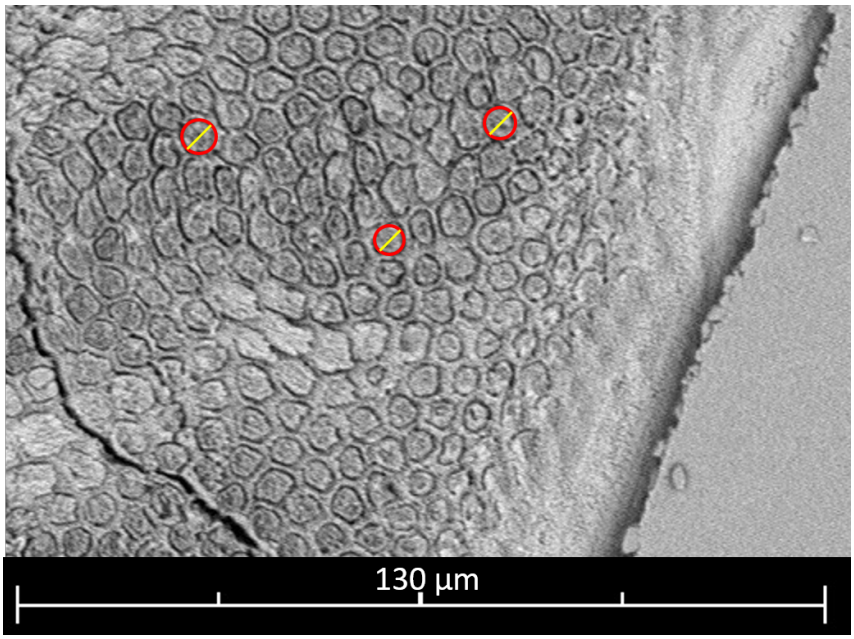


**Figure 3.8:** Prism diameter measurement on longitudinal section of Oncilla (*Leopardus tigrinus)* molar

### 3.4.8 Prism orientation

Assuming that the prisms in diazones have an approximately circular cross-section and that the block $ABCDEFG$ represents a thin parallel-sided slice of the enamel that has been cut in a pre-determined position and angle with respect to the prism (Fig. 3.9), prism orientation can be determined from the intersection of the prism with the surfaces ($ABCD$ and $EFGH$). Prism orientation $(Ang = \beta)$ is initially obtained from the projected length $(l_p)$ of the prism and the thickness of the thin section $(t)$

(Fig. 3.9a). Furthermore, assuming that the prism intersects both surfaces, $\beta$ can be calculated as $\beta = \sin^{-1}(b/a)$, where $2b$ is the diameter of the prism and $2a$ is the length of the mayor axis of the ellipse (Fig. 3.9b) (Hull and Clyne, 1996).

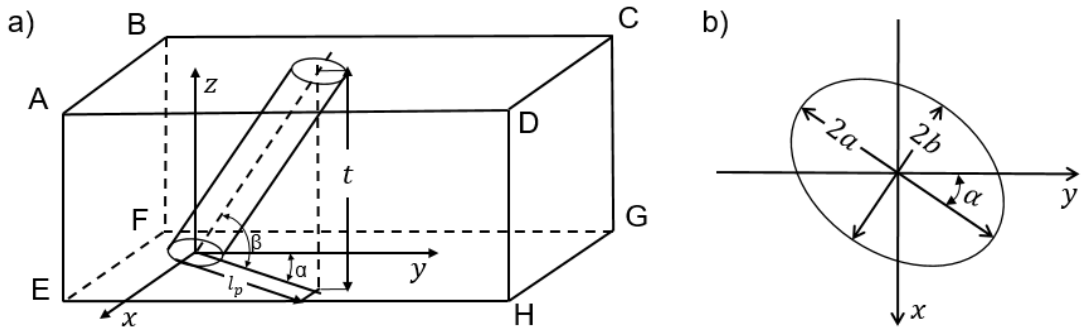


**Figure 3.9:** Determination of the prism orientation in a thin section (Adapted from Hull and Clyne Hull and Clyne (1996))

## 3.5 Linear correlation

Pearson correlation coefficient (Kirch, 2008) was calculated between the properties to determine the existence of relationships between mechanical, chemical and ultrastructural properties with $BFQ$.

## 3.6 Statistical analysis

The differences in the results obtained for the measured variables were evaluated using a one-way ANOVA with a significance of $0.05$, and when necessary, a Tukey post-hoc analysis was used to determine differences between the groups (Animal or Region). The software used for the statistical analysis was Minitab®.

# 4 Results

Nanoindentation and Raman microspectroscopy experiments were carried out on three regions of dental enamel, furthermore, these values were mapped from the DEJ to the outer enamel surface. In addition, SEM images were obtained to characterize enamel ultrastructure and its variations. This chapter presents the results of mechanical, chemical and ultrastructural properties and the comparisons of the values between the evaluated specimens. Unless otherwise specified, all results (in figures and in text) are presented in descending order of the $BFQ$ value (see Fig. 3.1).

## 4.1 Mechanical properties

### 4.1.1 Elastic Modulus

Average elastic modulus ($E$) for the evaluated specimens is shown in table 4.1 and figure 4.1, while elastic modulus in cervical, cuspal and intercuspal regions for the evaluated specimens is shown figure 4.2.

**Table 4.1:** Average elastic modulus and hardness for the evaluated specimens

| **Animal** | **Elastic modulus** ($GPa$) | **Hardness** ($GPa$) |
|---|---|---|
| Gray wolf (Gw) | $56.24 \pm 6.37$ | $2.78 \pm 0.71$ |
| Common opossum (Co) | $75.79 \pm 4.65$ | $3.52 \pm 0.30$ |
| Lion (L) | $76.74 \pm 0.68$ | $3.40 \pm 0.72$ |
| Snow leopard (Sl) | $78.11 \pm 0.95$ | $3.32 \pm 0.32$ |
| Oncilla (O) | $74.13 \pm 8.97$ | $2.70 \pm 0.71$ |
| Black bear (Bb) | $85.58 \pm 3.45$ | $4.61 \pm 0.17$ |

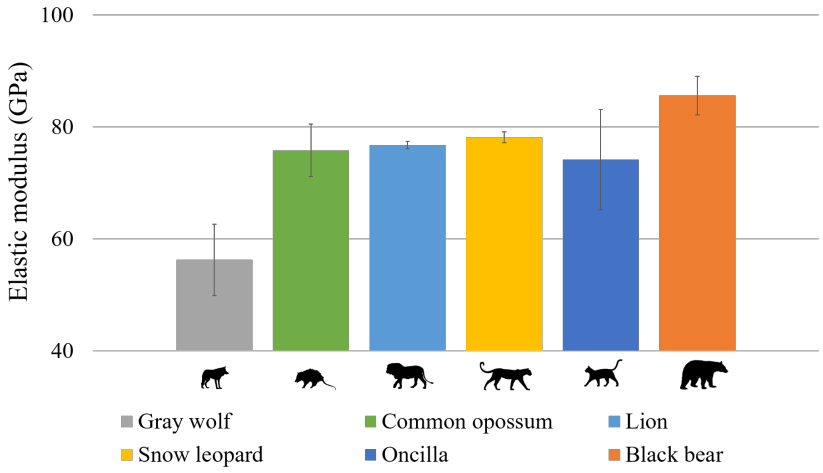


**Figure 4.1:** Average elastic modulus ($E$) the evaluated specimens

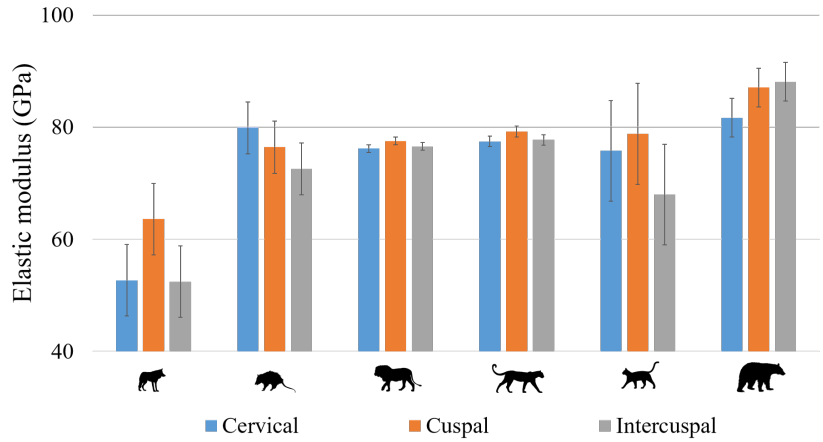


**Figure 4.2:** Elastic modulus ($E$) in cervical, cuspal and intercuspal regions for the evaluated specimens

Confidence interval plots for elastic modulus when comparing between animals and between regions is shown in figure 4.3. When elastic modulus is compared between animals (Fig. 4.3a), the confidence interval for Gray wolf does not overlap with the confidence intervals of the other animals, which indicates that there is a significant difference in elastic modulus for Gray wolf with respect to the other animals ($p < 0.05$). On the other hand, when comparing elastic modulus between regions (Fig. 4.3b), the three confidence intervals (cervical, cuspal and intercuspal) overlap, which indicates that there are no significant differences in elastic modulus between regions ($p = 0.6591$). The statistical difference in

elastic modulus between Gray wolf and the other animals is shown in figure 4.4, in which none of the confidence intervals of Gray wolf contains zero (Gw-Co, $p = 0.0053$; Gw-L, $p = 0.0036$; Gw-Sl, $p = 0.0022$; Gw-O, $p = 0.0103$; Gw-Bb, $p = 0.0002$).

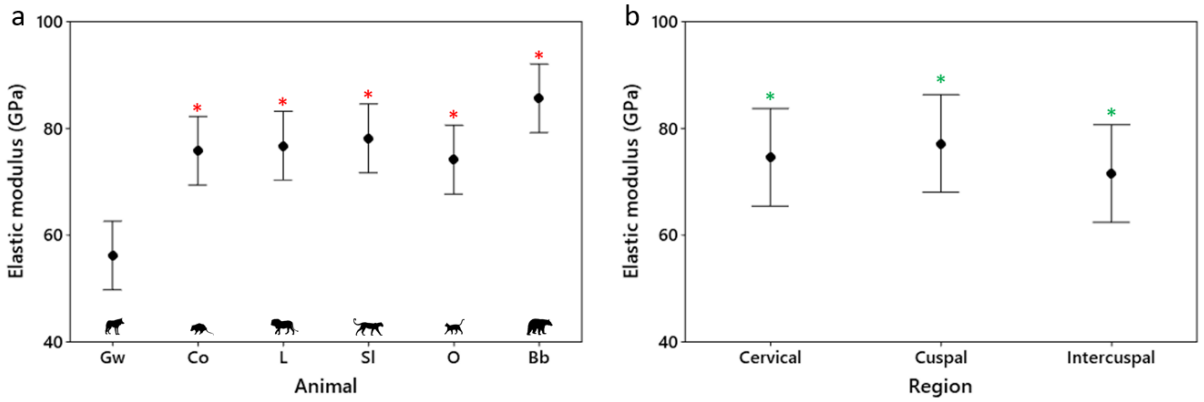


**Figure 4.3:** Tukey confidence intervals for elastic modulus ($E$). a) comparison between animals (average for all the regions); b) comparison between regions (average for all the animals). Intervals with the same marker do not show a statistically significant difference

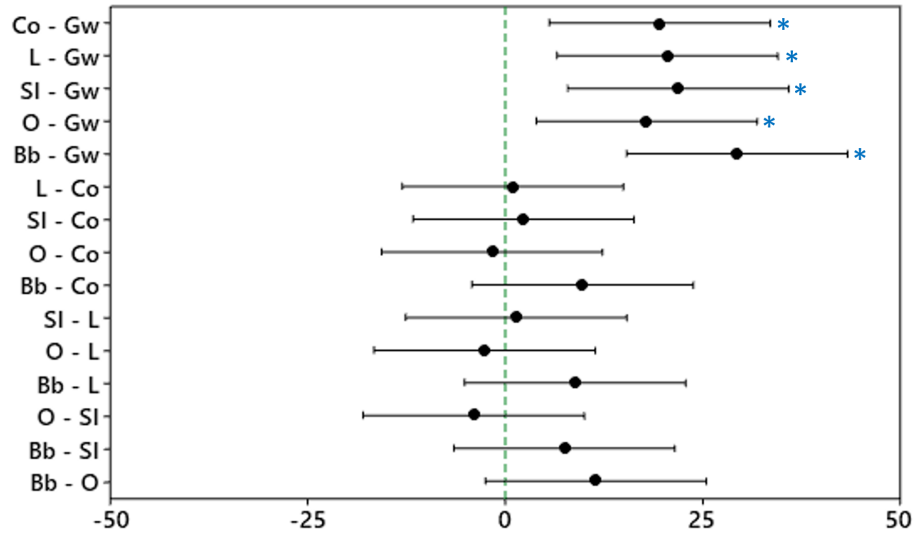


**Figure 4.4:** Tukey confidence intervals for elastic modulus ($E$) comparing the evaluated specimens. There is statistical difference in elastic modulus between the animals that share confidence intervals that do not contain zero (Blue asterisk)

Elastic modulus mapping was performed measuring $E$ as a function of the distance to the DEJ (Fig. 4.5). For all animals, a slight increase in elastic modulus is observed as the distance to the DEJ increases.

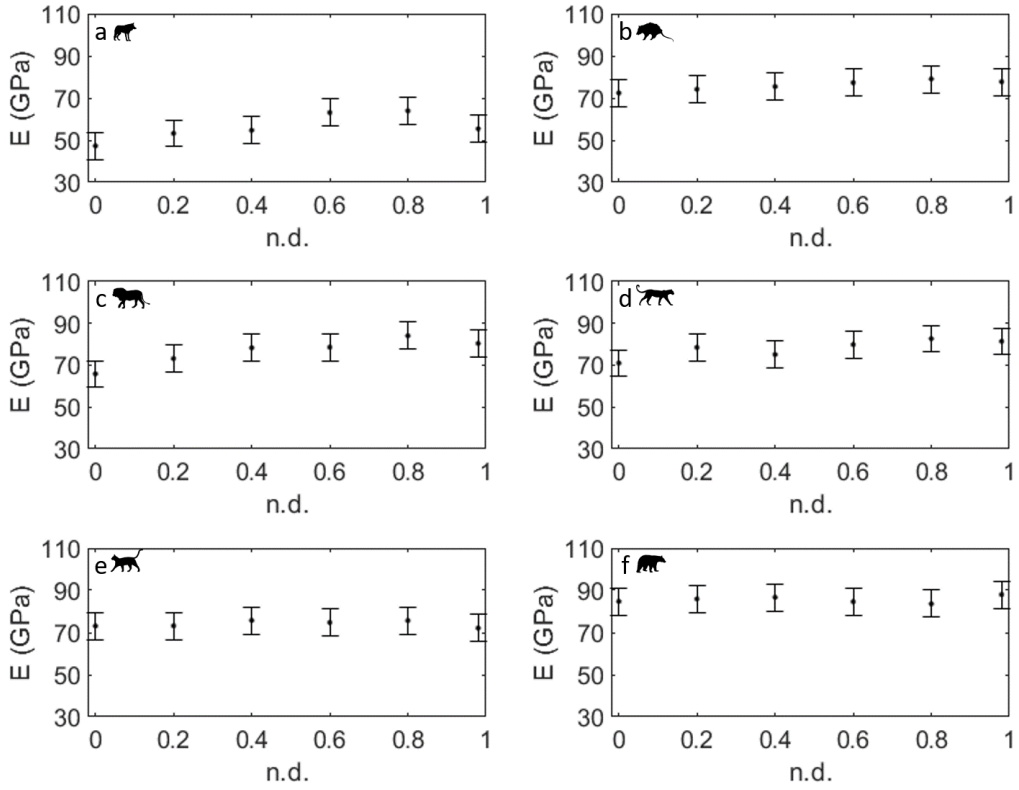


**Figure 4.5:** Elastic modulus mapping by animal. a) Gray wolf; b) Common opossum; c) Lion; d) Snow leopard; e) Oncilla; f) Black bear (*n.d.* = normalized distance, $0$ = DEJ, $1$ = outer enamel surface)

### 4.1.2 Hardness

Average hardness ($H$) for the evaluated specimens is shown in table 4.1 and figure 4.6, while hardness for all the evaluated specimens in cervical, cuspal and intercuspal regions is shown in figure 4.7. When comparing hardness between animals (Fig. 4.8a), Black bear confidence interval does not overlap with Gray wolf and Oncilla confidence intervals (i.e. there is a statistical difference ($p = 0.0113$) in hardness between Gray wolf and Black bear and between Oncilla and Black bear), but it overlaps with Common opossum, Lion and Snow leopard confidence intervals, this means that there is no statistical difference in hardness between Common opossum, Lion, Snow leopard and Black bear. It is also observed that there

are no statistical differences in hardness between Gray wolf, Common opossum, Lion, Snow Leopard and Oncilla. Furthermore, when comparing between regions (Fig. 4.8b) there are no significant differences in hardness as all the confidence intervals overlap ($p = 0.3186$). The statistical difference in hardness between Gray wolf and Black bear and between Oncilla and Black bear is shown in figure 4.9 in which intervals Gw-Bb and O-Bb intervals do not contain zero ($p = 0.0128$ and $p = 0.0094$ respectively).

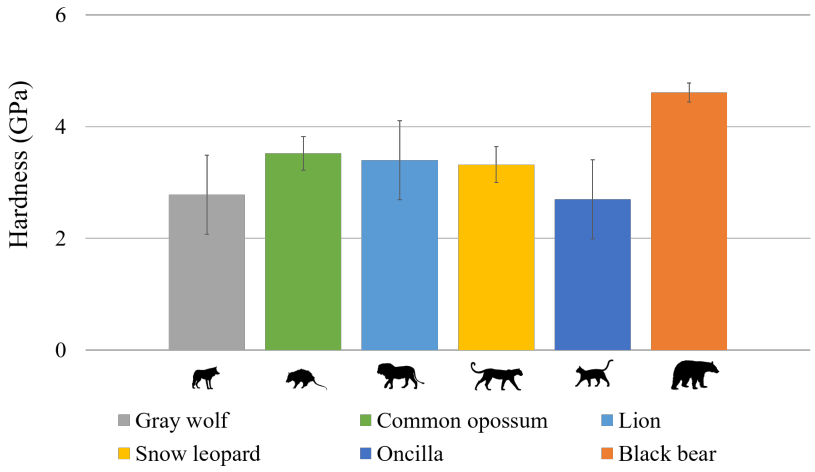


**Figure 4.6:** Average hardness ($H$) for the evaluated specimens

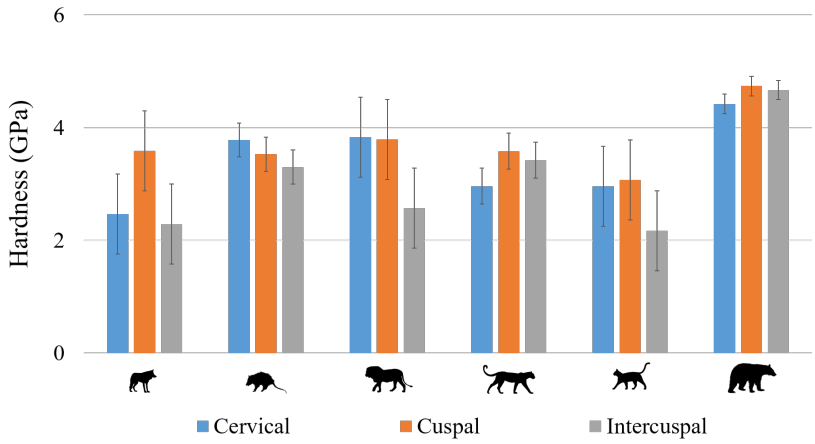


**Figure 4.7:** Hardness ($H$) in cervical, cuspal and intercuspal regions for the evaluated specimens

Hardness mapping (Fig. 4.10) shows a slight increase as the distance to the DEJ increases in all animals except in the Oncilla (Fig. 4.10e) in which a reduction in hardness is observed.

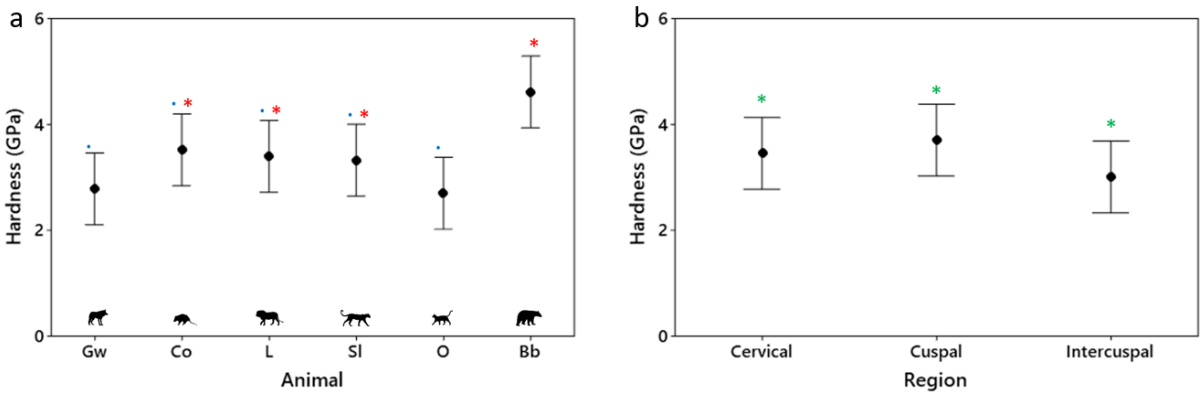


**Figure 4.8:** Tukey confidence intervals for hardness ($H$). a) comparison between animals (average for all the regions); b) comparison between regions (average for all the animals). Intervals with the same marker do not show a statistically significant difference

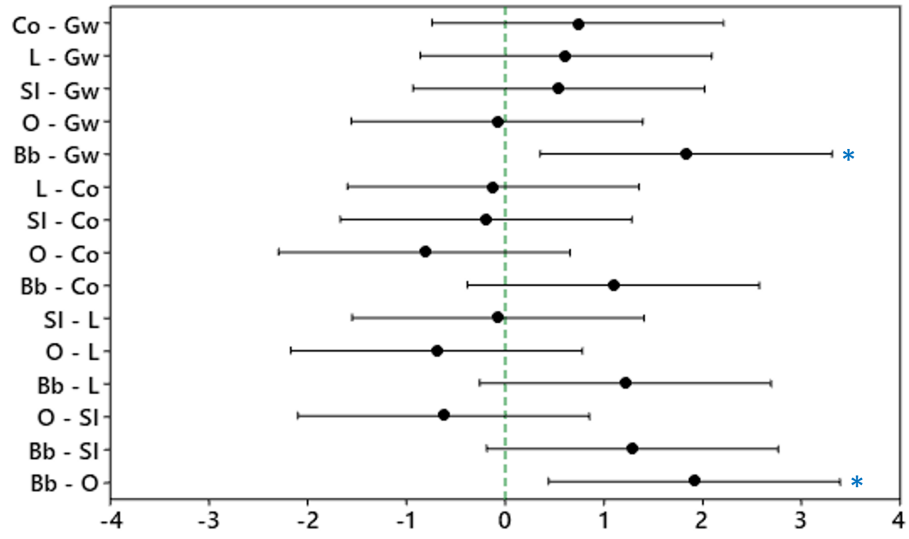


**Figure 4.9:** Tukey confidence intervals for hardness ($H$) comparing the evaluated specimens. There is statistical difference in hardness between the animals that share confidence intervals that do not contain zero (Blue asterisk)

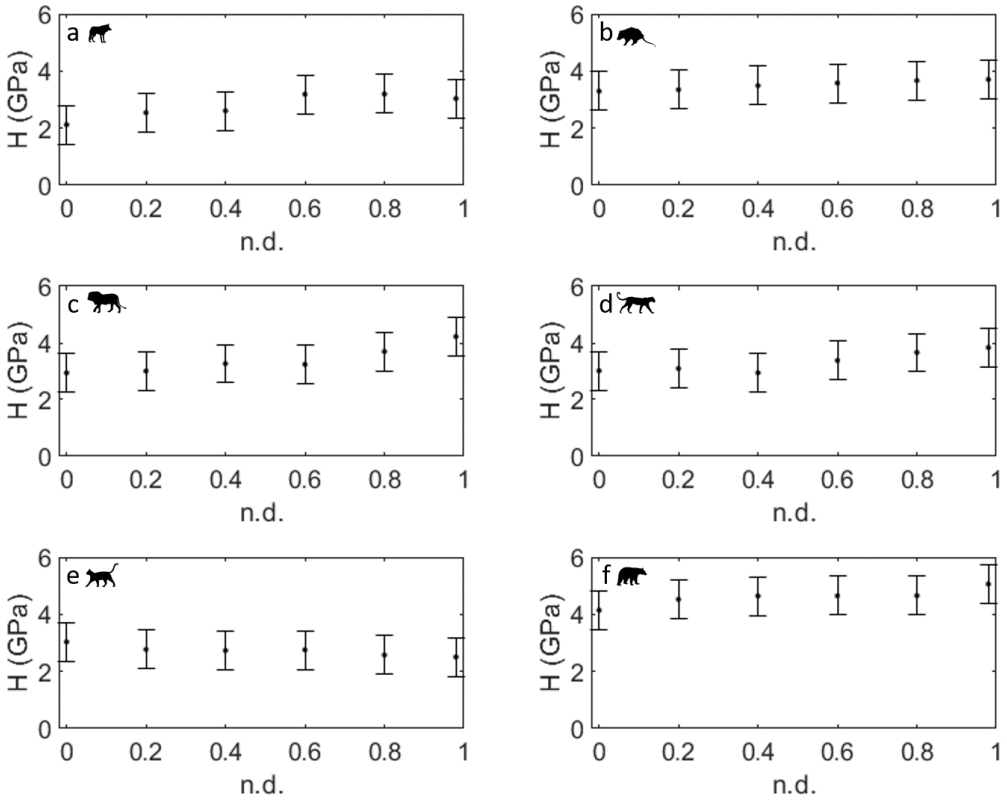


**Figure 4.10:** Hardness mapping by animal. a) Gray wolf, b) Common opossum, c) Lion, d) Snow leopard, e) Oncilla and f) Black bear (*n.d.* = normalized distance, $0 =$ DEJ, $1 =$ outer enamel surface)

## 4.2 Chemical properties

### 4.2.1 Phosphate peak position

Average phosphate peak position ($PP$) is shown in figure 4.11 and table 4.2, while figure 4.12 shows phosphate peak position in cervical, cuspal and intercuspal regions for the evaluated specimens. Figure 4.13 shows the confidence interval plot for phosphate peak position when comparing between animals and between regions. When phosphate peak position is compared between animals (Fig. 4.13a), there is no statistical difference between Gray wolf, Common opossum, Lion and Black bear, neither between Common opossum, Snow leopard and Black bear nor between Snow leopard and Oncilla. When comparing phosphate peak position between regions (Fig. 4.13b), there is no statistical difference because the three confidence intervals (cervical, cuspal and intercuspal) overlap ($p = 0.9593$). The statistical differences in phosphate peak position are shown in figure 4.14 in which intervals Gw-Sl ($p = 0.0002$), Gw-O ($p = 0.0128$), Co-Sl ($p = 0.0132$), L-Sl ($p = 0.0004$), L-O ($p = 0.0257$) and Sl-Bb ($p = 0.0008$) do not contain zero.

**Table 4.2:** Average phosphate peak position, phosphate peak width and carbonate substitution for the evaluated specimens

| **Animal** | **Peak position** ($cm^{-1}$) | **Peak width** ($cm^{-1}$) | **Carbonate substitution** |
|---|---|---|---|
| Gray wolf | $960.45 \pm 0.14$ | $13.19 \pm 0.07$ | $0.11 \pm 0.01$ |
| Common opossum | $960.69 \pm 0.14$ | $13.36 \pm 0.20$ | $0.08 \pm 0.00$ |
| Lion | $960.49 \pm 0.10$ | $12.96 \pm 0.04$ | $0.11 \pm 0.00$ |
| Snow leopard | $961.08 \pm 0.00$ | $13.03 \pm 0.02$ | $0.11 \pm 0.00$ |
| Oncilla | $960.84 \pm 0.08$ | $13.22 \pm 0.08$ | $0.10 \pm 0.01$ |
| Black bear | $960.53 \pm 0.15$ | $12.59 \pm 0.17$ | $0.10 \pm 0.01$ |

Mapping for phosphate peak position is shown in figure 4.15, there is a reduction in phosphate peak position as the distance to the DEJ increases for all the animals.

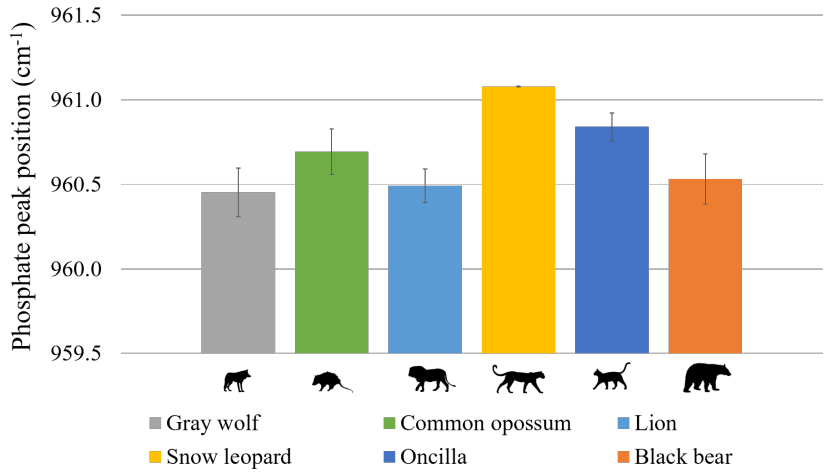


**Figure 4.11:** Average phosphate peak position ($PP$) for the evaluated specimens

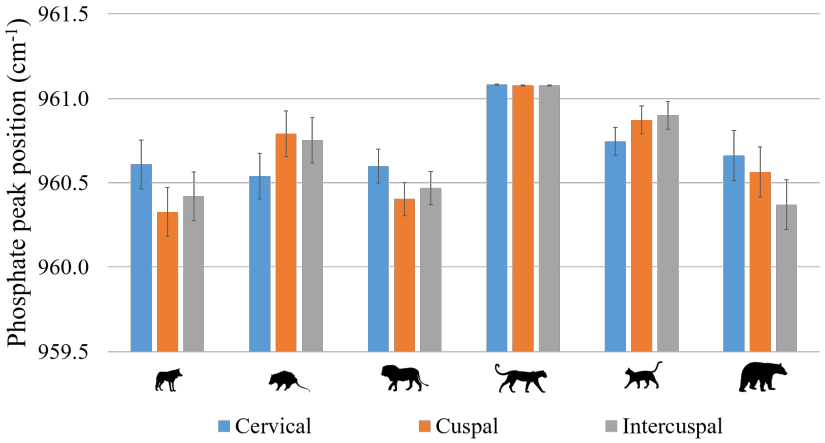


**Figure 4.12:** Phosphate peak position ($PP$) in cervical, cuspal and intercuspal regions for the evaluated specimens

### 4.2.2 Phosphate peak width

Average phosphate peak width ($PW$) is shown in figure 4.16 and table 4.2, while phosphate peak width in cervical, cuspal and intercuspal for all the evaluated specimens is shown in figure 4.17. Phosphate peak width was compared between animals (Fig. 4.18a) and between regions (Fig. 4.18b). When compared between animals, there is no statistical difference in phosphate peak width between Gray wolf, Common opossum, Lion and Black bear, neither between Common opossum, Oncilla and Black bear nor between Snow leopard and Oncilla. By the other hand, when comparing phosphate peak width

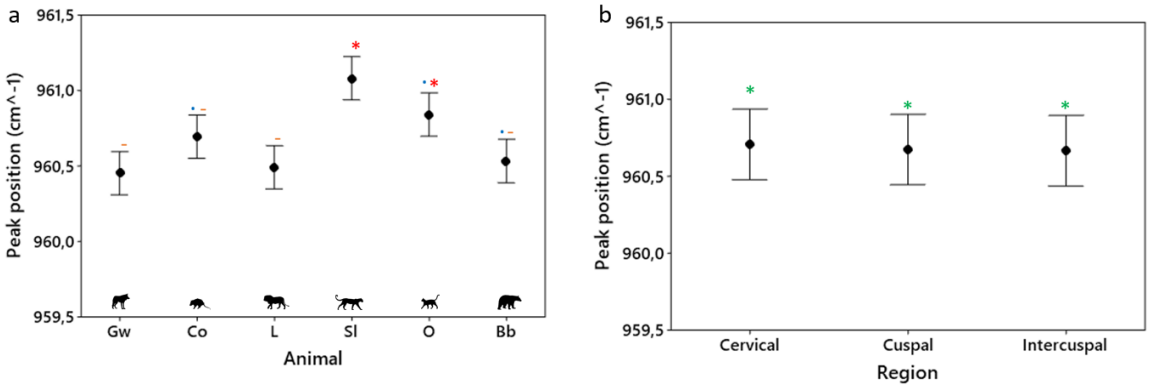


**Figure 4.13:** Tukey confidence intervals for phosphate peak position ($PP$). a) comparison between animals (average for all the regions); b) comparison between regions (average for all the animals). Intervals with the same marker do not show a statistically significant difference

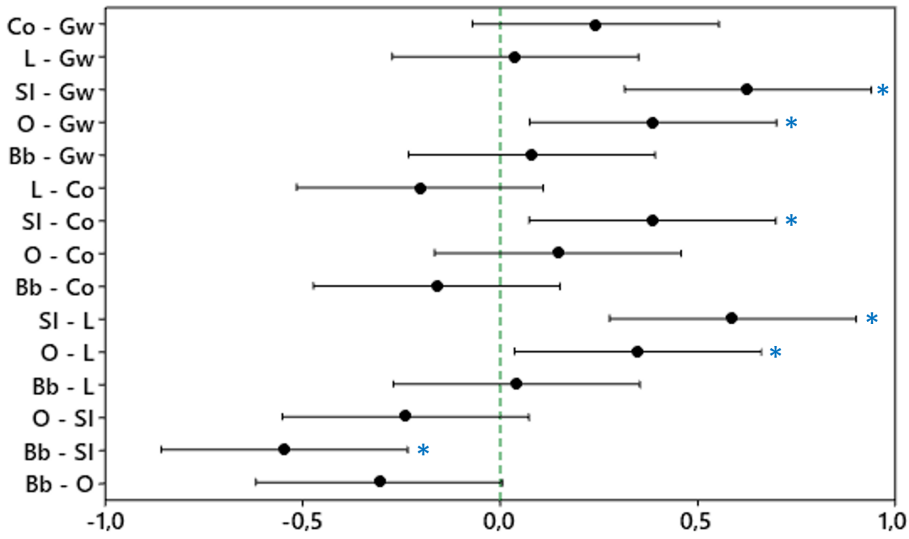


**Figure 4.14:** Tukey confidence intervals for phosphate peak position ($PP$) comparing the evaluated specimens. There is statistical difference in phosphate peak position between the animals that share confidence intervals that do not contain zero (Blue asterisk)

between regions, there is no statistical difference because the three confidence intervals (cervical, cuspal and intercuspal) overlap ($p = 0.8092$). The statistical differences in phosphate peak width are shown in figure 4.19 in which intervals Gw-Bb ($p = 0.0004$), Co-L ($p = 0.0117$), Co-Sl ($p = 0.0430$), Co-Bb ($p = 0.0000$), L-Bb ($p = 0.0202$), Sl-Bb ($p = 0.0056$) and O-Bb ($p = 0.0003$) do not contain zero.

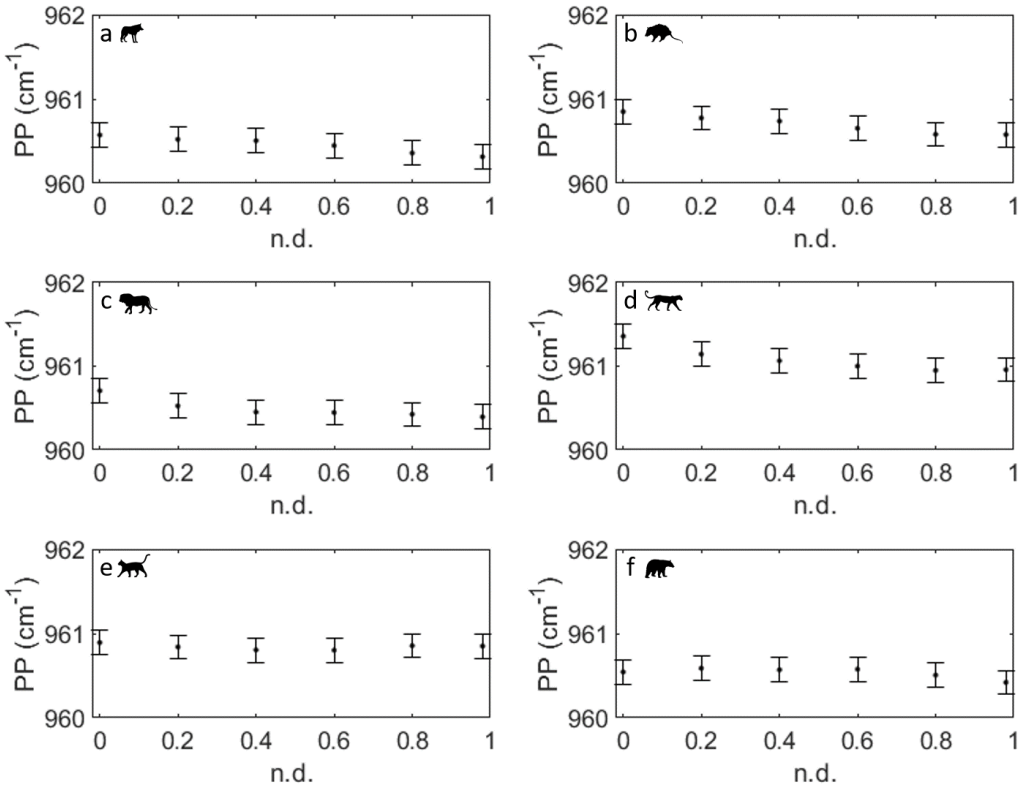


**Figure 4.15:** Phosphate peak position mapping by animal. a) Gray wolf, b) Common opossum, c) Lion, d) Snow leopard, e) Oncilla and f) Black bear (*n.d.* = normalized distance, 0 = DEJ, 1 = outer enamel surface)

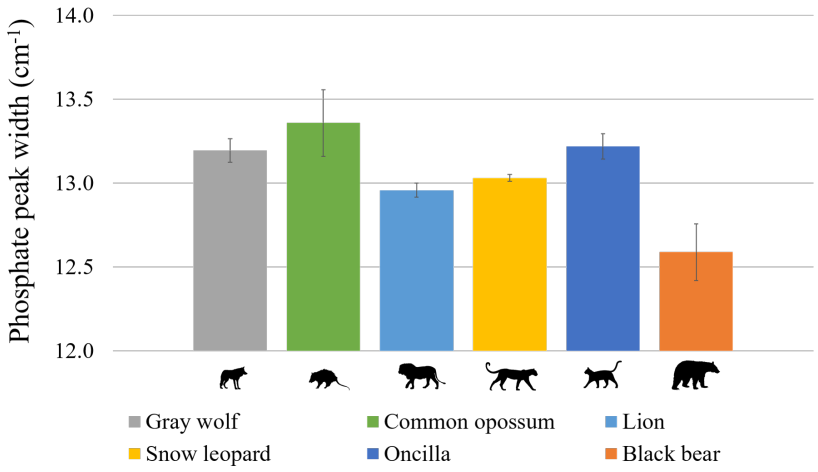


**Figure 4.16:** Average phosphate peak width ($PW$) for the evaluated specimens

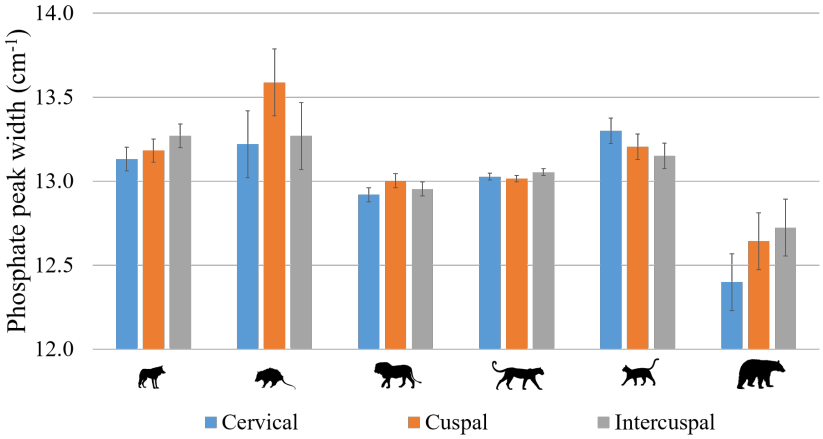


**Figure 4.17:** Phosphate peak width ($PW$) in cervical, cuspal and intercuspal regions for the evaluated specimens

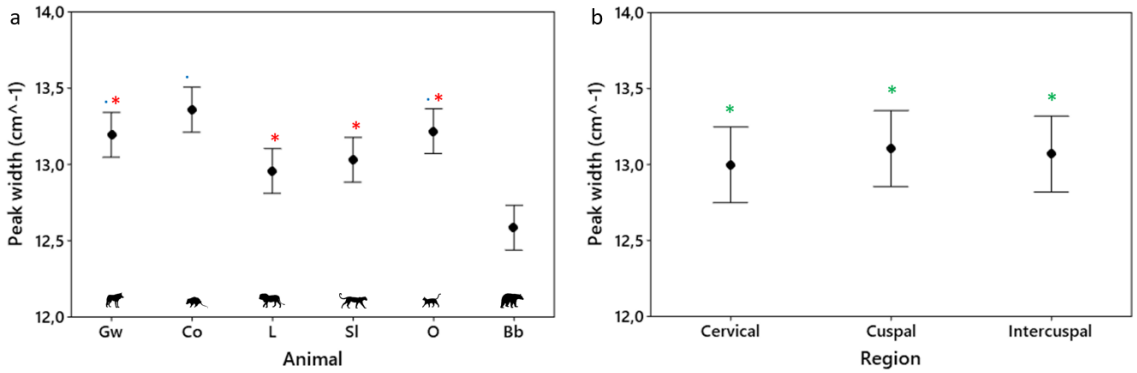


**Figure 4.18:** Tukey confidence intervals for phosphate peak width ($PW$). a) comparison between animals (average for all the regions); b) comparison between regions (average for all the animals). Intervals with the same marker do not show a statistically significant difference

Phosphate peak width was also measured from the DEJ to the external enamel surface (Fig. 4.20). In all animals there is an increase in phosphate peak width as the distance to the DEJ increases. This increase is less evident in Black bear with respect to the other animals.

### 4.2.3 Carbonate substitution

Avereage carbonate substitution ($CO_3$) is shown in figure 4.21 and table 4.2, while figure 4.22 shows carbonate substitution in cervical, cuspal and intercuspal for all the evaluated specimens. Tukey confidence interval plot for carbonate substitution when comparing between animals and between regions

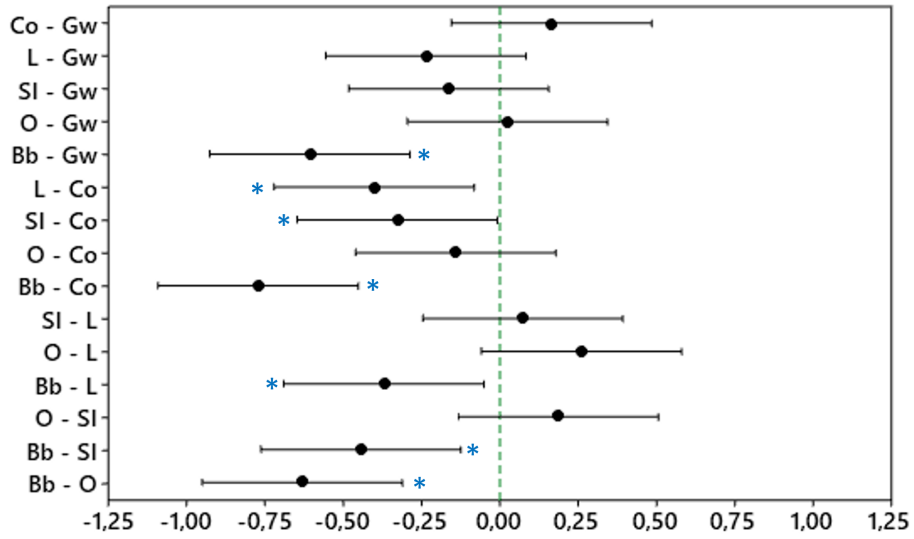


**Figure 4.19:** Tukey confidence intervals for phosphate peak width ($PW$) comparing the evaluated specimens. There is statistical difference in phosphate peak width between the animals that share confidence intervals that do not contain zero (Blue asterisk)

is shown in figure 4.23. When carbonate substitution is compared between animals (Fig. 4.23a), there is a difference between Common opossum and the other animals except Black bear ($p = 0.0003$). Also, as carbonate substitution confidence intervals between regions overlap (Fig. 4.23b), there is no statistical difference between cervical, cuspal and intercuspal regions ($p = 0.6503$). The statistical differences in carbonate substitution are shown in figure 4.24 in which intervals Gw-Co ($p = 0.0007$), Co-L ($p = 0.0011$), Co-Sl ($p = 0.0005$), and Co-O ($p = 0.0092$) do not contain zero.

Carbonate substitution was also measured from the DEJ to the external enamel surface (Fig. 4.25). In all animals there is an increase in carbonate substitution as the distance to the DEJ increases.

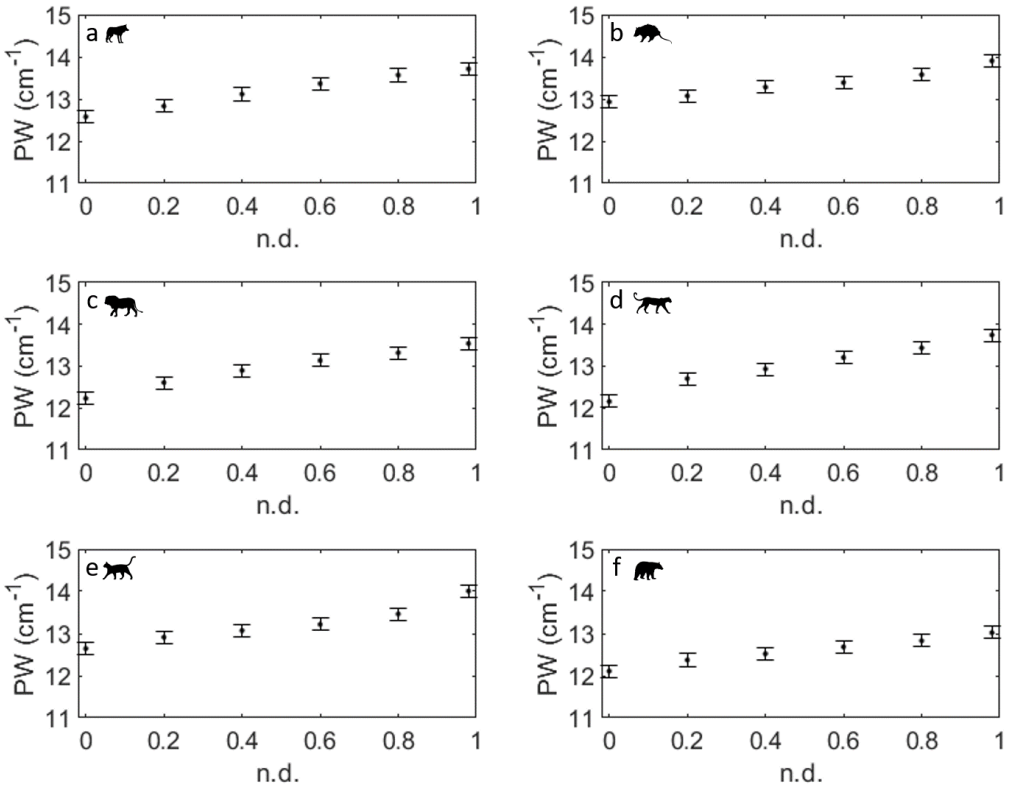


**Figure 4.20:** Phosphate peak width mapping by animal. a) Gray wolf, b) Common opossum, c) Lion, d) Snow leopard, e) Oncilla and f) Black bear (*n.d.* = normalized distance, 0 = DEJ, 1 = outer enamel surface)

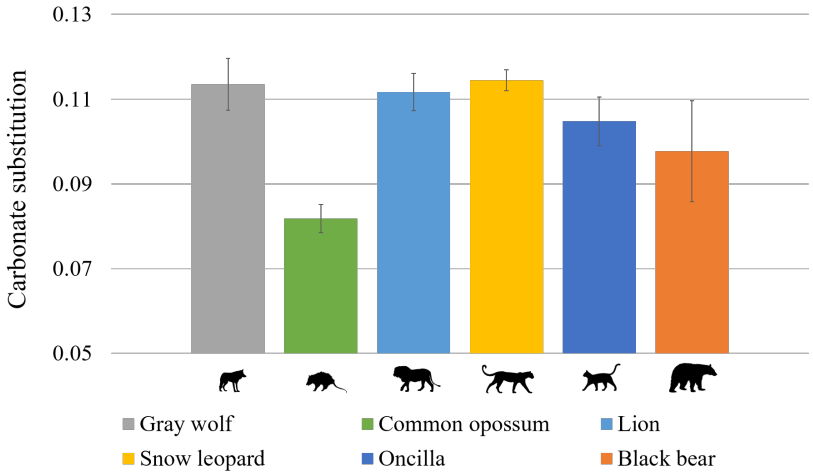


**Figure 4.21:** Average carbonate substitution ($CO_3$) for the evaluated specimens

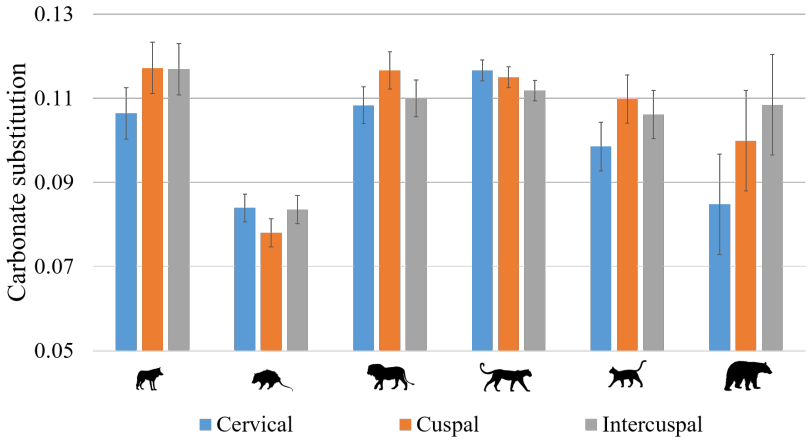


**Figure 4.22:** Carbonate substitution ($CO_3$) in cervical, cuspal and intercuspal regions for the evaluated specimens

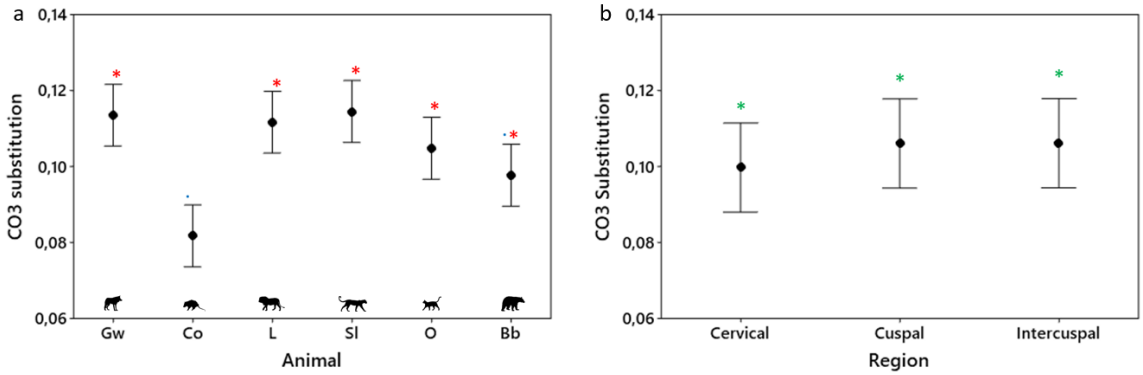


**Figure 4.23:** Tukey confidence intervals for carbonate substitution ($CO_3$). a) comparison between animals (average for all the regions); b) comparison between regions (average for all the animals). Intervals with the same marker do not show a statistically significant difference

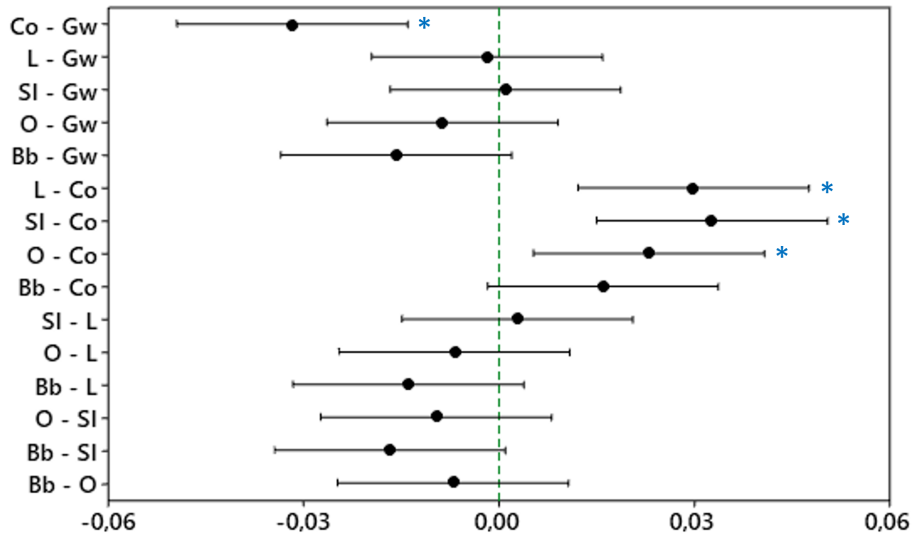


**Figure 4.24:** Tukey confidence intervals for carbonate substitution ($CO_3$) comparing the evaluated specimens. There is statistical difference in carbonate substitution between the animals that share confidence intervals that do not contain zero (Blue asterisk)

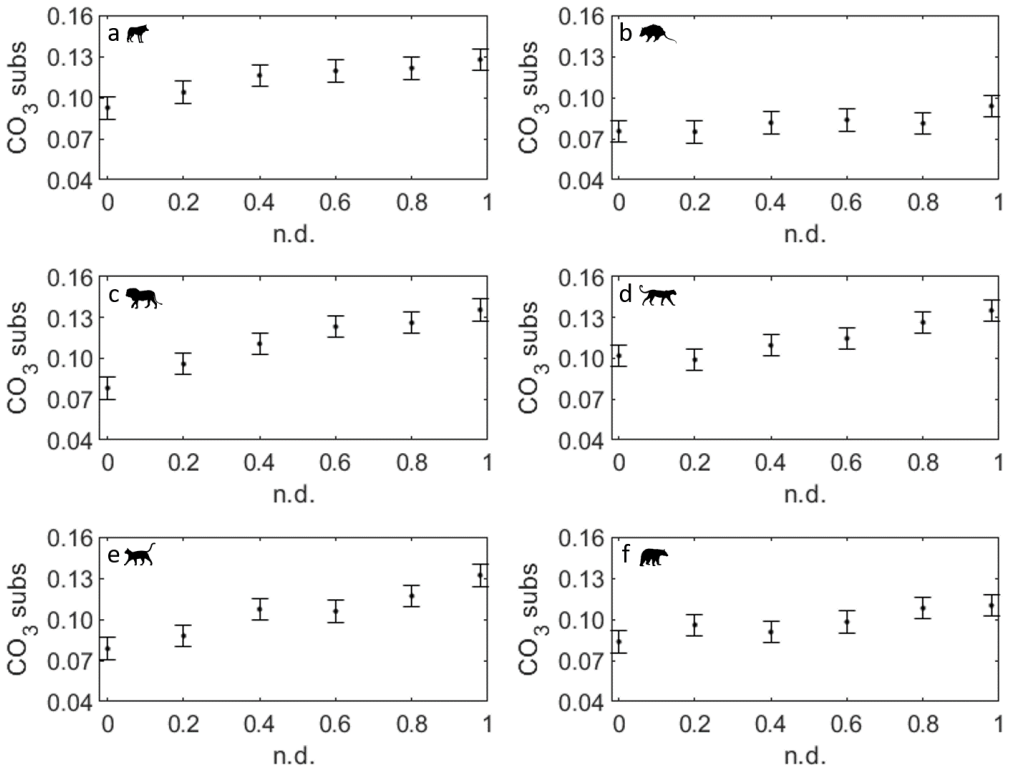


**Figure 4.25:** Carbonate substitution mapping by animal. a) Gray wolf, b) Common opossum, c) Lion, d) Snow leopard, e) Oncilla and f) Black bear (*n.d.* = normalized distance, $0$ = DEJ, $1$ = outer enamel surface)

## 4.3 Enamel ultrastructure

### 4.3.1 Ultrastructure description

Table 4.3 shows a summary of the main characteristics of the enamel in each of the analyzed specimens in terms of the prism shape, prism pattern and enamel type present in each of the three analyzed regions. The same ultrastructural features are seen in the three regions (cervical, cuspal and intercuspal) of all the analyzed specimens.

Prism shape and pattern (Fig. 4.26) vary between the analyzed specimens, in Gray wolf and Black bear the prism is key-hole shaped (pattern II) while in the other specimens it is closed (pattern I). In the common opossum and Oncilla it is circular shaped, in the Lion the prism has an irregular shape and in the Snow leopard it is hexagonal.

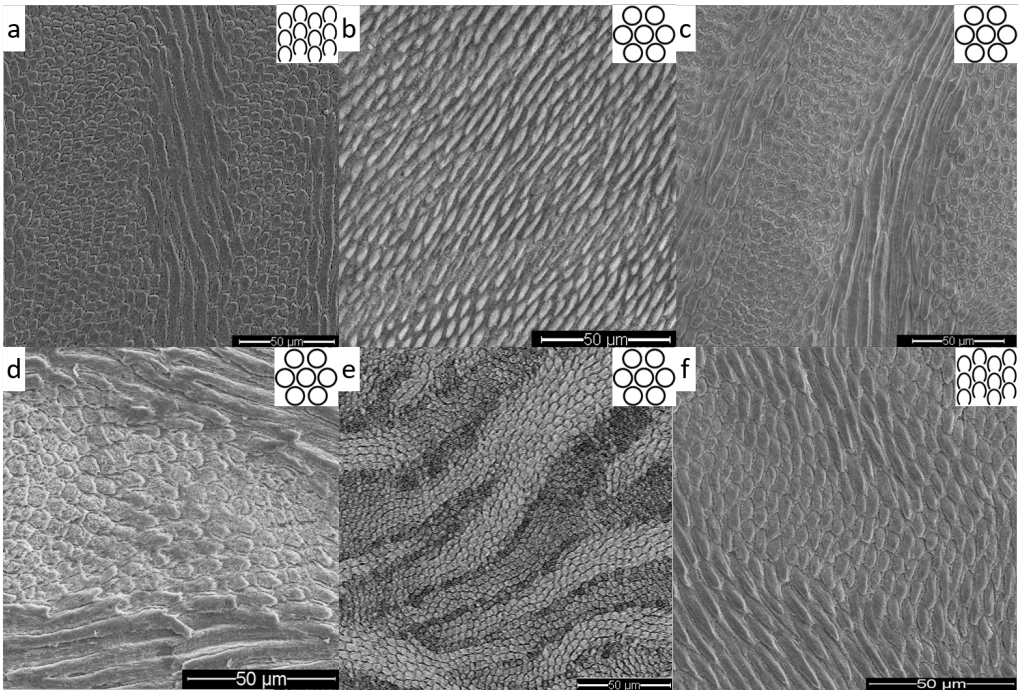


**Figure 4.26:** Enamel prism patterns in the evaluated specimens. a) Gray wolf, b) Common opossum, c) Lion, d) Snow leopard, e) Oncilla and f) Black bear. Gray wolf and Black bear have key-hole shaped prisms (pattern II) while the other specimens have closed prisms (pattern I). In the upper right corner of each image there is a diagram of the pattern of prisms, according to Maas and Dumont (1999), for each analyzed specimen

**Table 4.3:** Enamel ultrastructure description. I: Inner, O: Outer

| **Animal** | **Region** | **Prism shape** | **Prism pattern** | **Enamel type** |
|---|---|---|---|---|
| Gray wolf | Cervical | Key-hole | II | I: Decussated, O: Radial |
| | Cuspal | Key-hole | II | I: Decussated, O: Radial |
| | Intercuspal | Key-hole | II | I: Decussated, O: Radial |
| Common opossum | Cervical | Closed - Circular | I | I: Decussated, O: Radial |
| | Cuspal | Closed - Circular | I | I: Decussated, O: Radial |
| | Intercuspal | Closed - Circular | I | I: Decussated, O: Radial |
| Lion | Cervical | Closed - Irregular | I | I: Decussated, O: Radial |
| | Cuspal | Closed - Irregular | I | I: Decussated, O: Radial |
| | Intercuspal | Closed - Irregular | I | I: Decussated, O: Radial |
| Snow leopard | Cervical | Closed - Hexagonal | I | I: Decussated, O: Radial |
| | Cuspal | Closed - Hexagonal | I | I: Decussated, O: Radial |
| | Intercuspal | Closed - Hexagonal | I | I: Decussated, O: Radial |
| Oncilla | Cervical | Closed - Circular | I | I: Decussated, O: Radial |
| | Cuspal | Closed - Circular | I | I: Decussated, O: Radial |
| | Intercuspal | Closed - Circular | I | I: Decussated, O: Radial |
| Black bear | Cervical | Key-hole | II | I: Decussated, O: Radial |
| | Cuspal | Key-hole | II | I: Decussated, O: Radial |
| | Intercuspal | Key-hole | II | I: Decussated, O: Radial |

Finally, in all the specimens, inner enamel is decussated while outer enamel is radial, figure 4.27 shows enamel pattern for Oncilla and Black bear.

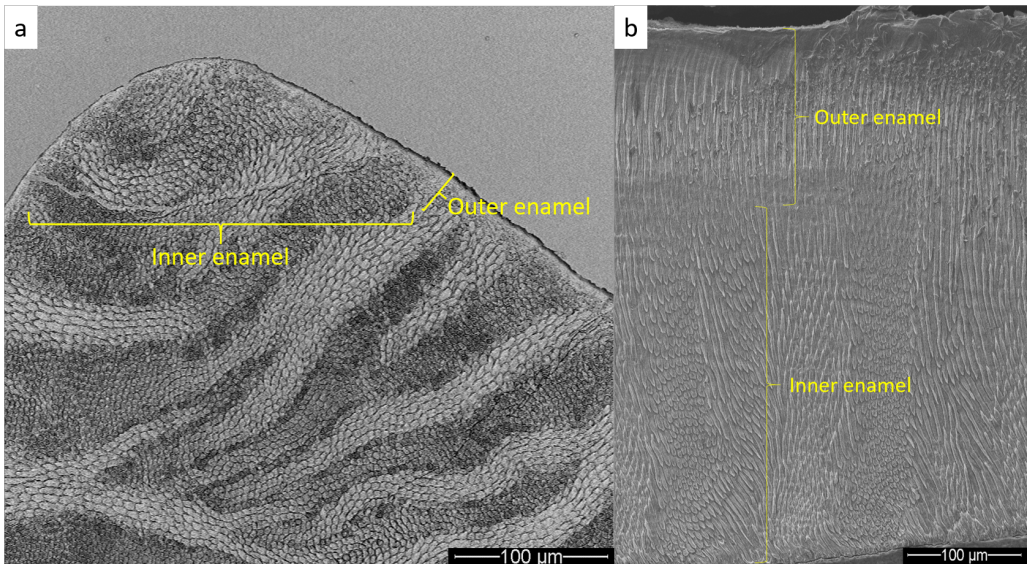


**Figure 4.27:** Enamel types for Oncilla (a) and Black bear (b). Enamel type on the Oncilla (a) and the Black Bear (b). In both samples, the enamel of the Oncilla (cuspal region) and of the black bear (cervical region), the internal enamel is decussated while the external enamel is radial

### 4.3.2 Enamel thickness

Average enamel thickness ($ET$) for the evaluated specimens is shown in table 4.4 and in figure 4.28, while figure 4.29 shows enamel thickness in cervical, cuspal and intercuspal for all the evaluated specimens.

**Table 4.4:** Average enamel thickness, decussated thickness and decussated fraction for the evaluated specimens

| **Animal** | **Enamel thickness** ($\mu m$) | **Decussated thickness** ($\mu m$) | **Decussated fraction** |
|---|---|---|---|
| Gray wolf | $531.77 \pm 46.99$ | $439.48 \pm 36.89$ | $0.83 \pm 0.02$ |
| Common opossum | $193.14 \pm 59.47$ | $156.80 \pm 54.17$ | $0.80 \pm 0.03$ |
| Lion | $701.36 \pm 116.02$ | $597.85 \pm 109.51$ | $0.85 \pm 0.02$ |
| Snow leopard | $269.44 \pm 86.36$ | $222.83 \pm 59.52$ | $0.84 \pm 0.07$ |
| Oncilla | $318.87 \pm 132.78$ | $288.22 \pm 113.86$ | $0.91 \pm 0.02$ |
| Black bear | $457.37 \pm 27.29$ | $384.55 \pm 20.94$ | $0.84 \pm 0.01$ |

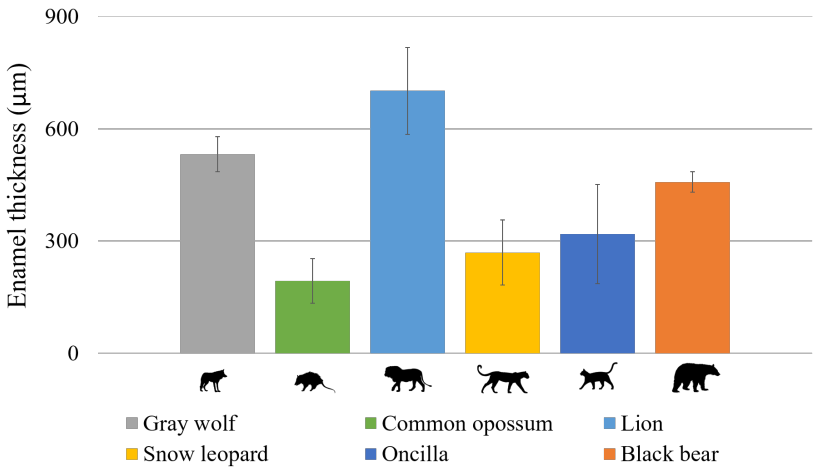


**Figure 4.28:** Average enamel thickness ($ET$) for the evaluated specimens

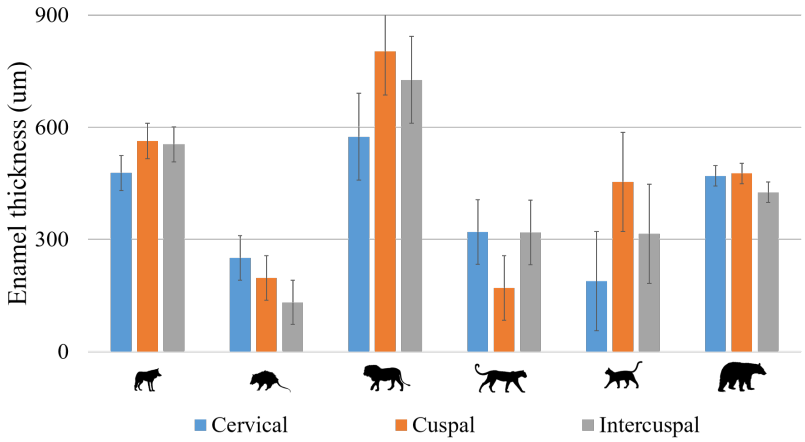


**Figure 4.29:** Enamel thickness ($ET$) in cervical, cuspal and intercuspal regions for the evaluated specimens

Enamel thickness was compared between animals and regions, this comparison (Fig. 4.30a) shows that there are no statistically significant differences between Gray wolf and Lion, between Gray wolf, Oncilla and Black bear, neither between Snow leopard, Oncilla and Black bear nor between Common opossum, Snow leopard and Oncilla. As in the previous properties, there are no differences in enamel thickness between the cervical, cuspal and intercuspal regions (Fig. 4.30b) as their confidence intervals overlap ($p = 0.8623$). The statistical differences in enamel thickness between specimens are shown in

figure 4.31, in which intervals Gw-Co ($p = 0.0046$), Gw-Sl ($p = 0.0278$), Co-L ($p = 0.0001$), Co-Bb ($p = 0.0265$), L-Sl ($p = 0.0006$), L-O ($p = 0.0017$) and L-Bb ($p = 0.0430$) do not contain zero.

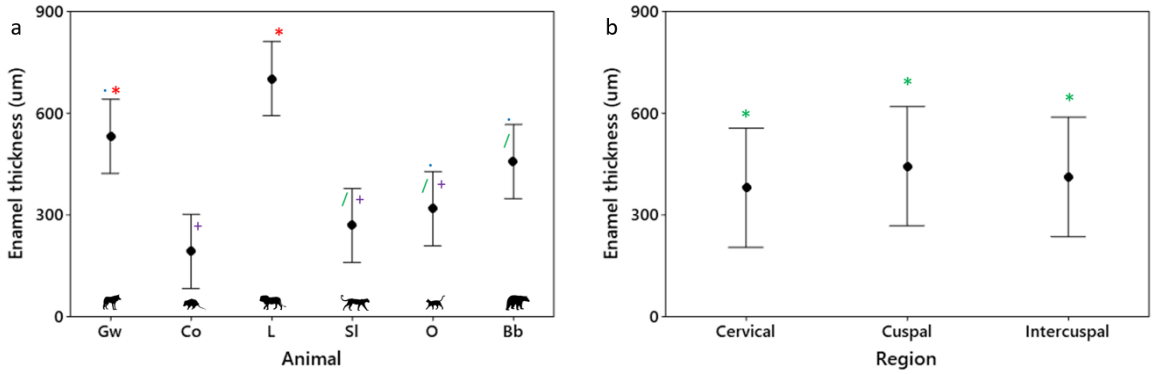


**Figure 4.30:** Tukey confidence intervals for enamel thickness ($ET$). a) comparison between animals (average for all the regions); b) comparison between regions (average for all the animals). Intervals with the same marker do not show a statistically significant difference

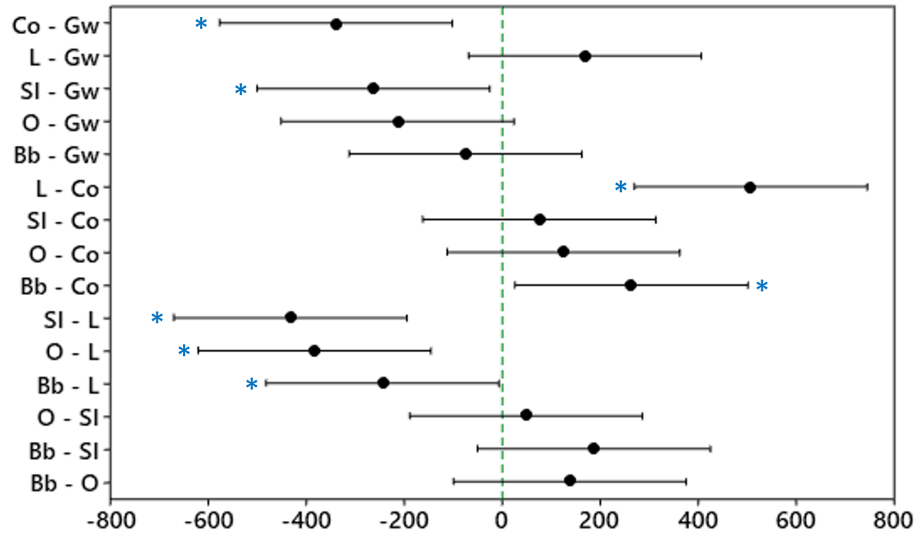


**Figure 4.31:** Tukey confidence intervals for enamel thickness ($ET$) comparing the evaluated specimens. There is statistical difference in enamel thickness between the animals that share confidence intervals that do not contain zero (Blue asterisk)

### 4.3.3 Decussated thickness

Average decussated thickness ($DT$) is shown in figure 4.32 and table 4.4, while decussated thickness in cervical, cuspal and intercuspal for all the evaluated specimens is shown in figure 4.33.

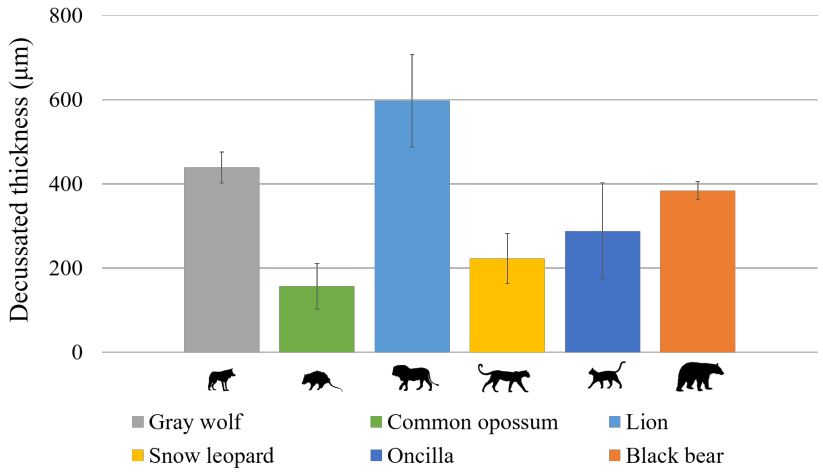


**Figure 4.32:** Average decussated thickness ($DT$) for the evaluated specimens

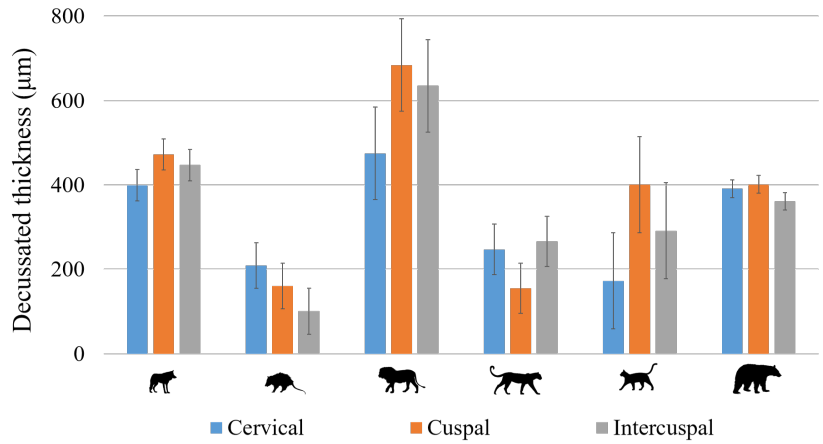


**Figure 4.33:** Decussated thickness ($DT$) in cervical, cuspal and intercuspal regions for the evaluated specimens

Tukey confidence interval plot for animals (Fig. 4.34a) and regions (Fig. 4.34b) shows that, when comparing animals, there are not statistical differences in decussated thickness between Gray wolf and Lion, between Gray wolf, Oncilla and Black bear; Common opossum, Snow leopard and Oncilla nor

between Snow leopard, Oncilla and Black bear. Furthermore, there are no differences between the evaluated regions ($p = 0.8166$). The statistical differences in decussated thickness are shown in figure 4.35, in which intervals Gw-Co ($p = 0.0057$), Gw-Sl ($p = 0.0354$), Co-L ($p = 0.0001$), Co-Bb ($p = 0.0260$), L-Sl ($p = 0.0005$), L-O ($p = 0.0028$) and L-Bb ($p = 0.0388$) do not contain zero.

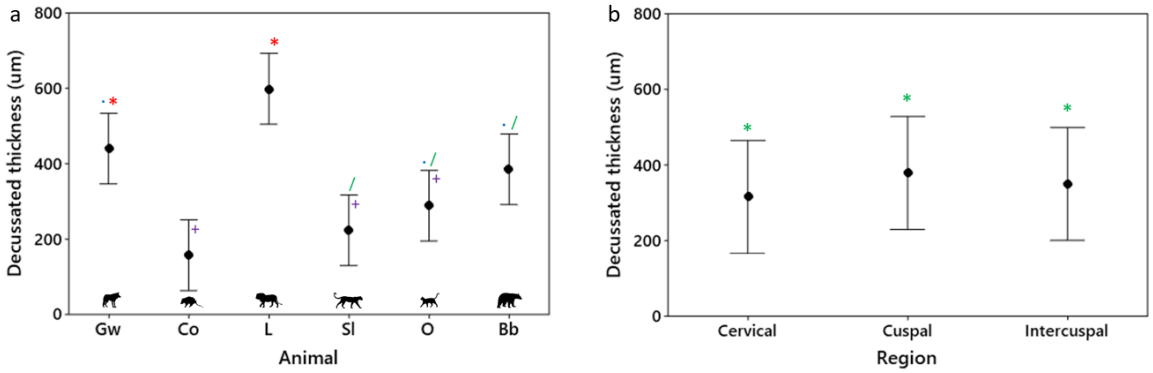


**Figure 4.34:** Tukey confidence intervals for decussated thickness ($DT$). a) comparison between animals (average for all the regions); b) comparison between regions (average for all the animals). Intervals with the same marker do not show a statistically significant difference

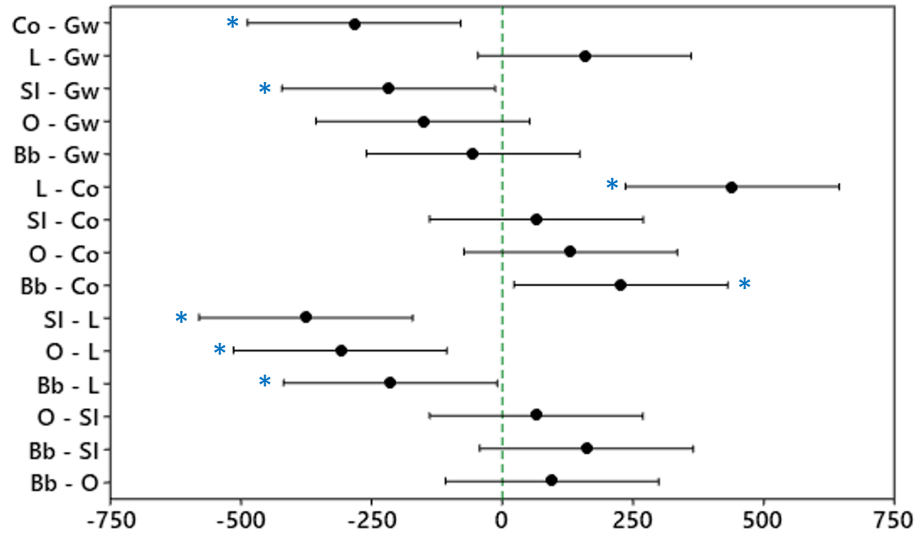


**Figure 4.35:** Tukey confidence intervals for decussated thickness ($DT$) comparing the evaluated specimens. There is statistical difference in decussated thickness between the animals that share confidence intervals that do not contain zero (Blue asterisk)

### 4.3.4 Decussated fraction

Average decussated fraction ($DF$) is shown in table 4.4 and in figure 4.36 while figure 4.37 shows decussated fraction in cervical, cuspal and intercuspal for all the evaluated specimens. Comparison between animals (Fig. 4.38a) and regions (Fig. 4.38b) shows that there is a statistical difference in decussated fraction between Common opossum and Oncilla, but not between the other analyzed specimens, and that there is no significant difference between the evaluated regions ($p = 0.7257$). The statistical differences in decussated fraction are shown in figure 4.39, in which the interval Co-O ($p = 0.0029$) does not contain zero.

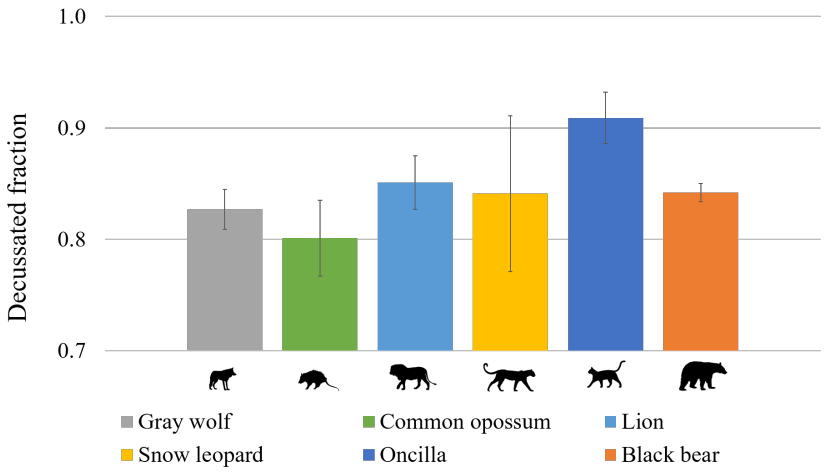


**Figure 4.36:** Average decussated fraction ($DF$) for the evaluated specimens

### 4.3.5 Decussated band thickness

Average decussated band thickness ($DBT\mu m$) is shown in table 4.5 and figure 4.40, while decussated band thickness in cervical, cuspal and intercuspal for all the evaluated specimens is shown in figure 4.41. Comparison between animals (Fig. 4.42a) and regions (Fig. 4.42b) shows that decussated band thickness in Common opossum is statistically different from decussated band thickness in the other animals but not from the thickness of the decussated band of the Oncilla ($p = 0.0013$) and that there is no significant difference in decussated band thickness between the evaluated regions ($p = 0.5026$). Statistical differences in decussated band thickness are shown in figure 4.43, in which the intervals

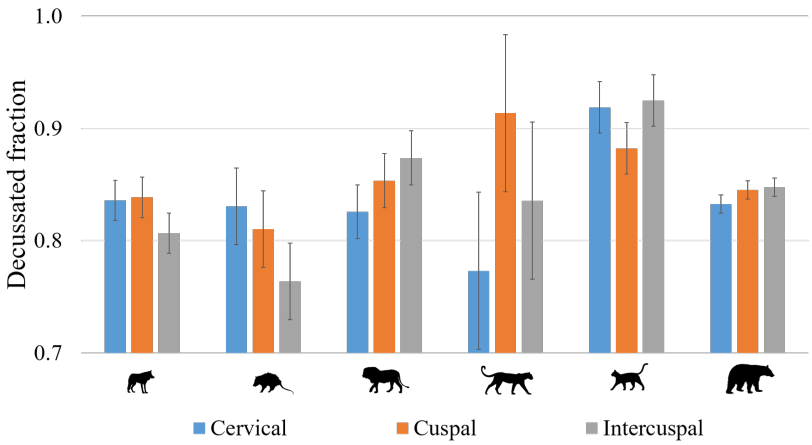


**Figure 4.37:** Decussated fraction ($DF$) in cervical, cuspal and intercuspal regions for the evaluated specimens

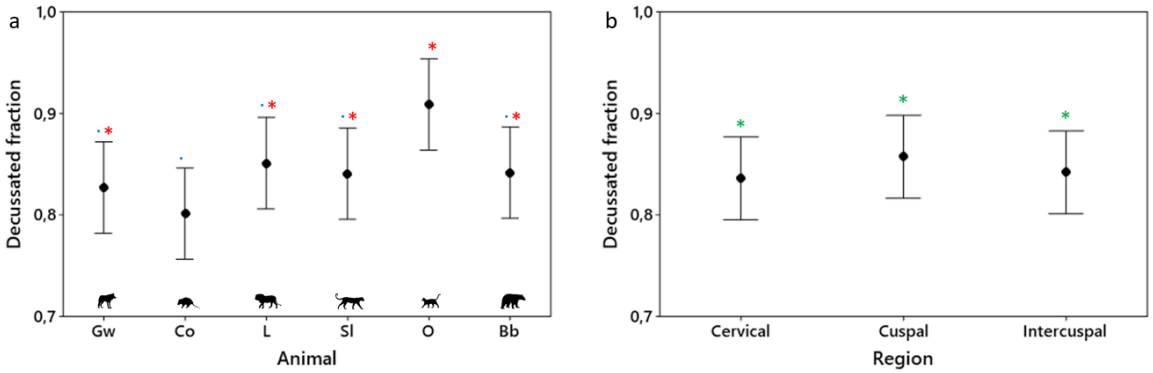


**Figure 4.38:** Tukey confidence intervals for decussated fraction ($DF$). a) comparison between animals (average for all the regions); b) comparison between regions (average for all the animals). Intervals with the same marker do not show a statistically significant difference

Gw-Co ($p = 0.0242$), Co-L ($p = 0.0135$), Co-Sl ($p = 0.0020$), and Co-Bb ($p = 0.0015$) not contain zero.

### 4.3.6 Number of prisms in decussation band

Average number of prisms in decussated band ($DBp$) is shown in figure 4.44 and table 4.5, while the number of prisms in decussated band in cervical, cuspal and intercuspal for all the evaluated specimens is shown in figure 4.45. Comparison between animals (Fig. 4.46a) and regions (Fig. 4.46b) shows that there are not statistical differences in the number of prisms in decussation band between Gray wolf,

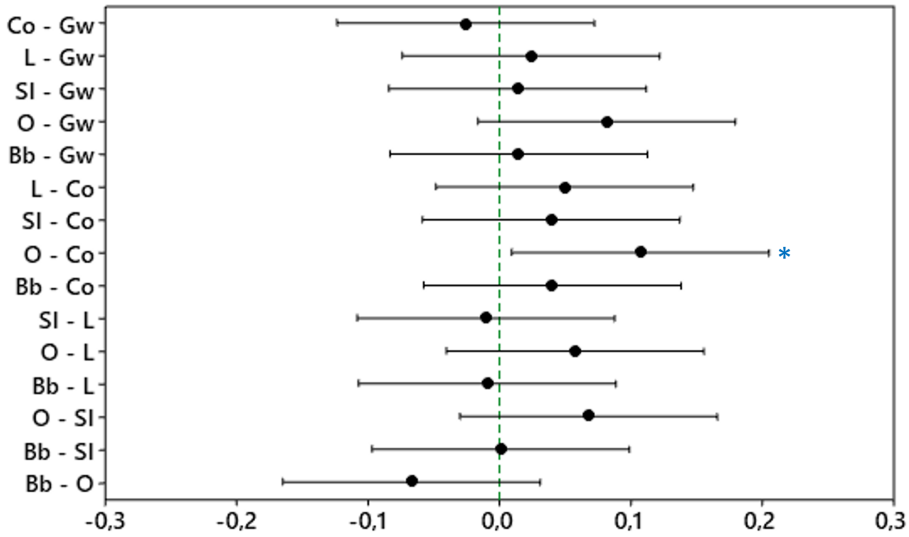


**Figure 4.39:** Tukey confidence intervals for decussated fraction ($DF$) comparing the evaluated specimens. There is statistical difference in decussated fraction between the animals that share confidence intervals that do not contain zero (Blue asterisk)

**Table 4.5:** Average decussated band thickness, number of prisms in decussated band, prism diameter and prism orientation for the evaluated specimens

| **Animal** | **Decussated band thickness** ($\mu m$) | **Number of prisms in decussated band** | **Prism diameter** ($\mu m$) | **Prism orientation** ($Deg$) |
|---|---|---|---|---|
| Gray wolf | $54.38 \pm 11.95$ | $9.70 \pm 1.37$ | $5.17 \pm 0.85$ | $46.78 \pm 5.90$ |
| Common opossum | $14.71 \pm 7.06$ | $3.70 \pm 2.28$ | $3.39 \pm 0.46$ | $47.71 \pm 15.13$ |
| Lion | $57.62 \pm 13.66$ | $8.37 \pm 0.17$ | $6.15 \pm 0.95$ | $54.47 \pm 9.04$ |
| Snow leopard | $68.41 \pm 7.07$ | $10.30 \pm 0.57$ | $5.65 \pm 0.34$ | $58.29 \pm 1.01$ |
| Oncilla | $43.10 \pm 12.70$ | $7.78 \pm 0.95$ | $6.64 \pm 0.53$ | $62.17 \pm 5.91$ |
| Black bear | $70.36 \pm 9.71$ | $12.78 \pm 2.78$ | $5.20 \pm 0.48$ | $40.04 \pm 0.21$ |

Lion, Snow leopard and Black bear; between Gray wolf, Lion, Snow leopard and Oncilla, and between Common opossum and Oncilla and as in the previous properties, there is no significant difference in the number of prisms in decussation band between the evaluated regions ($p = 0.7269$). The statistical differences in the number of prisms in decussation band are shown in figure 4.47, in which the intervals

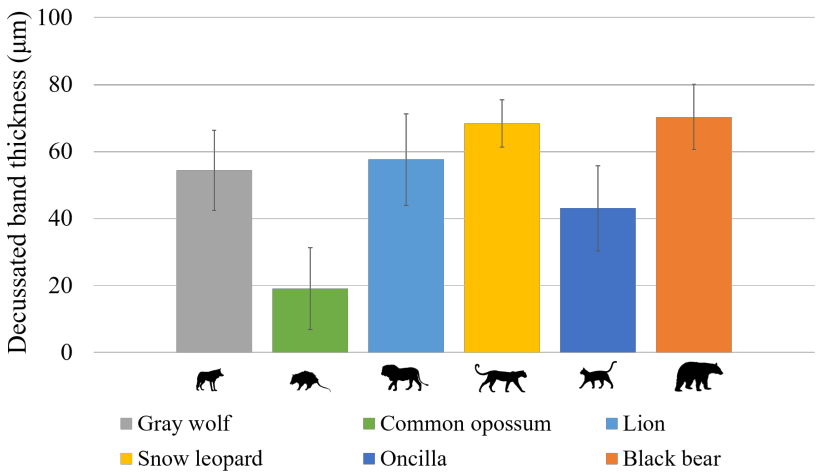


**Figure 4.40:** Average decussated band thickness ($DBT\mu m$) for the evaluated specimens

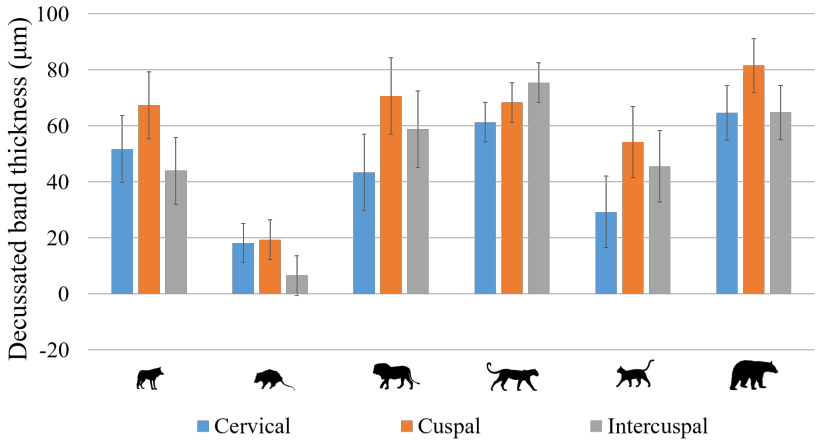


**Figure 4.41:** Decussated band thickness ($DBT\mu m$) in cervical, cuspal and intercuspal regions for the evaluated specimens

Gw-Co ($p = 0.0075$), Co-L ($p = 0.0402$), Co-Sl ($p = 0.0036$), Co-Bb ($p = 0.0002$), and O-Bb ($p = 0.0264$) do not contain zero.

### 4.3.7 Prism diameter

Average prism diameter ($D$) is shown in figure 4.48 and table 4.5, while prism diameter in cervical, cuspal and intercuspal for all the evaluated specimens is shown in figure 4.49. Comparison between animals (Fig. 4.50a) and regions (Fig. 4.50b) shows that only Common opossum shows statistical

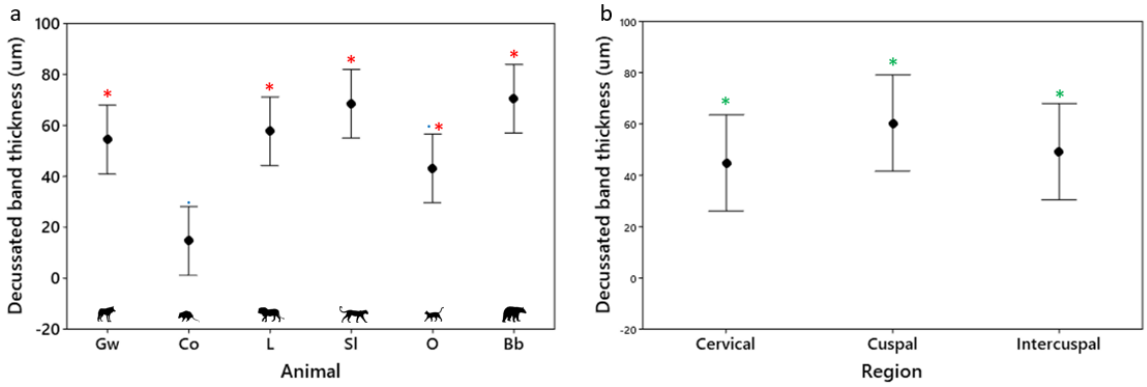


**Figure 4.42:** Tukey confidence intervals for decussated band thickness ($DBT\mu m$). a) comparison between animals (average for all the regions); b) comparison between regions (average for all the animals). Intervals with the same marker do not show a statistically significant difference

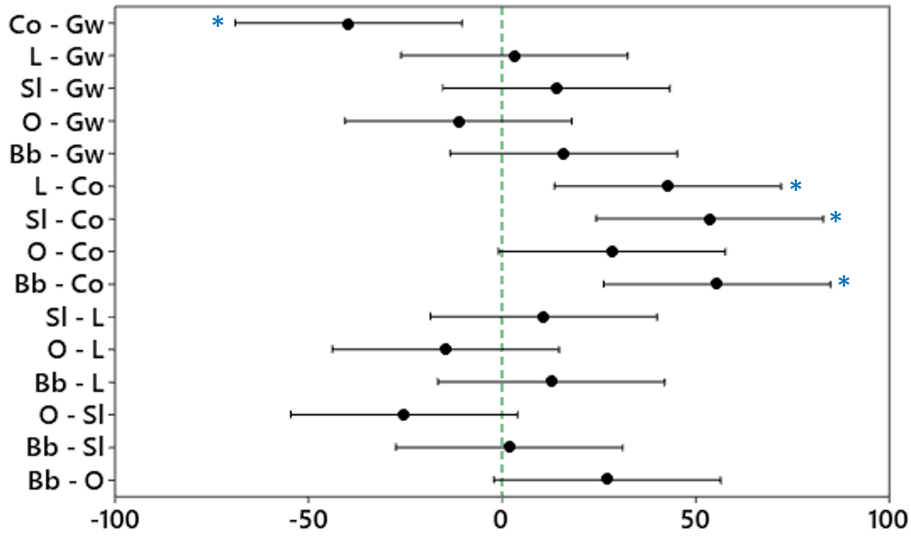


**Figure 4.43:** Tukey confidence intervals for decussated band thickness ($DBT\mu m$) comparing the evaluated specimens. There is statistical difference in decussated band thickness between the animals that share confidence intervals that do not contain zero (Blue asterisk)

difference in prism diameter with the other animals ($p = 0.0009$). Also, as prism diameter confidence intervals between regions overlap, there is not statistical difference in prism diameter between regions ($p = 0.9597$). The statistical differences in prism diameter are shown in figure 4.51, in which the intervals Gw-Co ($p = 0.0475$), Co-L ($p = 0.0022$), Co-Sl ($p = 0.0101$), Co-O ($p = 0.0005$) and Co-Bb ($p = 0.0440$) do not contain zero.

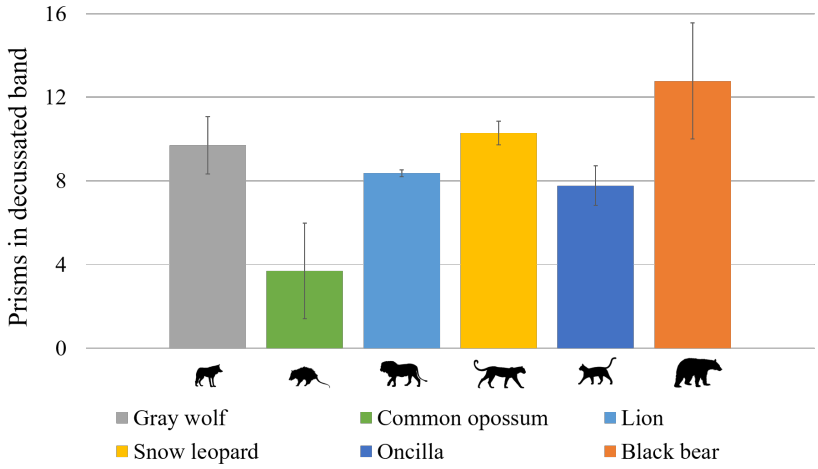


**Figure 4.44:** Average number of prisms in decussated band ($DBp$) for the evaluated specimens

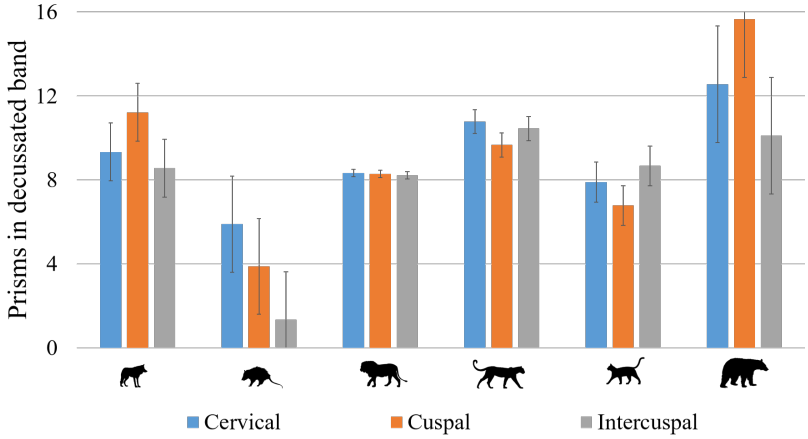


**Figure 4.45:** Number of prisms in decussated band ($DBp$) in cervical, cuspal and intercuspal regions for the evaluated specimens

### 4.3.8 Prism orientation

Average prism orientation ($Ang$) is shown in figure 4.52 and table 4.5, while prism orientation diameter in cervical, cuspal and intercuspal for all the evaluated specimens is shown in figure 4.53. When comparing between animals (Fig. 4.54a) there is only statistical difference in prism orientation between Oncilla and Black bear. Also, comparison between regions (Fig. 4.54b) shows that there is no statistical difference in prism orientation between regions as the confidence intervals overlap ($p = 0.7787$). The

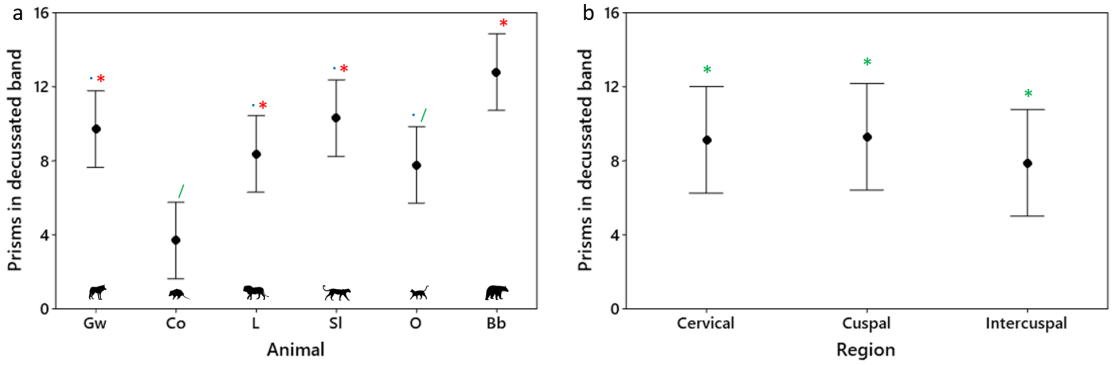


**Figure 4.46:** Tukey confidence intervals for number of prisms in decussated band ($DBp$). a) comparison between animals (average for all the regions); b) comparison between regions (average for all the animals). Intervals with the same marker do not show a statistically significant difference

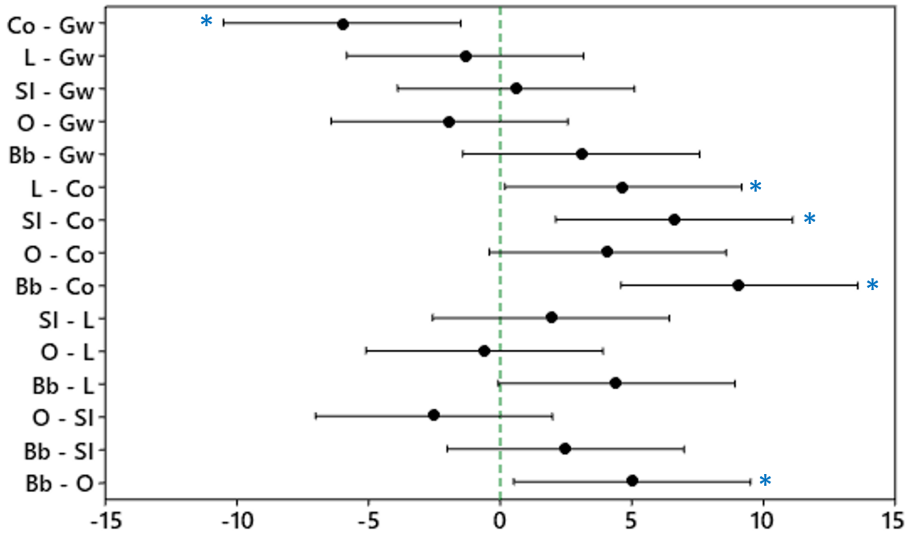


**Figure 4.47:** Tukey confidence intervals for the number of prisms in decussation band comparing the evaluated specimens. There is statistical difference in the number of prisms in decussation band between the animals that share confidence intervals that do not contain zero (Blue asterisk)

statistical difference in prism orientation is shown in figure 4.55, in which the interval O-Bb ($p = 0.0467$) does not contain zero .

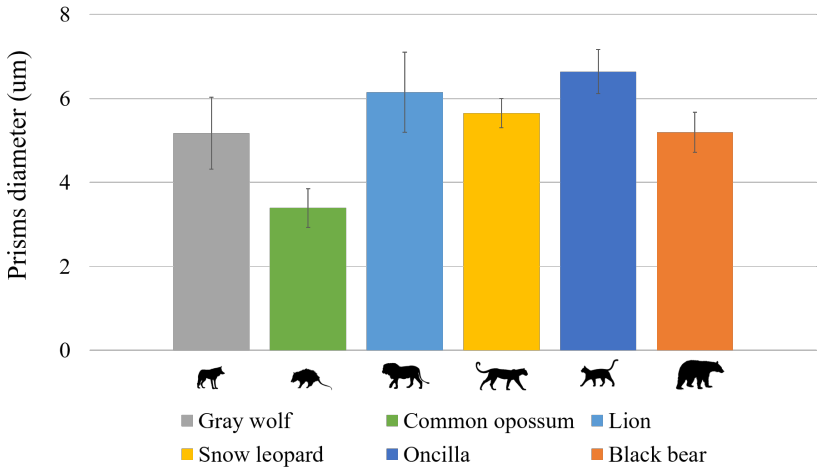


**Figure 4.48:** Average prism diameter ($D$) for the evaluated specimens

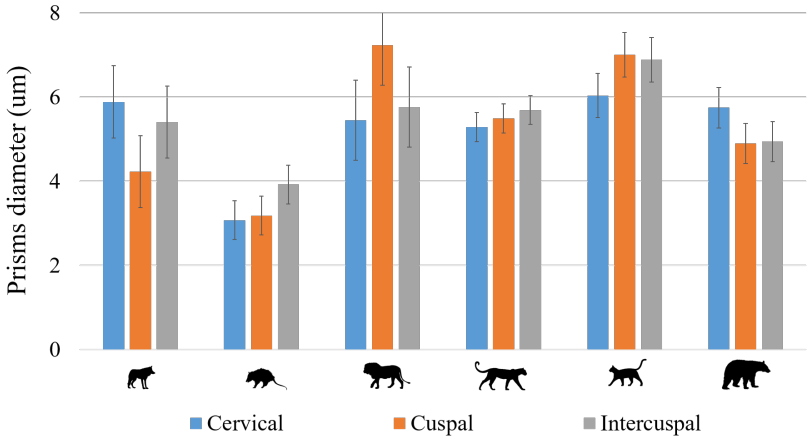


**Figure 4.49:** Prism diameter ($D$) in cervical, cuspal and intercuspal regions for the evaluated specimens

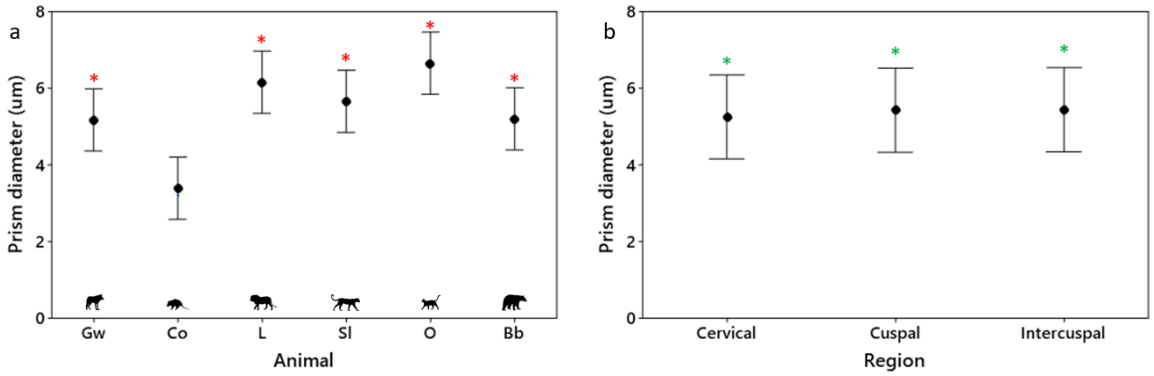


**Figure 4.50:** Tukey confidence intervals for prism diameter ($D$). a) comparison between animals (average for all the regions); b) comparison between regions (average for all the animals). Intervals with the same marker do not show a statistically significant difference

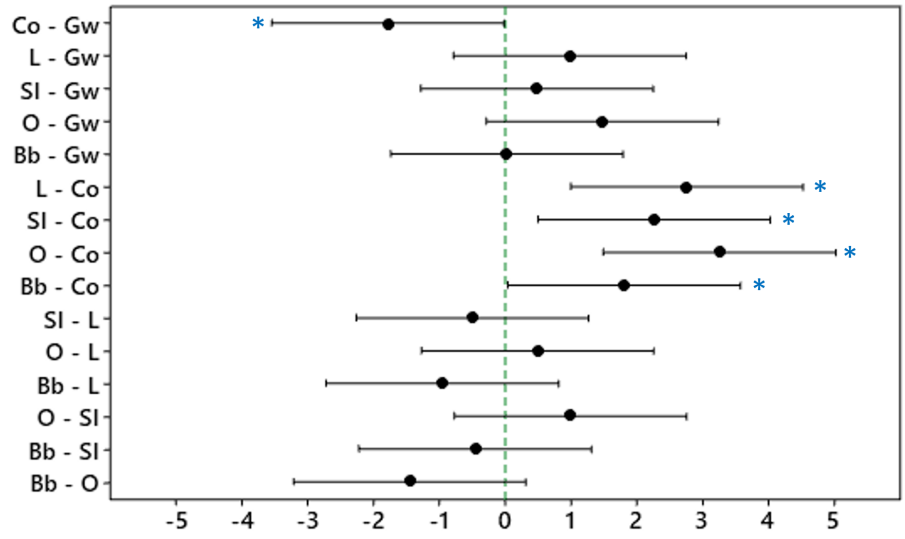


**Figure 4.51:** Tukey confidence intervals for prism diameter ($D$) comparing the evaluated specimens. There is statistical difference in prism diameter between the animals that share confidence intervals that do not contain zero (Blue asterisk)

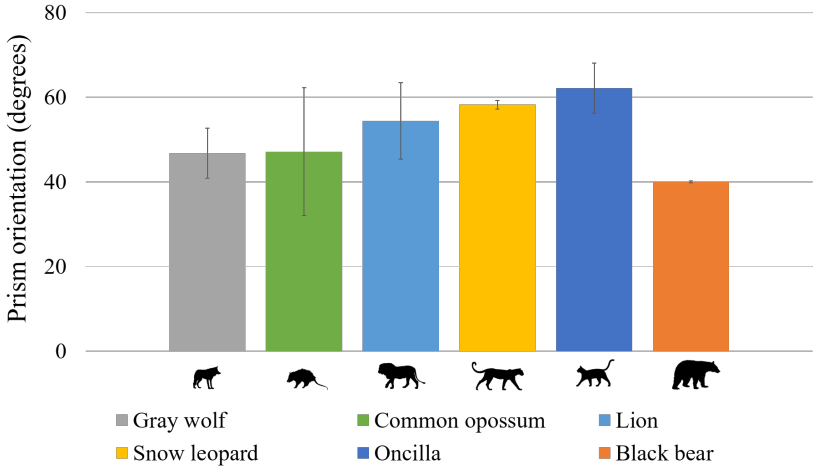


**Figure 4.52:** Average prism orientation ($Ang$) for the evaluated specimens

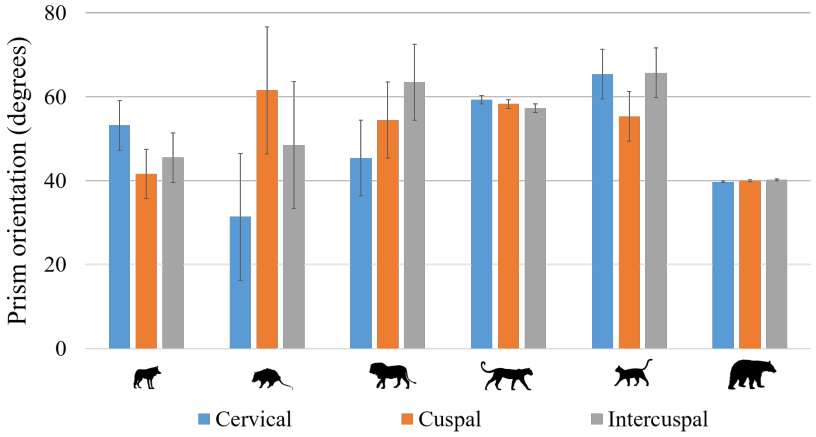


**Figure 4.53:** Prism orientation ($Ang$) in cervical, cuspal and intercuspal regions for the evaluated specimens

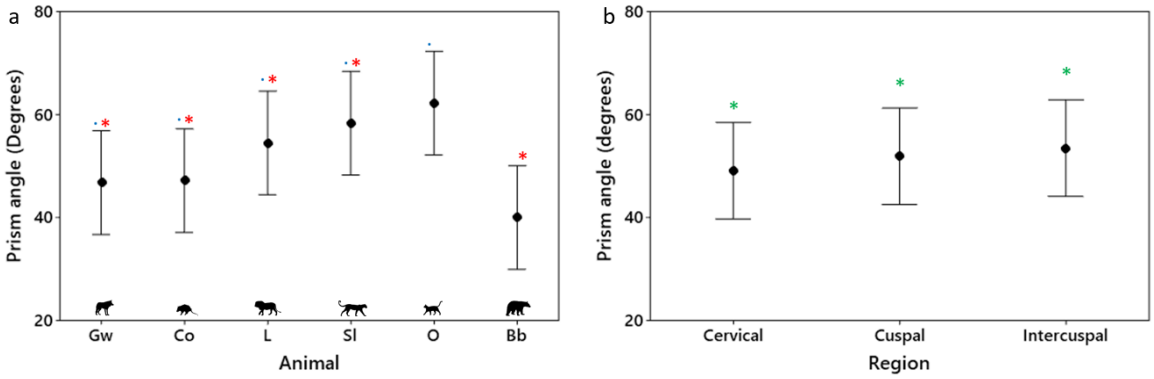


**Figure 4.54:** Tukey confidence intervals for prism orientation ($Ang$). a) comparison between animals (average for all the regions); b) comparison between regions (average for all the animals). Intervals with the same marker do not show a statistically significant difference

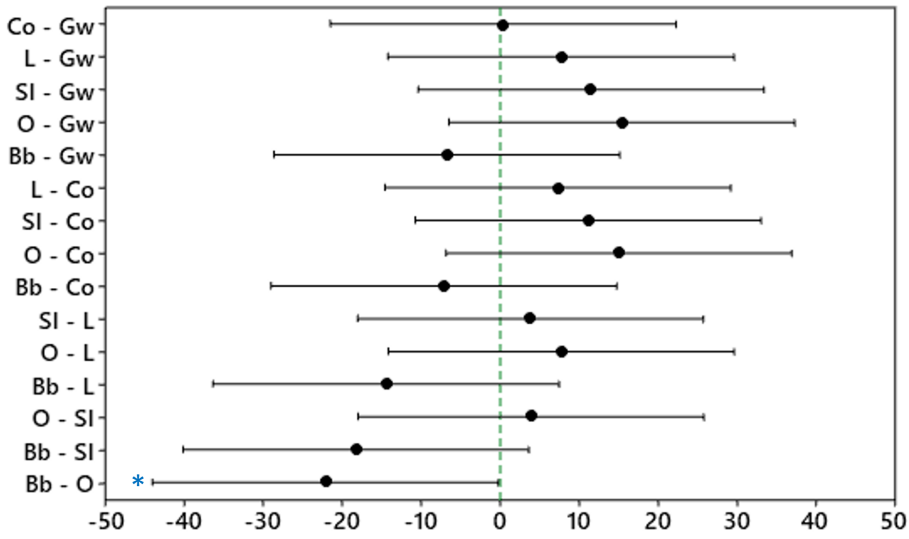


**Figure 4.55:** Tukey confidence intervals for prism orientation ($Ang$) comparing the evaluated specimens. There is statistical difference in prism orientation between the animals that share confidence intervals that do not contain zero (Blue asterisk)

## 4.4 Linear correlation

Pearson correlation coefficient ($\rho$) between $BFQ$ and all the analyzed properties is shown in figure 4.56. Size and color intensity of the circle shown in the upper diagonal matrix are indicators of the correlation between the properties shown, however, for ease of interpretation, the correlation coefficient is shown in the lower diagonal matrix.

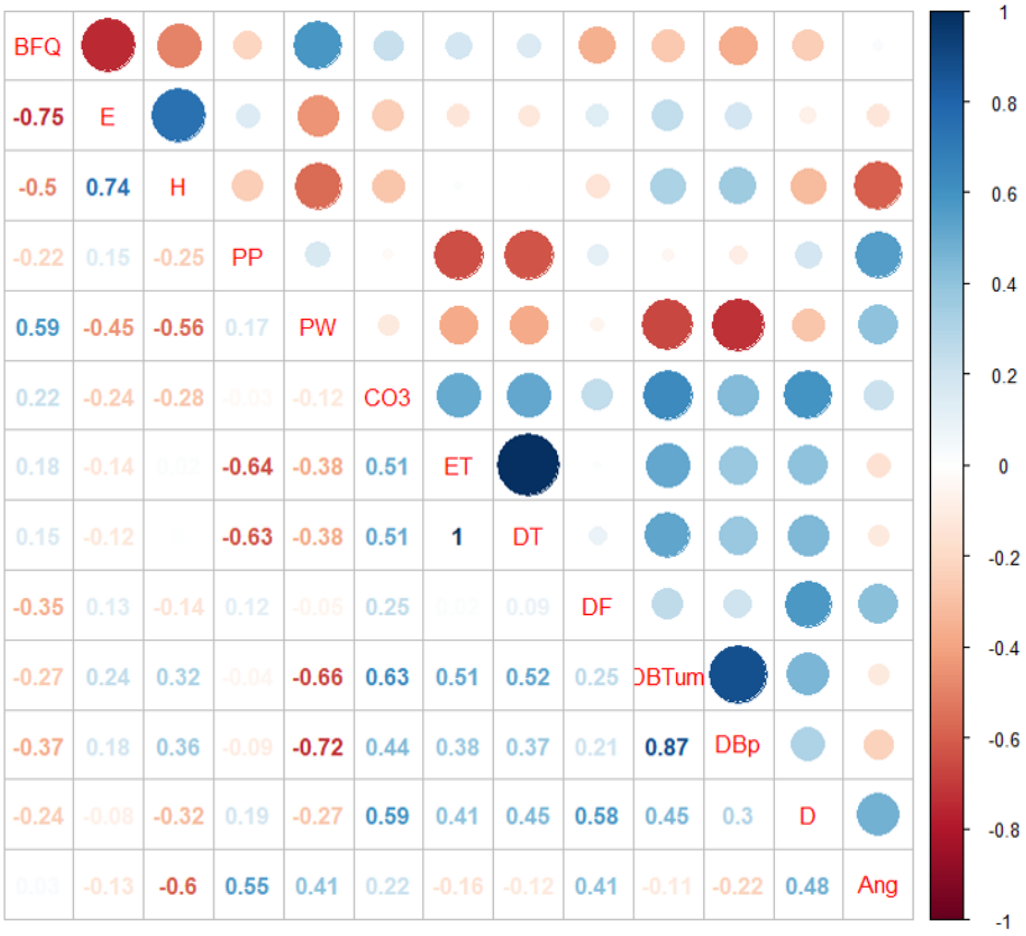


**Figure 4.56:** Pearson correlation coefficient between $BFQ$ and all the evaluated properties. Values in blue show a positive correlation while values in red show a negative correlation

Among the possible 92 paired combinations of the analyzed properties, only 21 of them show a significant correlation ($p < 0.05$), Pearson correlation coefficient ($\rho$) and $p$-value for those combinations are shown in table 4.6.

**Table 4.6:** Significant pairwise Pearson correlation for the analyzed properties

| **Sample** 1 | **Sample** 2 | $\rho$ | $p$**-value** | **Sample** 1 | **Sample** 2 | $\rho$ | $p$**-value** |
|---|---|---|---|---|---|---|---|
| $BFQ$ | $E$ | $-0.75$ | 0.0004 | $CO_3$ | $ET$ | 0.51 | 0.0309 |
| $BFQ$ | $H$ | $-0.50$ | 0.0361 | $CO_3$ | $DT$ | 0.51 | 0.0297 |
| $BFQ$ | $PW$ | 0.59 | 0.0101 | $CO_3$ | $DBT\mu m$ | 0.63 | 0.0048 |
| $E$ | $H$ | 0.74 | 0.0004 | $CO_3$ | $D$ | 0.59 | 0.0093 |
| $H$ | $PW$ | $-0.56$ | 0.0151 | $ET$ | $DT$ | 0.99 | 0.0000 |
| $H$ | $Ang$ | $-0.60$ | 0.0087 | $ET$ | $DBT\mu m$ | 0.51 | 0.0291 |
| $PP$ | $ET$ | $-0.64$ | 0.0041 | $DT$ | $DBT\mu m$ | 0.52 | 0.0269 |
| $PP$ | $DT$ | $-0.63$ | 0.0051 | $DF$ | $D$ | 0.58 | 0.0117 |
| $PP$ | $Ang$ | 0.55 | 0.0179 | $DBp$ | $DBT\mu m$ | 0.87 | 0.0000 |
| $PW$ | $DBp$ | $-0.72$ | 0.0007 | $D$ | $Ang$ | 0.48 | 0.0448 |
| $PW$ | $DBT\mu m$ | $-0.66$ | 0.0026 | | | | |

# 5 Discussion

In this chapter the analysis of the previously shown results is performed. Initially, an analysis of the mechanical and chemical properties evaluated is carried out, later the correlation between $BFQ$ and these properties is analyzed, and finally the relationship between these variables and the taxonomic classification or feeding patterns of the evaluated specimens is analyzed.

The measured properties are compared between the analyzed specimens, grouped either by their feeding pattern (carnivores and omnivores) or by their taxonomic classification (Table 3.1). When comparing specimens by their taxonomic classification, only those belonging to the order Carnivora are compared: Lion, Snow leopard and Oncilla (sub-order Feliformia); Gray wolf and Black bear (sub-order Caniformia). Since the Common opossum belongs to the order Didelphimorphia, it was not compared with the other specimens studied in this research, in terms of its taxonomic classification.

## 5.1 General findings

### 5.1.1 Property mapping

When analyzing the mapping performed on the mechanical and chemical properties, it was observed that, in general, as the distance to the DEJ increases, there is an increase in elastic modulus (Fig. 4.5) and hardness (Fig. 4.10), a reduction in phosphate peak position (Fig. 4.15) but an increase in phosphate peak width (Fig. 4.20) and in carbonate substitution (Fig. 4.25). When these results are compared with those obtained in human (Park et al., 2008; Constantino et al., 2011; Xu et al., 2012) non-human primate enamel (Darnell et al., 2009; Campbell et al., 2012; Constantino et al., 2012), as well as other terrestrial (O'Brien et al., 2014; Wang et al., 2019) and aquatic mammals (Constantino et al., 2011), the same changes in mechanical and chemical properties are observed with increasing distance to the DEJ. These

changes in enamel properties may be due to the way in which the prisms are organized, that is, to the variation in enamel ultrastructure from the DEJ to the outter enamel.

### 5.1.2 Linear correlations

As the relationship between enamel mechanical and chemical properties has been reported (Baldassarri, Margolis, and Beniash, 2008; Xu et al., 2012; Akkus, Karasik, and Roperto, 2017; Mansoor et al., 2019), the correlation between $BFQ$ and these properties was analyzed. Table 4.6 and the correlation matrix (Fig. 5.1) show that:

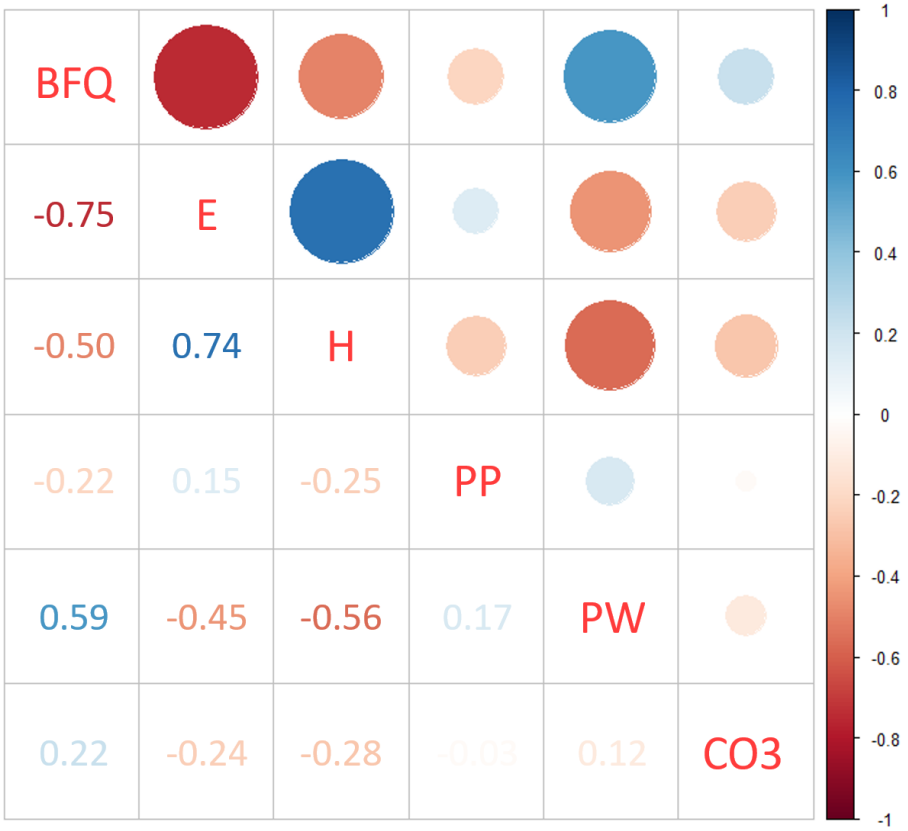


**Figure 5.1:** Pearson correlation coefficient between $BFQ$, mechanical and chemical properties. Positive correlations are shown in blue and negative ones in red. There is a significant correlation between: $BFQ$ and elastic modulus; $BFQ$ and hardness; elastic modulus and hardness; $BFQ$ and phosphate peak width, and hardness and phosphate peak width ($p < 0.05$)

- There is a negative correlation between $BFQ$ and elastic modulus ($\rho = -0.75$, $p = 0.0004$) and between $BFQ$ and hardness ($\rho = -0.50$, $p = 0.0361$). Both elastic modulus and hardness are lower in Gray wolf (animal with higher $BFQ$) and higher in Black bear (animal with lower $BFQ$). To the best of my knowledge, no study has yet been conducted that correlates $BFQ$ with enamel mechanical and chemical properties.

- There is a positive correlation between elastic modulus and hardness ($\rho = 0.74$, $p = 0.0004$), this correlation has been previously reported for human enamel (Cuy et al., 2002; Park et al., 2008; Zhang et al., 2014; Mansoor et al., 2019).

- There is a positive correlation between $BFQ$ and phosphate peak width ($PW$) ($\rho = 0.59$, $p = 0.0101$) and a negative correlation between hardness and phosphate peak width ($\rho = -0.56$, $p = 0.0151$). As for the mechanical properties, it is not known that a correlation between $BFQ$ and enamel chemical properties has been reported. Correlation between enamel mechanical an chemical properties has been previously reported for humans (Cuy et al., 2002; Xu et al., 2012).

Correlation between the ultrastructural properties and $BFQ$ was also analyzed. Table 4.6 and figure 5.2 show that there is no significant correlation between $BFQ$ and any of the ultrastructural properties. However, a correlation was found between some of the ultrastructural properties, such as:

- Positive correlation ($\rho = 0.99$, $p = 0.0000$) between enamel thickness ($ET$) and decussated thickness ($DT$), this implies that in all the analyzed specimens, changes in enamel thickness are almost fully reflected in changes in decussated thickness.

- Positive correlation between enamel thickness and decussated band thickness ($DBT\mu m$), and between decussated thickness and decussated band thickness ($\rho = 0.51$, $p = 0.0291$, and $\rho = 0.52$, $p = 0.0269$ respectively). Taking into account that the decussated region is responsible for preventing crack growth (the longer the winding path that the cracks must travel, the more energy is required), it could be concluded that crack growth prevention occurs not only from the outer to

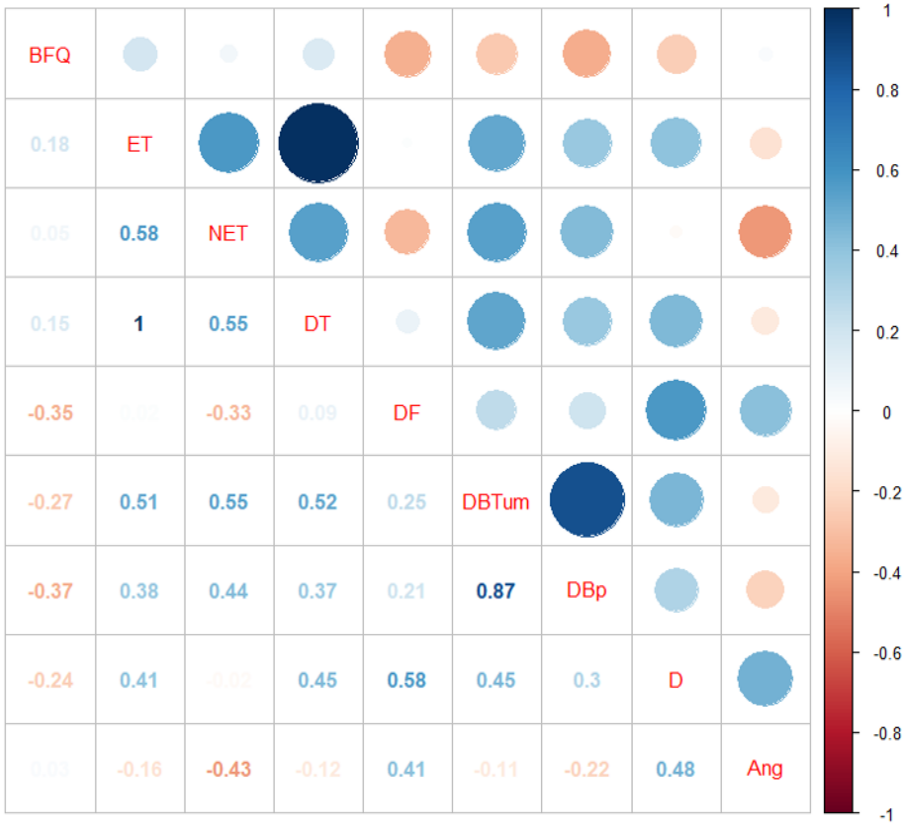


**Figure 5.2:** Pearson correlation coefficient between $BFQ$ and ultrastructural properties. Positive correlations ares shown in blue and negative ones in red. There is no significant correlation between $BFQ$ any ultrastructural properties

the inner enamel but also occurs in a direction parallel to the DEJ, increasing the path a crack must follow to cause enamel fracture.

- Positive correlation ($\rho = 0.58, p = 0.0117$) between decussated fraction ($DF$) and prism diameter ($D$). Decussated fraction is defined as the ratio between decussated thickness and enamel thickness. Although the correlation between decussated thickness and prism diameter is not significant ($p > 0.05$), it can be assumed that part of the variation in decussated thickness can be explained from the variation in the prism diameter. That is, the thickness of the decussation region does not depend solely on the number of prisms in this region (property that was not measured) but also the diameter of the prisms.

- Positive correlation ($\rho = 0.87$, $p = 0.0000$) between decussated band thickness and the number of prisms in the decussated band. Decussated band thickness depends on the number of prisms in the band and their diameter. This high correlation can be explained by taking into account the way in which decussated band thickness was measured (Fig. 3.7) and the non-significant correlation between prism diameter and decussated band thickness ($p > 0.05$). That is, changes in decussated band thickness are largely due to changes in the number of prisms in the band (which explains this correlation) and the other part to changes in prism diameter (non significant correlation). Decussated band thickness is traditionally measured in the number of prisms per band. In most mammals that have HSBs, the thickness of these bands is about six to fifteen prisms, but larger mammals tend to have thicker HSBs (Kawai, 1955; von Koenigswald, Holbrook, and Rose, 2011; Mao, Wang, and Meng, 2015; Yilmaz, Koldehoff, and Schneider, 2018).

- Finally, there is only one significant correlation between mechanical and ultrastructural properties: hardness ($H$) and prism orientation ($Ang$) are negatively correlated ($\rho = -0.60$, $p = 0.0087$). However, the analysis of this correlation must be carried out with special care, since, due to the way in which the $Ang$ were measured (always on the prisms over the diazones), this property can not be easily compared with the mechanical or chemical properties, which were made in prisms located in both diazones and parazones

Although mammalian enamel ultrastructure has been extensively studied, the investigations found in the literature are mainly descriptive, do not show ultrastructural properties measurements (von Koenigswald and Goin, 2000; Stefen, 2001; Wiszniowska et al., 2010; von Koenigswald, Holbrook, and Rose, 2011; von Koenigswald and Reumer, 2020) or do not compare these measurements between different species (Na Ayudhya and Wannaprasert, 2020), neither relate mechanical, chemical and ultrastructure enamel properties with mammalian bite force.

Even though there are 21 combinations of statistically significant correlations, only in five of those combinations the coefficient of determination ($R^2 = \rho^2$) is greater than 0.50 (Table 5.1), that is, in these

correlations more than $50\%$ of the proportion of the variation in one property can be explained from the variation of the other, which implies a high dependence of the value of one property on the other.

**Table 5.1:** Significant correlations with coefficient of determination ($R^2$) greater than $0.5$

| **Sample** $1$ | **Sample** $2$ | $\rho$ | $p$**-value** | $R^2$ |
|---|---|---|---|---|
| $BFQ$ | $E$ | $-0.75$ | $0.0004$ | $0.56$ |
| $E$ | $H$ | $0.74$ | $0.0004$ | $0.55$ |
| $PW$ | $DBp$ | $-0.72$ | $0.0007$ | $0.53$ |
| $ET$ | $DT$ | $0.99$ | $0.0000$ | $0.99$ |
| $DBp$ | $DBT\mu m$ | $0.87$ | $0.0000$ | $0.76$ |

Taking into account the correlations shown in table 5.1, the analysis of the results of this research were carried out on the following properties: elastic modulus, hardness, phosphate peak width, enamel thickness, decussated thickness, decussated band thickness and number of prisms in the decussated band. However, the correlations will not be the starting point of the analysis, as some correlations do not have a reasonable theoretical or practical explanation (such as the correlation between the phosphate peak width and the number of prisms in the decussated band). Correlation is an important criterion for the selection of variables (among all existing ones), but it is not decisive. These properties will be analyzed in terms of their importance in enamel mechanical behavior (i.e. elastic modulus and hardness), of the relationships previously established with others properties (Phosphate peak width has already been reported as a variable that influences enamel mechanical properties) and of their apparent importance in the behavior of enamel in response to mechanical loads produced during chewing (enamel thickness, decussated thickness, decussated band thickness and number of prisms in the decussated band).

## 5.2 Relationship between enamel ultrastructure characteristics, taxonomic classification and feeding patterns

When the specimens are analyzed based on their taxonomic classification, only five of the six analyzed specimens (those belonging to the order Carnivora) can be compared, these specimens are classified

into two sub-orders: Feliformia (Lion, Snow leopard and Oncilla) and Caniformia (Gray wolf and Black bear) (Wilson and Reeder, 2005). On the other hand, taking into account their feeding patterns, the analyzed specimens are grouped as carnivores (Gray wolf, Lion, Snow leopard and Oncilla) and omnivores (Common opossum and Black bear) (Christiansen and Adolfssen, 2005; Hillson, 2005; Brito et al., 2018b; Brito et al., 2018a; Berkovitz and Shellis, 2018d; Berkovitz and Shellis, 2018a; Ferretti et al., 2020).

Carnivore are those that feed on meat and omnivores are those that feed on plants and meat (Bellani, 2020). Gray wolf, Lion, Snow leopard and Oncilla are carnivores and belong to a group described as "hypercarnivores" because their diet is almost exclusively based on meat (more than 70%), more specifically, Gray wolf, Lion and Snow leopard are "large-prey hypercarnivores", that is, they often prey on animals larger than themselves (Berkovitz and Shellis, 2018a), while the Oncilla is a "small-prey hypercarnivore", that is, Oncilla eats animals smaller than itself (Wang, 2002). Common opossum and Black bear are omnivores (Tardieu, Adogwa, and Garcia, 2017; Popp et al., 2018), Common opossum has a omnivorous diet with a preference for animal matter, but they also feed on fruit (Tardieu, Adogwa, and Garcia, 2017; Berkovitz and Shellis, 2018d), while Black bear center his diet on vegetation, however, salmon is an important seasonal prey in its diet (Larivière, 2001). In general, omnivorous mammals consume soft foods, however, when their preferred foods are scarce, they can fall back onto hard foods such as nuts and seeds (Lawn et al., 2013), therefore enamel in omnivores must be able to resist fracture in contact with these different types of food.

When jointly analyzing the feeding patterns and the taxonomic classification, it is found that for animals of the order Carnivora, it has been reported that there is a reduction in $BFQ$ with feeding pattern and prey size, since the larger the prey, the greater the force that is needed to penetrate a bigger tissue (Meers, 2002; Christiansen and Wroe, 2007). The median bite force quotient in different dietary groups is 131 (large prey carnivores), 120 (medium prey carnivores), 92 (small prey carnivores) and 89 (omnivores) (Berkovitz and Shellis, 2018a).

Description of enamel ultrastructure main characteristics (Table 4.3) in terms of taxonomical classification shows that both specimens belonging to the Caniformia sub-order have key-hole shaped prisms (pattern

II) and that prisms are closed (pattern I) in the specimens of the Feliformia sub-order (Lion, Snow leopard and Oncilla). This could imply that the taxonomic classification may influence the shape and pattern of the prisms present in mammalian enamel.

Taking into account the feeding patterns there does not seem to be a relationship. In the two omnivore specimens, prism shape and prism pattern are different: closed-circular (pattern I) in Common opossum and key-hole (pattern II) in Black bear. The same happens in the carnivore specimens: key-hole (pattern II) in Gray wolf, closed (irregular, hexagonal and circular, pattern I) in Lion, Snow Leopard and Oncilla respectively. Furthermore, it should be noted that the enamel types (decussated or radial) are the same for all specimens.

The great ultrastructural complexity of dental enamel is the result of an evolutionary process (von Koenigswald, 1997). Enamel ultrastructure may be a factor that allows mammals to be grouped either by their feeding pattern (Peres Line and Duarte Novaes, 2005) or by their taxonomic classification (von Koenigswald, Martin, and Pfretzschner, 1993). Prism type (define by shape and pattern) can characterize some orders, the enamel type can typify taxa at about the family rank and finally, the *Schmelzmuster* can characterize a genus.

In terms of ultrastructure, the *Schmelzmuster* is defined as a specific combination of enamel types and is related to the functionality of the tooth (von Koenigswald, 1997). Different enamel types (decussated or radial), which are defined according to the orientation of the prisms, also have different functional meanings, therefore the taxonomic value of enamel structures is largely limited to the Schmelzmuster level (von Koenigswald and Pfretzschner, 1991).

## 5.3 Relationship between enamel properties, taxonomic classification and feeding patterns

### 5.3.1 Elastic modulus

The inverse correlation between $BFQ$ and elastic modulus ($\rho = -0.75$, Fig. 5.3 and table 4.6) may imply that the diet of specimens with higher $BFQ$ include large preys or hard foods. When animals feed

on hard food or on large preys, elastic modulus must be small to withstand the stress generated, in order to prevent enamel fracture and loss of tooth functionality.

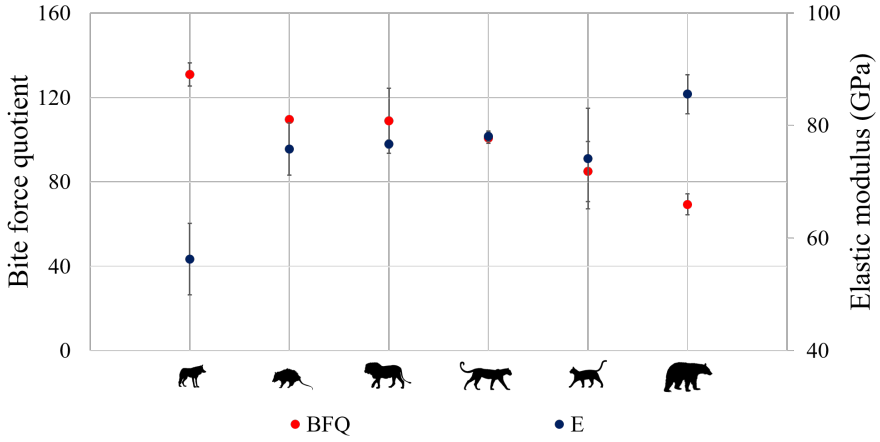


**Figure 5.3:** Bite force quotient ($BFQ$) and elastic modulus ($E$) for the analyzed specimens. The negative correlation ($\rho = -0.75$, $p = 0.0004$) between $BFQ$ and elastic modulus is observed

Figure 5.3 shows simultaneously the changes in $BFQ$ and elastic modulus. Gray wolf, Lion and Snow leopard are large-prey hypercarnivores and Common opossum is omnivore (feeds on meat, fruits and hard seeds). As elastic modulus increases, $BFQ$ decreases, which coincides with what would be expected in the Oncilla, which although it is carnivore, specializes in small prey. However, the higher elastic modulus in the Black bear goes against what would be expected of the dental enamel of an animal that can include hard foods in its diet since a high elastic modulus would cause the enamel to become more brittle on contact with these foods. Elastic modulus does not seem to be related either with feeding patterns or with taxonomic classification. Elastic modulus is significantly different only in Gray wolf compared with the other analyzed specimens (Fig. 4.3), but it is not significantly different between other carnivore specimens (Lion, Snow Leopard and Oncilla) and in the other specimen belonging to the sub-order Caniformia (Black bear).

### 5.3.2 Hardness

There is a significant positive correlation between hardness and elastic modulus (Fig. 5.4 and table 5.1). The correlation between hardness and elastic modulus in anisotropic materials that show gradual changes in their mechanical properties (as enamel) has been previously reported (Labonte, Lenz, and Oyen, 2017).

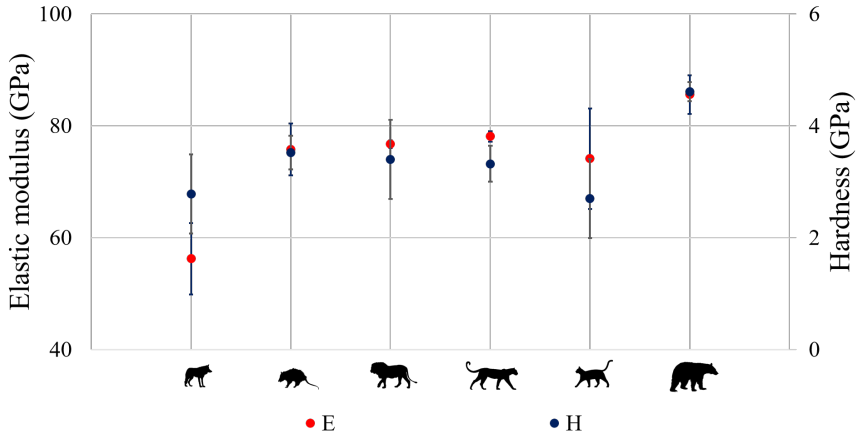


**Figure 5.4:** Elastic modulus ($E$) and hardness ($H$) the analyzed specimens. There is a positive correlation between elastic modulus and hardness ($\rho = 0.74$, $p = 0.0004$)

Figure 5.4 shows that there is a significant difference in hardness between Gray wolf and Black bear (both specimens belong to the sub-order Caniformia) and between Oncilla and Black bear (the former belongs to the sub-order Feliformia and the latter belongs to the sub-order Caniformia). There is also no significant difference in hardness between the two omnivore animals (Common opossum and Black bear), neither between these and two of the carnivore specimens (Lion and Snow leopard), nor between the Common opossum and the Oncilla (omnivore and small-prey hypercarnivore respectively). Therefore, it cannot be said that feeding pattern or taxonomic classification affects enamel hardness.

### 5.3.3 Phosphate peak width

The correlation between phosphate peak width and enamel hardness has been previously reported (Xu et al., 2012). However, the results of this research show that although there is a significant correlation

($p < 0.05$), less than $50\%$ of the change in hardness is produced by a change in phosphate peak width ($R^2 < 0.5$). This low correlation is also observed in figure 5.5.

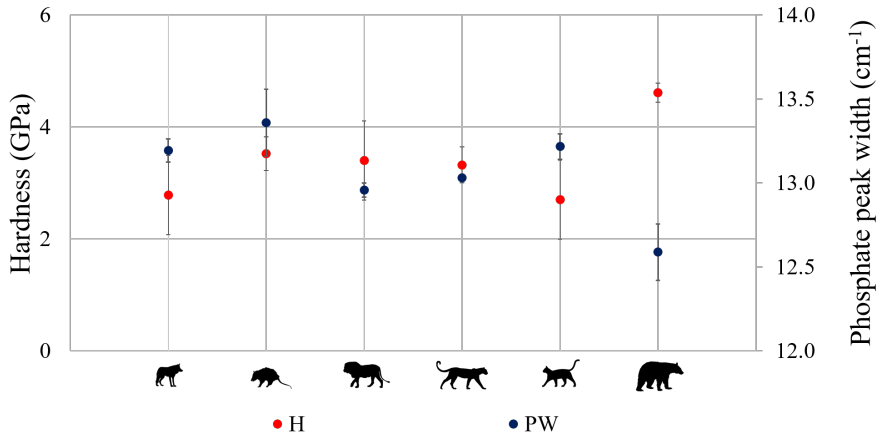


**Figure 5.5:** Hardness ($H$) and phosphate peak width ($PW$) for the analyzed specimens, there is a negative but weak correlation ($\rho = -0.56$, $R^2 = 0.31$) between hardness and phosphate peak width

There is no significant difference in phosphate peak width between the analyzed carnivore specimens (Gray wolf, Lion, Snow leopard and Oncilla), this would indicate that taxonomic classification (Canifformia vs Feliformia) does not influence on phosphate peak width. There are significant differences in the phosphate peak width between Common opossum (omnivore), Lion and Snow leopard (the latter are large-prey carnivores), and between Black bear (omnivore) and all other specimens. Therefore, it could be concluded that the type of food (even within the same food pattern) does influence on phosphate peak width. Phosphate peak width is inversely related to enamel crystallinity. Changes in enamel crystallinity are caused by food intake and enamel maturation time (Curson and Duggal, 2003; Humphrey et al., 2008; Kallistová et al., 2018). Variations in enamel crystallinity produce variations in its mechanical properties; the higher the crystallinity, the better its mechanical properties (Xu et al., 2012; Kallistová et al., 2018).

### 5.3.4 Enamel thickness and Decussated thickness

Enamel thickness and decussated thickness are jointly analyzed due to the high correlation between them ($\rho = 0.99$). Two of the large-prey hypercarnivores (Gray wolf and Lion) have the thickest enamel,

followed by the Black bear (omnivore), the Oncilla and the Snow leopard (both hypercarnivores) and lastly the Common opossum (omnivore). In other words, according to these values, there does not seem to be an influence on enamel thickness, either due to the type of diet or by the taxonomic classification.

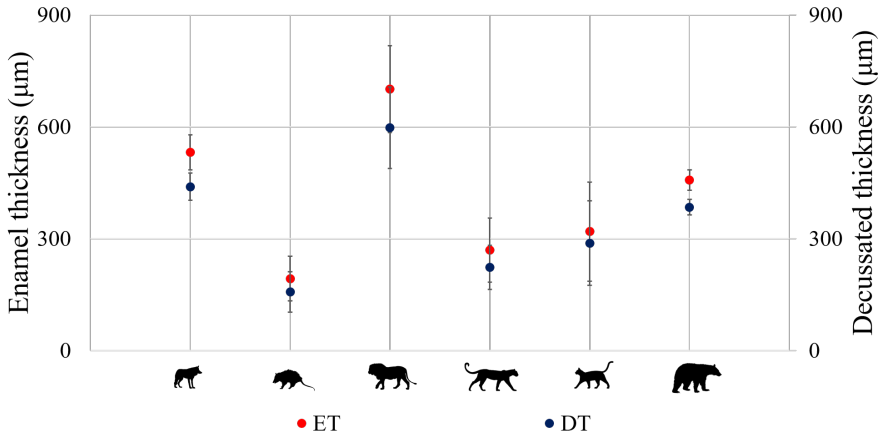


**Figure 5.6:** Enamel thickness ($ET$) and decussated thickness ($DT$) for the analyzed specimens

Enamel thickness is a relevant factor in terms of feeding patterns since it can influence the response of the tooth from two points of view: morphological (the shape of the enamel coating on the dental crown) and mechanical (wear and fracture resistance caused by the permanent contact with other teeth and with food) (Shellis et al., 1998). Enamel thickness has been evaluated in humans (Daubert et al., 2016), non-human primates (Lucas et al., 2009) and other mammals (Yilmaz, Koldehoff, and Schneider, 2018; Häkkinen et al., 2019; Wang et al., 2019; Zhang et al., 2020a). Considering diet as a comparison factor, several authors have found that, in animals that feed on hard foods, enamel is thicker (Teaford, 2007; Ungar, 2008; Schwartz, McGrosky, and Strait, 2020). Differences have also been reported between the thickness of tooth enamel between the buccal and lingual regions (in mandibular and maxillary molars respectively) (Gantt and Rafter, 2008). Although in this investigation three different regions of the tooth were evaluated (cervical, cuspal and intercuspal), different teeth were not compared nor the sides (buccal or lingual) of the specimens were compared. However, the fact that the enamel is thick is not enough to be able to feed on hard objects, this must be accompanied by a structural reinforcement, in this case, enamel decussation (Rensberger, 2000)

In the same way as in enamel thickness, there is no evidence that decussated thickness is influenced by feeding patterns or by the taxonomic classification of the analyzed specimens (Fig. 5.6). The almost perfect correlation between enamel thickness and decussated thickness may be due to an evolutionary mechanism of enamel, regardless of the feeding pattern or taxonomy. The dependence between these variables could be a fundamental parameter in the ultrastructure, helping to withstand repeated mechanical loads during dental function, keeping the decussation fraction almost constant and therefore the energy required for the creation and growth of cracks.

### 5.3.5 Decussated band thickness and Number of prisms in the decussated band

The high but not perfect correlation between decussated band thickness and number of prisms in the decussated band ($\rho = 0.87$, Fig. 5.7) could be explained from the fact that a greater number of prisms in the decussated band would cause an increase in the thickness of the decussated band, but it should also be taken into account that the thickness of the decussated band also depends on prism diameter.

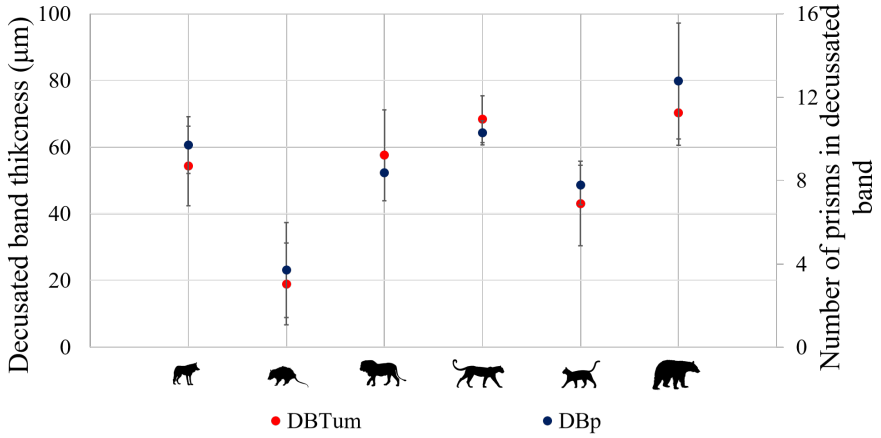


**Figure 5.7:** Decussated band thickness ($DBT\mu m$) and number of prism in the decussated band ($DBp$) for the analyzed specimens

Both the prism diameter and the number of prisms in the decussated band in Common opossum (omnivore) are the lowest among all the analyzed specimens, therefore the thickness of the decussated band in this specimen is lower than in the other specimens. In the Oncilla (carnivore), the thickness of the decussated band is low, but it does not show significant differences either with the Common opossum or

with the other specimens. This low value is mainly due to the small number of prisms in the decussated band that are not compensated with prism diameter (Table 4.5). There is no evidence that decussated band thickness (Fig. 4.42) or the number of prisms in the decussated band (Fig. 4.46) are influenced by feeding patterns or taxonomic classification since there are no significant differences between Black Bear (omnivore and belonging to the sub-order Caniformia) and the hypercarnivore specimens (from both sub-orders) or between Common opossum (omnivore) and Oncilla (hypercarnivore).

# 6 Conclusions and Recommendations

This is the first time that the mechanical, chemical and ultrastructural properties of the dental enamel of different mammals have been studied in search of coincidences and / or differences that lead to an understanding of whether these enamel characteristics are due to general conditions of mammals or to specific conditions of each species.

The correlation found by Park et al. (2008), Zhang et al. (2014), and Mansoor et al. (2019) between elastic modulus and hardness ($H$) in human enamel was found in this study for the analyzed specimens ($\rho = 0.74$). In the same way, changes in mechanical and chemical properties are observed with increasing distance to the DEJ in all the specimens analyzed in this study. These changes have been previously reported by Park et al. (2008) and Xu et al. (2012) for human enamel; Darnell et al. (2009) and Campbell et al. (2012) for non-human primate enamel and by O'Brien et al. (2014) and Wang et al. (2019) for other mammals. These variations in enamel mechanical and chemical properties should be taken into account in the design of similar materials (brittle and with high fracture toughness, for example) to achieve mechanical responses similar to those provided by enamel in response to chewing loads.

Furthermore, there is a negative correlation ($\rho = -0.75$) between $BFQ$ and elastic modulus ($E$), which is consistent with the importance of having a low elastic modulus when feeding on hard foods, so that the enamel can withstand the stresses generated without fracturing and without losing tooth functionality. Finally, phosphate peak width ($PW$) is positively correlated with $BFQ$ ($\rho = 0.59$) and negatively correlated with hardness ($\rho = -0.56$), the correlation between mechanical and chemical properties of human enamel was reported by Cuy et al. (2002) and Xu et al. (2012). Neither elastic modulus nor hardness seem to be related either with feeding patterns or taxonomic classification. Finally, phosphate peak width does not depend on the classification but it does seem to depend on feeding pattern.

Considering ultrastructural properties, there is no significant correlation between $BFQ$ and any of the ultrastructural properties, which would allow to conclude that mammalian enamel ultrastructure is independent of taxonomic classification or feeding patterns.

Mammalian prism shape and pattern may be influenced by taxonomic classification but not by feeding patterns, however, enamel types seem to be independent of taxonomic classification or feeding patterns. There is a positive correlation ($\rho = 0.99$) between enamel thickness ($ET$) and decussated thickness ($DT$), which implies that for all samples analyzed, changes in enamel thickness are almost completely reflected in changes in decussated thickness. This high correlation between enamel thickness and decussated thickness and the fact that decussated fraction (defined as the fraction of enamel thickness that is composed of decussated rods, $DF = DT/ET$) is higher than $0.8$ in all the analyzed specimens (regardless of the taxonomic classification or feeding patterns of the analyzed species), could imply that as Yahyazadehfar, Bajaj, and Arola (2013) reported, decussated fraction may be important in retarding crack extension.

Enamel thickness is a relevant factor in terms of feeding patterns since it can influence the response of the tooth from a morphological and a mechanical point of view. In other words, according to the data found in this study, there does not seem to be an influence on enamel thickness, either due to the feeding patterns or by the taxonomic classification. In the same way as in enamel thickness, there is no evidence that decussated thickness is influenced by feeding patterns or by the taxonomic classification of the analyzed specimens. Furthermore, the correlation between enamel thickness and decussated thickness may be due to an evolutionary mechanism of enamel regardless of the feeding pattern or taxonomy. Enamel thickness and decussated band thickness ($DBT\mu m$) as well as decussated thickness and decussated band thickness are positive correlated ($\rho = 0.51$ and $\rho = 0.52$ respectively).

Considering that enamel decussation is responsible for retarding crack extension, it can be concluded that crack growth retarding may occur from the external to the internal enamel and in a direction parallel to the DEJ. In other words, the path that a crack must follow to cause enamel fracture may be longer. There is no evidence that decussated band thickness or the number of prisms in the decussated band are influenced by feeding patterns or taxonomic classification. There is a positive correlation ($\rho = 0.58$)

between decussated fraction ($DF$) and prism diameter ($D$) and between decussated band thickness and the number of prisms in the decussated band ($DBp$) ($\rho = 0.87$). Decussated fraction depends on both enamel thickness and decussated thickness, in turn these two properties as well as decussated fraction depend on prism diameter. It could be concluded that both the number of prisms and their diameter are important ultrastructural properties to retard the growth of cracks.

The spatial variation of enamel decussation patterns has not yet been explored in different species of animals (mammals or not) and may be an important factor in the design of natural materials with high fracture toughness. Finally, von Koenigswald and Goin (2000), Stefen (2001), Wiszniowska et al. (2010), von Koenigswald, Holbrook, and Rose (2011), and von Koenigswald and Reumer (2020) have extensively studied mammalian enamel ultrastructure. However, these studies cannot be directly compared with what has been done in this study since: 1) they do not show measurements of ultrastructural properties, 2) they do not compare these measurements between different species or 3) they do not relate the mechanical, chemical and ultrastructural properties of the enamel with the bite force of mammals.

An important recommendation that arises from the analysis of the data of this study is to increase the number of samples analyzed by each species, both in the number of teeth of the same specimen, and in the number of specimens of each species analyzed, in addition to analyzing the variations on the different surfaces of the tooth (buccal, lingual, palatal, occlusal, medial and distal, for example). It would also be appropriate to analyze different types of teeth (incisors, canines, premolars and molars) in order to look for variations in their properties according to their function when cutting, tearing and grinding food.

It would also be appropriate to study the correlation between the chemical properties of enamel, mainly the width of the phosphate peak, with feeding patterns to determine the exact degree of correlation and its relationship with phylogenetics.

# Bibliography

Akkus, A, D Karasik, and R Roperto (2017). "Correlation between micro-hardness and mineral content in healthy human enamel". In: *Journal of Clinical and Experimental Dentistry* 9.4, e569–e573. DOI: 10.4317/jced.53345.

An, B et al. (2012). "The role of property gradients on the mechanical behavior of human enamel". In: *Journal of the Mechanical Behavior of Biomedical Materials* 9, pp. 63–72. DOI: 10.1016/j.jmbbm.2012.01.009.

Arango-Santander, S et al. (2020). "Chemical, structural and mechanical characterization of bovine enamel". In: *Archives of Oral Biology* 109.1, p. 104573. DOI: 10.1016/j.archoralbio.2019.104573.

Bajaj, D and D Arola (2009a). "On the R-curve behavior of human enamel". In: *Biomaterials* 30.23-24, pp. 4037–4046. DOI: 10.1016/j.biomaterials.2009.04.017.ON.

— (2009b). "Role of prism decussation on fatigue crack growth and fracture of human enamel". In: *Acta Biomaterialia* 5.8, pp. 3045–3056. DOI: 10.1016/j.actbio.2009.04.013.

Baldassarri, M, H C Margolis, and E Beniash (2008). "Compositional determinants of mechanical properties of enamel". In: *Journal of Dental Research* 87.7, pp. 645–649. DOI: 10.1177/154405910808700711.

Bechtle, S, S F Ang, and G A Schneider (2010). "On the mechanical properties of hierarchically structured biological materials". In: *Biomaterials* 31.25, pp. 6378–6385. DOI: 10.1016/j.biomaterials.2010.05.044.

Bellani, G G (2020). "Order of carnivores (Carnivora)". In: *Felines of the world - Discovery in taxonomic classification and history*. Elsevier. Chap. 1, pp. 1–12. DOI: 10.1016/B978-0-12-816503-4.00001-5.

Beniash, E et al. (2019). "The hidden structure of human enamel". In: *Nature Communications* 10.1, p. 4383. DOI: 10.1038/s41467-019-12185-7.

Bergqvist, L P and W von Koenigswald (2017). "The dentition of *Carodnia vieirai* (Mammalia: Xenungulata): enamel microstructure and mastication pattern". In: *Palaeontologia Electronica* 20.2.30A, pp. 1–15. DOI: 10.26879/703.

Berkovitz, B K B (2013). *Nothing but the tooth: a dental odyssey*. 1st ed. London, UK: Elsevier, p. 264. DOI: 10.1016/C2011-0-06944-2.

Berkovitz, B K B, G R Holland, and B J Moxham (2017). *Oral anatomy histology and embryology*. 5th. Elsevier Health Sciences, p. 472.

Berkovitz, B K B and P Shellis (2018a). "Carnivora". In: *The teeth of mammalian vertebrates*. Vol. 38. 2. Elsevier. Chap. 15, pp. 267–304. DOI: 10.1016/B978-0-12-802818-6.00015-6.

— (2018b). "General introduction". In: *The teeth of mammalian vertebrates*. Elsevier. Chap. 1, pp. 1–24. DOI: 10.1016/B978-0-12-802818-6.00001-6.

— (2018c). "Mammalian tooth structure and function". In: *The teeth of mammalian vertebrates*. Elsevier. Chap. 2, pp. 25–46. DOI: 10.1016/B978-0-12-802818-6.00002-8.

— (2018d). "Monotremata and Marsupialia". In: *The teeth of mammalian vertebrates*. Elsevier. Chap. 4, pp. 57–74. DOI: 10.1016/B978-0-12-802818-6.00004-1.

Biswas, N et al. (2012). "Orientational effect in nanohardness of functionally graded microstructure in enamel". In: *Journal of The Institution of Engineers (India): Series D* 93.2, pp. 87–95. DOI: 10.1007/s40033-012-0011-z.

Boyde, A (1964). "The structure and development of mammalian enamel." Doctoral thesis.

— (1997). "Microstructure of enamel". In: *Ciba Foundation Symposium 205 - Dental Enamel*. Ed. by D J Chadwick and G Cardew. 205. CIBA foundation, pp. 18–31. DOI: 10.1002/9780470515303.ch3.

Brito, J et al. (2018a). *Mamíferos de la costa - Guía dinámica*. Museo de Zoología, Pontificia Universidad Católica del Ecuador, p. 731.

Brito, J et al. (2018b). *Mamíferos de los Andes - Guía dinámica*. Museo de Zoología, Pontificia Universidad Católica del Ecuador, p. 1033.

Burke Museum (2020). *Mammalogy | Burke Museum*.

Campbell, S E et al. (2012). "Nanoindentation of lemur enamel: An ecological investigation of mechanical property variations within and between sympatric species". In: *American Journal of Physical Anthropology* 148.2, pp. 178–190. DOI: 10.1002/ajpa.21582.

Carden, A and M D Morris (2000). "Application of vibrational spectroscopy to the study of mineralized tissues (review)". In: *Journal of Biomedical Optics* 5.3, p. 259. DOI: 10.1117/1.429994.

Carreon, A H and P D Funkenbusch (2019). "Nanoscale properties and deformation of human enamel and dentin". In: *Journal of the Mechanical Behavior of Biomedical Materials* 97, pp. 74–84. DOI: 10.1016/j.jmbbm.2019.05.009.

Chai, H et al. (2009a). "A simple model for enamel fracture from margin cracks". In: *Acta Biomaterialia* 5.5, pp. 1663–1667. DOI: 10.1016/j.actbio.2008.11.007.

Chai, H et al. (2009b). "Remarkable resilience of teeth". In: *National Academy of Sciences*. Vol. 106. 18, pp. 7289–7293. DOI: 10.1073/pnas.0902466106.

Cheng, Z J et al. (2010). "The mechanical anisotropy on a longitudinal section of human enamel studied by nanoindentation". In: *Journal of Materials Science: Materials in Medicine* 21.6, pp. 1811–1816. DOI: 10.1007/s10856-010-4052-2.

Christiansen, P (2007). "Canine morphology in the larger Felidae: implications for feeding ecology". In: *Biological Journal of the Linnean Society* 91.4, pp. 573–592. DOI: 10.1111/j.1095-8312.2007.00819.x.

Christiansen, P and J S Adolfssen (2005). "Bite forces, canine strength and skull allometry in carnivores (Mammalia, Carnivora)". In: *Journal of Zoology* 266.2, pp. 133–151. DOI: 10.1017/S0952836905006643.

Christiansen, P and S Wroe (2007). "Bite forces and evolutionary adaptations to feeding ecology in carnivores". In: *Ecology* 88.2, pp. 347–358.

Constantino, P J et al. (2009). "The influence of fallback foods on great ape tooth enamel". In: *American Journal of Physical Anthropology* 140.4, pp. 653–660. DOI: 10.1002/ajpa.21096.

Constantino, P J et al. (2011). "Adaptation to hard-object feeding in sea otters and hominins". In: *Journal of Human Evolution* 61.1, pp. 89–96. DOI: 10.1016/j.jhevol.2011.02.009.

Constantino, P J et al. (2012). "The role of tooth enamel mechanical properties in primate dietary adaptation". In: *American Journal of Physical Anthropology* 148.2, pp. 171–177. DOI: 10.1002/ajpa.21576.

Curson, M E J and M S Duggal (2003). "Dental disease - Structure of teeth". In: *Encyclopedia of Food Sciences and Nutrition*. Ed. by B Caballero. Elsevier, pp. 1743–1746. DOI: 10.1016/B0-12-227055-X/00324-2.

Cuy, J L et al. (2002). "Nanoindentation mapping of the mechanical properties of human molar tooth enamel". In: *Archives of Oral Biology* 47.4, pp. 281–291. DOI: 10.1016/S0003-9969(02)00006-7.

Daculsi, G and B Kerebel (1978). "High-resolution electron microscope study of human enamel crystallites: Size, shape, and growth". In: *Journal of Ultrasructure Research* 65.2, pp. 163–172. DOI: 10.1016/S0022-5320(78)90053-9.

Darnell, L A et al. (2009). "Variations in the mechanical properties of *Alouatta palliata* molar enamel". In: *American Journal of Physical Anthropology* 141.1, pp. 7–15. DOI: 10.1002/ajpa.21126.

Daubert, D M et al. (2016). "Human enamel thickness and ENAM polymorphism". In: *International Journal of Oral Science* 8.2, pp. 93–97. DOI: 10.1038/ijos.2016.1.

Davis, B M (2011). "Evolution of the tribosphenic molar pattern in early mammals, with momments on the "Dual-Origin" hypothesis". In: *Journal of Mammalian Evolution* 18.4, pp. 227–244. DOI: 10.1007/s10914-011-9168-8.

Eimar, H (2011). "Tooth enamel ultrastructure: correlation between composition and physical properties". Master thesis. McGill University.

Eimar, H et al. (2011). "The role of enamel crystallography on tooth shade". In: *Journal of Dentistry* 39.SUPPL. 3, e3–e10. DOI: 10.1016/j.jdent.2011.11.008.

Ellis, J L et al. (2009). "Cranial dimensions and forces of biting in the domestic dog". In: *Journal of Anatomy* 214.3, pp. 362–373. DOI: 10.1111/j.1469-7580.2008.01042.x.

Evans, A R and S Pineda-Munoz (2018). "Inferring mammal dietary ecology from dental morphology". In: *Methods in Paleoecology*. Ed. by D A Croft, D F Su, and S W Simpson. Vertebrate Paleobiology and Paleoanthropology. Cham, Switzerland: Springer International Publishing. DOI: 10.1007/978-3-319-94265-0.

Fehrenbach, M J and T Popowics (2015). *Student workbook for illustrated dental embryology, histology, and anatomy*. Missouri, U.S., p. 272.

Ferretti, F et al. (2020). "Only the largest terrestrial carnivores increase their dietary breadth with increasing prey richness". In: *Mammal Review* 50.3, pp. 291–303. DOI: 10.1111/mam.12197.

Gantt, D G and J A Rafter (2008). "Evolutionary and functional significance of hominoid tooth enamel". In: *Connective Tissue Research* 39.1-3, pp. 195–206. DOI: 10.3109/03008209809023927.

Gao, S S et al. (2016). "Contact fatigue of human enamel: Experiments, mechanisms and modeling". In: *Journal of the Mechanical Behavior of Biomedical Materials* 60, pp. 438–450. DOI: 10.1016/j.jmbbm.2016.02.030.

Ghadimi, E et al. (2014). "Regulated fracture in tooth enamel: A nanotechnological strategy from nature". In: *Journal of Biomechanics* 47.10, pp. 2444–2451. DOI: 10.1016/j.jbiomech.2014.04.005.

Giacaman, R A, V A Perez, and C A Carrera (2016). "Mineralization processes in hard tissues: Teeth". In: *Biomineralization and Biomaterials*. Ed. by C Aparicio and M P Ginebra. Boston, U.S.: Woodhead Publishing. Chap. 5, pp. 147–185. DOI: 10.1016/B978-1-78242-338-6.00006-5.

Habelitz, S et al. (2001). "Mechanical properties of human dental enamel on the nanometre scale". In: *Archives of Oral Biology* 46, pp. 173–183. DOI: 10.1016/S0003-9969(00)00089-3.

Hájková, P, A Jíra, and L Řehounek (2018). "Verification of behaviour of human enamel for fracture toughness determination". In: *Acta Polytechnica* 58.4, pp. 226–231. DOI: 10.14311/AP.2018.58.0226.

Häkkinen, T J et al. (2019). "Modeling enamel matrix secretion in mammalian teeth". In: *PLoS Computational Biology* 15.5, pp. 1–12. DOI: 10.1371/journal.pcbi.1007058.

Hanlie, H, T Liyun, and J Tao (2006). "The crystal characteristics of enamel and dentin by XRD method". In: *Journal of Wuhan University of Technology-Mater. Sci. Ed.* 21.1, pp. 9–12. DOI: 10.1007/BF02861458.

Hayashi-Sakai, S et al. (2012). "Determination of fracture toughness of human permanent and primary enamel using an indentation microfracture method". In: *Journal of Materials Science: Materials in Medicine* 23.9, pp. 2047–2054. DOI: 10.1007/s10856-012-4678-3.

He, B et al. (2011). "Mineral densities and elemental content in different layers of healthy human enamel with varying teeth age". In: *Archives of Oral Biology* 56.10, pp. 997–1004. DOI: 10.1016/j.archoralbio.2011.02.015.

He, L H (2008). "Mechanical behaviour of human enamel and the relationship to its structural and compositional characteristics". Doctoral thesis. University of Sidney.

He, L H and M V Swain (2009). "Nanoindentation creep behavior of human enamel". In: *Journal of Biomedical Materials Research - Part A* 91.2, pp. 352–359. DOI: 10.1002/jbm.a.32223.

He, L H et al. (2013). "A natural functionally graded biocomposite coating-Human enamel". In: *Acta Biomaterialia* 9.5, pp. 6330–6337. DOI: 10.1016/j.actbio.2012.12.029.

Hillson, S (2005). *Teeth*. 2nd ed. New York, U.S.: Cambridge University Press, p. 373. DOI: 10.1017/CBO9780511614477.

Hite, N J et al. (2019). "The better to eat you with: Bite force in the Naked mole-rat (*Heterocephalus glaber*) is stronger than predicted based on body size". In: *Frontiers in Integrative Neuroscience* 13. DOI: 10.3389/fnint.2019.00070.

Hull, D and T W Clyne (1996). *An introduction to composite materials*. 2nd ed. Cambridge, UK: Cambridge University Press, p. 326. DOI: 10.1017/CBO9781139170130.

Humphrey, L T et al. (2008). "Unlocking evidence of early diet from tooth enamel". In: *National Academy of Sciences of the United States of America*. Vol. 105. 19, pp. 6834–6839. DOI: 10.1073/pnas.0711513105.

Kallistová, A et al. (2018). "Enamel apatite crystallinity significantly contributes to mammalian dental adaptations". In: *Scientific Reports* 8.1, pp. 1–9. DOI: 10.1038/s41598-018-23826-0.

Kawai, N (1955). "Comparative anatomy of the bands of Schreger". In: *Okajimas Folia Anatomica Japonica* 27.2-3, pp. 115–131. DOI: 10.2535/ofaj1936.27.2-3_115.

Kim, S E et al. (2018). "Bite forces and their measurement in dogs and cats". In: *Frontiers in Veterinary Science* 5.76. DOI: 10.3389/fvets.2018.00076.

Kirch, W, ed. (2008). *Encyclopedia of public health*. Dordrecht, NL: Springer Netherlands. DOI: 10.1007/978-1-4020-5614-7.

Koldehoff, J, M V Swain, and G A Schneider (2020). "The geometrical structure of interfaces in dental enamel: A FIB-STEM investigation". In: *Acta Biomaterialia* 104.1, pp. 17–27. DOI: 10.1016/j.actbio.2019.12.040.

Labonte, D, A K Lenz, and M L Oyen (2017). "On the relationship between indentation hardness and modulus, and the damage resistance of biological materials". In: *bioRxiv*. DOI: 10.1101/107284.

Larivière, S (2001). "*Ursus americanus*". In: *Mammalian Species* 647, pp. 1–11. DOI: 10.1644/1545-1410(2001)647<0001:UA>2.0.CO;2.

Lawn, B R et al. (2013). "Inferring biological evolution from fracture patterns in teeth". In: *Journal of Theoretical Biology* 338, pp. 59–65. DOI: 10.1016/j.jtbi.2013.08.029.

Leroy, G et al. (2002). "Human tooth enamel: A Raman polarized approach". In: *Applied Spectroscopy* 56.8, pp. 1030–1034. DOI: 10.1366/000370202760249765.

Lopes, C de C A et al. (2018). "Fourier transform infrared spectroscopy (FTIR) application chemical characterization of enamel, dentin and bone". In: *Applied Spectroscopy Reviews* 53.9, pp. 747–769. DOI: 10.1080/05704928.2018.1431923.

Lucas, P W (2004). *Dental function morphology - How teeth work*. New York, USA: Cambridge University Press, p. 355. DOI: 10.1017/CBO9780511735011.

Lucas, P W and A van Casteren (2015). "The wear and tear of teeth". In: *Medical Principles and Practice* 24.suppl 1, pp. 3–13. DOI: 10.1159/000367976.

Lucas, P W et al. (2008). "Dental enamel as a dietary indicator in mammals". In: *BioEssays* 30.4, pp. 374–385. DOI: 10.1002/bies.20729.

Lucas, P W et al. (2009). "Primate dental enamel: What it says about diet". In: *Comparative dental morphology*. Vol. 13. Basel: KARGER, pp. 44–48. DOI: 10.1159/000242389.

Lucas, P W et al. (2016). "Structure and scale of the mechanics of mammalian dental enamel viewed from an evolutionary perspective". In: *Evolution & Development* 18.1, pp. 54–61. DOI: 10.1111/ede.12169.

Lynch, C D et al. (2010). "Hunter-Schreger band patterns in human tooth enamel". In: *Journal of Anatomy* 217.2, pp. 106–115. DOI: 10.1111/j.1469-7580.2010.01255.x.

Maas, M C and E R Dumont (1999). "Built to last: The structure, function, and evolution of primate dental enamel". In: *Evolutionary Anthropology: Issues, News, and Reviews* 8.4, pp. 133–152. DOI: /10.1002/(SICI)1520-6505(1999)8:4<133::AID-EVAN4>3.0.CO;2-F.

Macchiarelli, R and S E Bailey (2007). "Introduction". In: *Dental perspectives on human evolution*. Ed. by S E Bailey and J J Hublin. Dordrecht, NL: Springer, pp. 139–146. DOI: 10.1007/978-1-4020-5845-5_9.

Mansoor, A et al. (2019). "Correlation between micro-hardness and mineral content in the healthy tooth enamel of humans belonging to different age groups". In: *Pakistan Armed Forces Medical Journal,* 69.6, pp. 1204–1209.

Mao, F, Y Wang, and J Meng (2015). "A systematic study on tooth enamel microstructures of *Lambdopsalis bulla* (multituberculate, mammalia) - Implications for multituberculate biology and phylogeny". In: *PLOS ONE* 10.5. Ed. by Thierry Smith, e0128243. DOI: 10.1371/journal.pone.0128243.

Meers, M B (2002). "Maximum bite force and prey size of *Tyrannosaurus rex* and their relationships to the inference of feeding behavior". In: *Historical Biology* 16.1, pp. 1–12. DOI: 10.1080/08912960210000507 55.

Na Ayudhya, J I and T Wannaprasert (2020). "Tooth morphology and enamel microstructure of the lesser bamboo rat (*Cannomys badius*)". In: *Mammal Study* 45.3, p. 1. DOI: 10.3106/ms2019-0074.

Nanci, A (2017). *Ten Cate's oral histology development, structure, and function*. 9th ed. St Louis, U.S.: Elsevier Health Sciences, p. 352.

O'Brien, S et al. (2014). "Revealing the structural and mechanical characteristics of ovine teeth". In: *Journal of the Mechanical Behavior of Biomedical Materials* 30, pp. 176–185. DOI: 10.1016/j.jmbbm.2013.11.006.

Oliver, W C and G M Pharr (1992). "An improved technique for determining hardness and elastic modulus using load and displacement sensing indentation experiments". In: *Journal of Materials Research* 7.6, pp. 1564–1583. DOI: 10.1557/JMR.1992.1564.

Padmanabhan, S K et al. (2010). "Micro-indentation fracture behavior of human enamel". In: *Dental Materials* 26.1, pp. 100–104. DOI: 10.1016/j.dental.2009.07.015.

Park, S et al. (2008). "Mechanical properties of human enamel as a function of age and location in the tooth". In: *Journal of Materials Science: Materials in Medicine* 19.6, pp. 2317–2324. DOI: 10.1007/s10856-007-3340-y.

Peres Line, S R and P Duarte Novaes (2005). "The development and evolution of mammalian enamel: structural and functional aspects". In: *Brazilian Journal of Morphological Sciences* 22.2, pp. 67–72.

Popowics, T E and S W Herring (2006). "Teeth, jaws and muscles in mammalian mastication." In: *Feeding in domestic vertebrates: from structure to behaviour*. Ed. by V Bels. Wallingford, UK: CABI, pp. 61–83. DOI: 10.1079/9781845930639.0061.

Popp, J N et al. (2018). "Black bear (*Ursus americanus*) and wolf (*Canis spp.*) summer diet composition and ungulate prey selectivity in Ontario, Canada". In: *Mammal Research* 63.4, pp. 433–441. DOI: 10.1007/s13364-018-0368-y.

Price, S A et al. (2012). "Tempo of trophic evolution and its impact on mammalian diversification". In: *Proceedings of the National Academy of Sciences* 109.18, pp. 7008–7012. DOI: 10.1073/pnas.1117133109.

Pro, J W and F Barthelat (2019). "Discrete element models of tooth enamel, a complex three-dimensional biological composite". In: *Acta Biomaterialia* 94, pp. 536–552. DOI: 10.1016/j.actbio.2019.04.058.

Ramakrishnaiah, R et al. (2015). "Applications of Raman spectroscopy in dentistry: Analysis of tooth structure". In: *Applied Spectroscopy Reviews* 50.4, pp. 332–350. DOI: 10.1080/05704928.2014.986734.

Rensberger, J M (2000). "Pathways to functional differentiation in mammalian enamel". In: *Development, function and evolution of teeth*. Ed. by M Teaford, M M Smith, and M W J Ferguson. New York, U.S.: Cambridge University Press. Chap. 18, pp. 252–268. DOI: 10.1017/CBO9780511542626.018.

Rensberger, J M and C Stefen (2006). "Functional differentiation of the microstructure in the upper carnassial enamel of the spotted hyena". In: *Palaeontographica Abteilung A* 278.1-6, pp. 149–162. DOI: 10.1127/pala/278/2006/149.

Rensberger, J M and W von Koenigswald (1980). "Functional and phylogenetic interpretation of enamel microstructure in rhinoceroses". In: *Paleobiology* 6.4, pp. 477–495. DOI: 10.1017/S009483730000364X.

Rensberger, J M and X Wang (2005). "Microstructural reinforcement in the canine enamel of the Hyaenid *Crocuta crocuta*, the Felid *Puma concolor* and the late miocene Canid *Borophagus secundus*". In: *Journal of Mammalian Evolution* 12, pp. 379–403. DOI: 10.1007/s10914-005-6964-z.

Sakae, T (2006). "Variations in dental enamel crystallites and micro-structure". In: *Journal of Oral Biosciences* 48.2, pp. 85–93. DOI: 10.2330/joralbiosci.48.85.

Sakae, T et al. (2011). "Three-dimensional orientation analysis of human enamel crystallites using X-ray diffraction". In: *Journal of Hard Tissue Biology* 20.1, pp. 7–10. DOI: 10.2485/jhtb.20.7.

Schwartz, G T, A McGrosky, and D S Strait (2020). "Fracture mechanics, enamel thickness and the evolution of molar form in hominins". In: *Biology Letters* 16.1, p. 20190671. DOI: 10.1098/rsbl.2019.0671.

Shellis, R P et al. (1998). "Variations in molar enamel thickness among primates". In: *Journal of Human Evolution* 35.4-5, pp. 507–522. DOI: 10.1006/jhev.1998.0238.

Shimizu, D and G A Macho (2008). "Effect of enamel prism decussation and chemical composition on the biomechanical behavior of dental tissue: A theoretical approach to determine the loading conditions to which modern human teeth are adapted". In: *Anatomical Record* 291.2, pp. 175–182. DOI: 10.1002/ar.20633.

Shore, R C et al. (1995). "Structure of mature enamel". In: *Dental enamel formation to destruction*. Ed. by C Robinson, J Kirkham, and R Shore. 1st ed. Boca Raton, U.S.: CRC Press. Chap. 7, pp. 151–166. DOI: 10.1201/9781315150925-7.

Stefen, C (1999a). "Enamel microstructure of recent and fossil Canidae (Carnivora: Mammalia)". In: *Journal of Vertebrate Paleontology* 19.3, pp. 576–587. DOI: 10.1080/02724634.1999.10011166.

— (1999b). "Tooth enamel structure of some Australian carnivorous marsupials". In: *Alcheringa: An Australasian Journal of Palaeontology* 23.2, pp. 111–132. DOI: 10.1080/03115519908619325.

— (2001). "Enamel structure of Arctoid Carnivora: Amphicyonidae, Ursidae, Procyonidae, and Mustelidae". In: *Journal of Mammalogy* 82.2, pp. 450–462. DOI: 10.1644/1545-1542(2001)082<0450:ESOACA>2.0.CO;2.

Stefen, C and J M Rensberger (1999). "The specialized enamel structure of hyaenids (Mammalia, Hyaenidae): Description and development within the lineage - Including percrocutids". In: *National Academy of Sciences*. Vol. 13. 2-3, pp. 363–380.

Svanbäck, R and D I Bolnick (2019). "Food specialization". In: *Encyclopedia of ecology*. Ed. by B Fath. 2nd ed. Elsevier, pp. 204–211. DOI: 10.1016/B978-0-12-409548-9.10924-8.

Tabuce, R et al. (2017). "Tooth enamel microstructure of living and extinct hyracoids reveals unique enamel types among mammals". In: *Journal of Mammalian Evolution* 24.1, pp. 91–110. DOI: 10.1007/s10914-015-9317-6.

Tardieu, L, A O Adogwa, and G W Garcia (2017). "Didelphis species, neo-tropical animals with the potential for intensive production: Part 1 Review of taxonomy, natural history, general biology, animal behaviour, and nutrition". In: *Tropical Agriculture* 94.3, pp. 312–334.

Teaford, M F (2007). "What do we know and not know about diet and enamel structure?" In: *Evolution of the human diet: the known, the unknown, and the unknowable*. Ed. by P S Ungar. New York, U.S.: Oxford University Press. Chap. 5, pp. 56–76.

The Smithsonian Institution (n.d.). *Smithsonian National Museum of Natural History*.

Thompson, V P (2020). "The tooth: An analogue for biomimetic materials design and processing". In: *Dental Materials* 36.1, pp. 25–42. DOI: 10.1016/j.dental.2019.08.106.

Ungar, P S (2008). "Strong teeth, strong seeds". In: *Nature* 452.7188, pp. 703–704. DOI: 10.1038/452703a.

— (2015). "Mammalian dental function and wear: A review". In: *Biosurface and Biotribology* 1.1, pp. 25–41. DOI: 10.1016/j.bsbt.2014.12.001.

van Casteren, A and S B Crofts (2019). "The materials of mastication: material science of the humble tooth". In: *Integrative and Comparative Biology* 59.6, pp. 1681–1689. DOI: 10.1093/icb/icz129.

von Koenigswald, W (1997). "Evolutionary trends in the differentiation of mammalian enamel ultrastructure". In: *Tooth enamel microstructure*. Ed. by W von Koenigswald and P M Sander. Rotterdam, NL: Balkema. Chap. 12, pp. 203–235.

— (2004). "Enamel microstructure of rodent molars, classification, and parallelisms, with a note on the systematic affiliation of the enigmatic eocene rodent protoptychus". In: *Journal of Mammalian Evolution* 11.2, pp. 127–142. DOI: 10.1023/B:JOMM.0000041192.79808.52.

— (2009). "Two different strategies in enamel differentiation: Marsupialia versus Eutheria". In: *Development, function and evolution of teeth*. Ed. by Mark F. Teaford, Moya Meredith Smith, and Mark W. J. Ferguson. Cambridge, UK: Cambridge University Press. Chap. 8, pp. 107–118. DOI: 10.1017/CBO9780511542626.008.

von Koenigswald, W and W A Clemens (1992). "Levels of complexity in the microstructure of mammalian enamel and their application in studies of systematics." In: *Scanning microscopy* 6.1, 195–217; discussion 217–8.

von Koenigswald, W and F J Goin (2000). "Enamel differentiation in South American marsupials and a comparison of placental and marsupial enamel". In: *Palaeontographica, Abteilung A: Palaozoologie - Stratigraphie* 255, pp. 129–168.

von Koenigswald, W, L T Holbrook, and K D Rose (2011). "Diversity and evolution of hunter-schreger band configuration in tooth enamel of perissodactyl mammals". In: *Acta Palaeontologica Polonica* 56.1, pp. 11–32. DOI: 10.4202/app.2010.0021.

von Koenigswald, W, D C Kalthoff, and G M Semprebon (2010). "The microstructure of enamel, dentine and cementum in advanced Taeniodonta (Mammalia) with comments on their dietary adaptations". In: *Journal of Vertebrate Paleontology* 30.6, pp. 1797–1804. DOI: 10.1080/02724634.2010.521931.

von Koenigswald, W, Th Martin, and H-U Pfretzschner (1993). "Phylogenetic interpretation of enamel structures in mammalian teeth: Possibilities and problems". In: *Mammal phylogeny - Mesozoic differentiation, Multituberculates, Monotremes, early Therians, and Marsupials*. Ed. by F S Szalay, M J Novacek, and M C McKenna. 1st ed. New York, U.S.: Springer-Verlag New York. Chap. 21, pp. 303–314. DOI: 10.1007/978-1-4613-9246-0.

von Koenigswald, W and H U Pfretzschner (1991). "Biomechanics in the enamel of mammalian teeth". In: *Constructional morphology and evolution*. Ed. by N Schmidt-Kittler and K Vogel. Berlin, Heidelberg: Springer Berlin Heidelberg, pp. 113–125. DOI: 10.1007/978-3-642-76156-0_9.

von Koenigswald, W and J W F Reumer (2020). "The enamel microstructure of fossil and extant shrews (Soricidae and Heterosoricidae, Mammalia) and its taxonomical significance". In: *Palaeontographica Abteilung A* 316.1-6, pp. 79–163. DOI: 10.1127/pala/2020/0095.

Wang, E (2002). "Diets of Ocelots (*Leopardus pardalis*), Margays (*L. wiedii*), and Oncillas (*L. tigrinus*) in the Atlantic Rainforest in Southeast Brazil". In: *Studies on Neotropical Fauna and Environment* 37.3, pp. 207–212. DOI: 10.1076/snfe.37.3.207.8564.

Wang, X et al. (2019). "Wild boar's tusk enamel: Structure and mechanical behavior". In: *Materials Science and Engineering C* 100.February, pp. 354–362. DOI: 10.1016/j.msec.2019.03.017.

Weng, Z Y et al. (2016). "Giant pandas tooth enamel: Structure, mechanical behavior and toughening mechanisms under indentation". In: *Journal of the Mechanical Behavior of Biomedical Materials* 64, pp. 125–138. DOI: 10.1016/j.jmbbm.2016.07.029.

Wilmers, J and S Bargmann (2020). "Nature's design solutions in dental enamel: Uniting high strength and extreme damage resistance". In: *Acta Biomaterialia* 107, pp. 1–24. DOI: 10.1016/j.actbio.2020.02.019.

Wilson, D E and D M Reeder, eds. (2005). *Mammal species of the world*. 3rd ed. Baltimore, US: Johns Hopkins University Press, p. 2142.

Wilson, G P et al. (2016). "A large carnivorous mammal from the Late Cretaceous and the North American origin of marsupials". In: *Nature Communications* 7, pp. 1–10. DOI: 10.1038/ncomms13734.

Wiszniowska, T et al. (2010). "Dental enamel structure in fossil bears *Ursus spelaeus* and *U. wenzensis* (=minimus) in comparison to selected representatives of other Carnivora". In: *Morphology and Systematics of Fossil Vertebrates*. Ed. by D Nowakowski. Wrocław, Poland: DN Publisher, pp. 125–142.

Wroe, S, C McHenry, and J J Thomason (2005). "Bite club: Comparative bite force in big biting mammals and the prediction of predatory behaviour in fossil taxa". In: *Proceedings of the Royal Society B: Biological Sciences* 272.1563, pp. 619–625. DOI: 10.1098/rspb.2004.2986.

Wroe, S and N Milne (2007). "Convergence and remarkably consistent constraint in the evolution of carnivore skull shape". In: *Evolution* 61.5, pp. 1251–1260. DOI: 10.1111/j.1558-5646.2007.00101.x.

Xing, S, M Martinón-Torres, and J M Bermúdez de Castro (2018). "The fossil teeth of the Peking Man". In: *Scientific Reports* 8, p. 2066. DOI: 10.1038/s41598-018-20432-y.

Xu, C et al. (2012). "The distribution of carbonate in enamel and its correlation with structure and mechanical properties". In: *Journal of Materials Science* 47.23, pp. 8035–8043. DOI: 10.1007/s10853-012-6693-7.

Yahyazadehfar, M and D Arola (2015). "The role of organic proteins on the crack growth resistance of human enamel". In: *Acta Biomaterialia* 19, pp. 33–45. DOI: 10.1016/j.actbio.2015.03.011.

Yahyazadehfar, M, D Bajaj, and D D Arola (2013). "Hidden contributions of the enamel rods on the fracture resistance of human teeth". In: *Acta Biomaterialia* 9.1, pp. 4806–4814. DOI: 10.1016/j.actbio.2012.09.020.

Yilmaz, E D, J Koldehoff, and G A Schneider (2018). "On the systematic documentation of the structural characteristics of bovine enamel: A critic to the protein sheath concept". In: *Dental Materials* 34.10, pp. 1518–1530. DOI: 10.1016/j.dental.2018.06.006.

Yilmaz, E D, G A Schneider, and M V Swain (2015). "Influence of structural hierarchy on the fracture behaviour of tooth enamel". In: *Philosophical Transactions of the Royal Society A: Mathematical, Physical and Engineering Sciences* 373.2038, p. 20140130. DOI: 10.1098/rsta.2014.0130.

Zamudio-Ortega, C M et al. (2014). "Morphological, chemical and structural characterisation of deciduous enamel: SEM, EDS, XRD, FTIR and XPS analysis". In: *European Journal of Paediatric Dentistry* 15.1, pp. 275–280.

Zavala-Alonso, V et al. (2012). "Analysis of the molecular structure of human enamel with fluorosis using micro-Raman spectroscopy". In: *Journal of Oral Science* 54.1, pp. 93–98. DOI: 10.2334/josnusd.54.93.

Zhang, N et al. (2020a). "Hierarchy structure and fracture mechanisms of the wild wolf tusk's enamel". In: *Materials Science and Engineering C* 106, p. 110277. DOI: 10.1016/j.msec.2019.110277.

Zhang, S et al. (2020b). "Enamel-inspired materials design achieving balance of high stiffness and large energy dissipation". In: *Journal of the Mechanical Behavior of Biomedical Materials* 103, p. 103587. DOI: 10.1016/j.jmbbm.2019.103587.

Zhang, Y R et al. (2014). "Review of research on the mechanical properties of the human tooth". In: *International Journal of Oral Science* 6.2, pp. 61–69. DOI: 10.1038/ijos.2014.21.

Zhao, Z, K M Weiss, and D W Stock (2000). "Development and evolution of dentition patterns and their genetic basis". In: *Development, function and evolution of teeth*. Ed. by M F Teaford, M M Smith, and M W J Ferguson. Cambridge University Press, pp. 152–172. DOI: 10.1017/CBO9780511542626.011.